COMPARATIVE GEOMORPHOLOGY OF TWO ACTIVE TECTONIC STRUCTURES, NEAR OXFORD, NORTH CANTERBURY

A thesis
submitted in partial fulfilment of the requirements for the Degree
of
Master of Science in Geology
at the
University of Canterbury
by
Bryce Derrick May

University of Canterbury
2004

Frontispiece:

Looking towards Christchurch from the Trig. Station on Starvation Hill.

ABSTRACT

The North Canterbury tectonic setting involves the southward propagating margin of easterly strike-slip activity intersecting earlier thrust activity propagating east from the Alpine Fault. The resulting tectonics contain a variety of structures caused by the way these patterns overlap, creating complexities on the regional and individual feature scale.

An unpublished map by Jongens et al. (1999) shows the Ashley-Loburn Fault System crossing the plains from the east connected with the Springfield Thrust Fault in the western margins, possibly the southern limit of the east-west trending strike-slip activity. Of note are two hill structures inferred to be affected by this fault system. View Hill to the west, is on the south side of this fault junction, and Starvation Hill further east, was shown lying on the north side of a left stepover restraining bend.

During thrust uplift and simple tilting of the View Hill structure, at least two uplift events post date last Pleistocene aggradation accounting for variations in scarp morphology. Broad constraints on fault dip and the age of the displacement surface suggest that slip-rates are in the order of 0.5 mm/year.

East from View Hill, the strike-slip fault was originally thought to curve northeast, around the southeast of Starvation Hill. But there is neither evidence of a scarp, nor other clear evidence of surface faulting at Starvation Hill, which poses the question of the extent to which folding may reflect both fault geometry and fault activity.

Starvation Hill is a triangular shape, with a series of distinctive smooth, semi-planar surfaces, lapping across both sides of the hill at a range of elevations and gradients. These surfaces are thought to be remnants of old river channels, and are indicative of tilting and upwarping of the hill structure. 3D computer modelling of these surfaces, combined with studies of the cover sequence on the hill, resulted in inferences being drawn as to the location of hinge lines of a dual-hinged anticline and an overview of the tectonic history of the hill. This illustrates the potential to apply topographical and geomorphic studies to the evolution of geometrically complex structures

Starvation Hill is interpreted to be the result of two fault-generated folds, one fault trending north, the other, more recent fault, trending east. These two faults are thought to be sequentially developed segments of the original fault zone inferred by Jongens et al. (1999) but with reinterpreted location and mechanism detail. The presence of two faults has resulted in overprinted differential uplift of the structure, which has been significantly degraded, especially in the southwest corner of the hill. The majority of the formation of the northerly trending structure of Starvation Hill is inferred to be pre-Otiran, with uplift of the later east trending structure continuing into the late Pleistocene and Holocene.

ACKNOWLEDGEMENTS

I would like to thank:

My parents and brothers for their support and encouragement throughout my time at university. My Supervisors Jocelyn Campbell and Phil Tonkin for their understanding when mine required repeated explanations, for the various entertaining experiences of multiple field trips, and for sharing their vast wealth of knowledge with me. My family, flatmates and rapidly diminishing number of friends for their help with the extensive and often gruelling fieldwork; thanks for enduring the steep slopes, gorse, livestock and blackberry bushes, varieties of weather conditions, and especially thanks to Matt for carrying those rocks, pity they never got used. My flatmates, for being great and entertaining flatmates, and providing often intriguing perspectives on life. The staff at the Arts Centre, especially the Venues staff, for making my 'second home' a friendly and often amusing work place of many happy memories. My room mates at Uni, Emily, Callum and Kerry, thanks for the encouragement and telling me off when I was being lazy. The Geology Department Technicians, especially Cathy Knight and Joyce Seale, for their fantastically positive, 'nothing's ever a problem' attitudes, their organisation, suggestions and encouragement to help me persevere and John Southward for helping me with numerous computer glitches. The farmers and landowners throughout my field areas, whose friendly and supportive attitudes have made fieldwork substantially less stressful. Mike Finnemore, Emma Davis, James Grindley and the staff and students of the ETH Zurich Geophysical Project, for the experience of seismic work, especially blowing up the North Island. The students and staff of the Geology Department of whom I have had the privilege of working beside, especially Andy Burgess for his inspiring motivational talks ("You gotta ask yourself what's the point, I mean what are we really doing here, don't you just want to give up?" - he finished before me too) and last but certainly not least, my thanks to Dave Bell for keeping me from taking life too seriously.

TABLE OF CONTENTS

PART TWO – VIEW HILL:

PART THREE – STARVATION HILL:

PART FOUR – SUMMARY & CONCLUSIONS:

LIST OF FIGURES

PART ONE – INTRODUCTION:

PART TWO – VIEW HILL:

PART THREE – STARVATION HILL:

PART ONE – INTRODUCTION:

1.1 Setting:

The focus of this study began at Starvation Hill, located 40 km northwest of central Christchurch. The Hill is an isolated topographic feature rising about 85 m above the surrounding North Canterbury Plains. The township of Oxford, nestled under the foothills of the Southern Alps, is located 3 km due west of Starvation Hill. The Hill lies 4 km from the nearest foothills and more than 6 km from the closest isolated topographic feature, the Cust Anticline.

The study extended to include a second such feature, View Hill, lying 13 km west-southwest of Starvation Hill. View Hill covers a smaller area than Starvation Hill and is comprised of two topographic highs with a saddle-like area between them. The two parts of View Hill rise about 70 and 90 m above the Plains.

Both Starvation Hill and View Hill are inferred to be underlain by tilted or folded pre-Quaternary sequences. Because of this, the question arises as to whether these features are currently actively deforming, or are preserved simply as relict elevated topography above the level of fluvio-glacial erosion and aggradation forming the surface of the Canterbury Plains.

Starvation Hill was initially of interest due to a fault line inferred along the southern side of the hill connecting the Ashley-Loburn Fault System in the northeast to the Springfield fault in the west (Jongens et al. 1999). The Hill was also inferred to be

an anticlinal structure, the anticline running approximately north-northeast and thought of as a possible restraining bend related structure.

Jongens et al. (1999) projects the fault at Starvation Hill to link to the Ashley-Loburn Fault System to the northeast. To the west of Starvation Hill, the fault is projected to link with a distinct fault scarp on the west side of View Hill, striking northeast and curving eastwards, towards Starvation Hill. Thus, there was an inference of a possible genetic linkage between the two structures of Starvation Hill and View Hill.

1.2 Objectives:

The initial objectives of this study evolved around the mapping of the fault near Starvation Hill, and determining its nature, with potential for improving seismic hazard assessment of the fault system for the Canterbury region. However, it became apparent that the fault does not have a clear surface expression amenable to conventional paleoseismic methods such as trenching. Attention then focussed on finding evidence of growth history of the Starvation Hill structure to determine the history and rate of fold growth as a reflection of possible fault driven activity at depth:

- **The production of a detailed topographic model of Starvation Hill and surrounding area.** This objective was approached through the following methods:

    - Examination of an existing digital elevation model (DEM) for use at the Starvation Hill site
    - A comprehensive GPS survey of the Starvation Hill structure resulting in a higher resolution DEM of the slopes of the hill than currently existed
    - Amalgamation of the existing and new DEM's to extend the topographic model

- **The determination of the age of distinctive surfaces eroded into the crest and flanks of Starvation Hill.** This objective was approached through the following methods:

    - Mapping of surface remnants determining potential correlations
    - Profiling of loessal soil cover, determining thickness and extent of the loess and the number of loess depositional cycles on the different topographic surfaces

- **Reconstruction of the gradients on distinctive surfaces to determine if Starvation Hill has been episodically tilted by fault movement.** This objective was approached through the following methods:

    - Incorporation of mapping of distinct surfaces with DEM and partial 3-D reconstruction of surface remnants
    - Comparisons of angles of tilt of the various surfaces and partial reconstruction of a relative chronology of deformation

- **Map the extent of the fault scarp at the View Hill site between the Waimakariri and Eyre Rivers and try to identify any linkage with the Starvation Hill Structure.** This objective was approached through the following methods:

    - A total station (integrated theodolite and electronic distance measurement instrument) survey across selected sections of the fault scarp
    - Examination of the Eyre River as a potential site for fault exposure
    - Examination of aerial photographs and identification of the relative age of surfaces affected by scarp growth

1.3 New Zealand Tectonic Setting:

1.3.1 Introduction:

To understand the tectonic setting of the field area, a brief overview of the New Zealand tectonic setting is given to place North Canterbury in its regional tectonic setting. For this purpose, the New Zealand tectonic setting is separated into three main zones:

- Northeast Subduction
- Southwest Subduction
- Transition zone between the two

The direction of movement of two plates on the Earth's lithosphere is usually described in terms of the relative motion at their boundary zones. In the case of the Australian and Pacific Plates, taking the Australian Plate as stationary, the relative motion of the Pacific Plate is as if it were moving towards the Australian Plate and rotating anticlockwise around a pole located towards the south of the present landmass. This implies that starting from due north of the pole of rotation, the relative motion will be from east to west, but further west on the plate, the direction of motion progressively includes a southward component. This is indicated in figure 1.1 by the arrows of convergence direction, showing more oblique convergence to the southwest until, due to the shape of the boundary, the interaction of the two plates becomes transpressive as the two plates appear to slide past each other along the Southern Alps.

1.3.2 Subduction:

As the Australian and Pacific plates are pushed relatively towards each other, in the northeast section (figure 1.1, Zone A) the Pacific Plate is thrust under the Australian Plate creating the Hikurangi Subduction Zone. This activity has created such features as the Kermadec Trench, Taupo Volcanic Zone, and the Accretionary Wedge as the Pacific Plate heads down under the overriding Australian Plate (see figure 1.2)

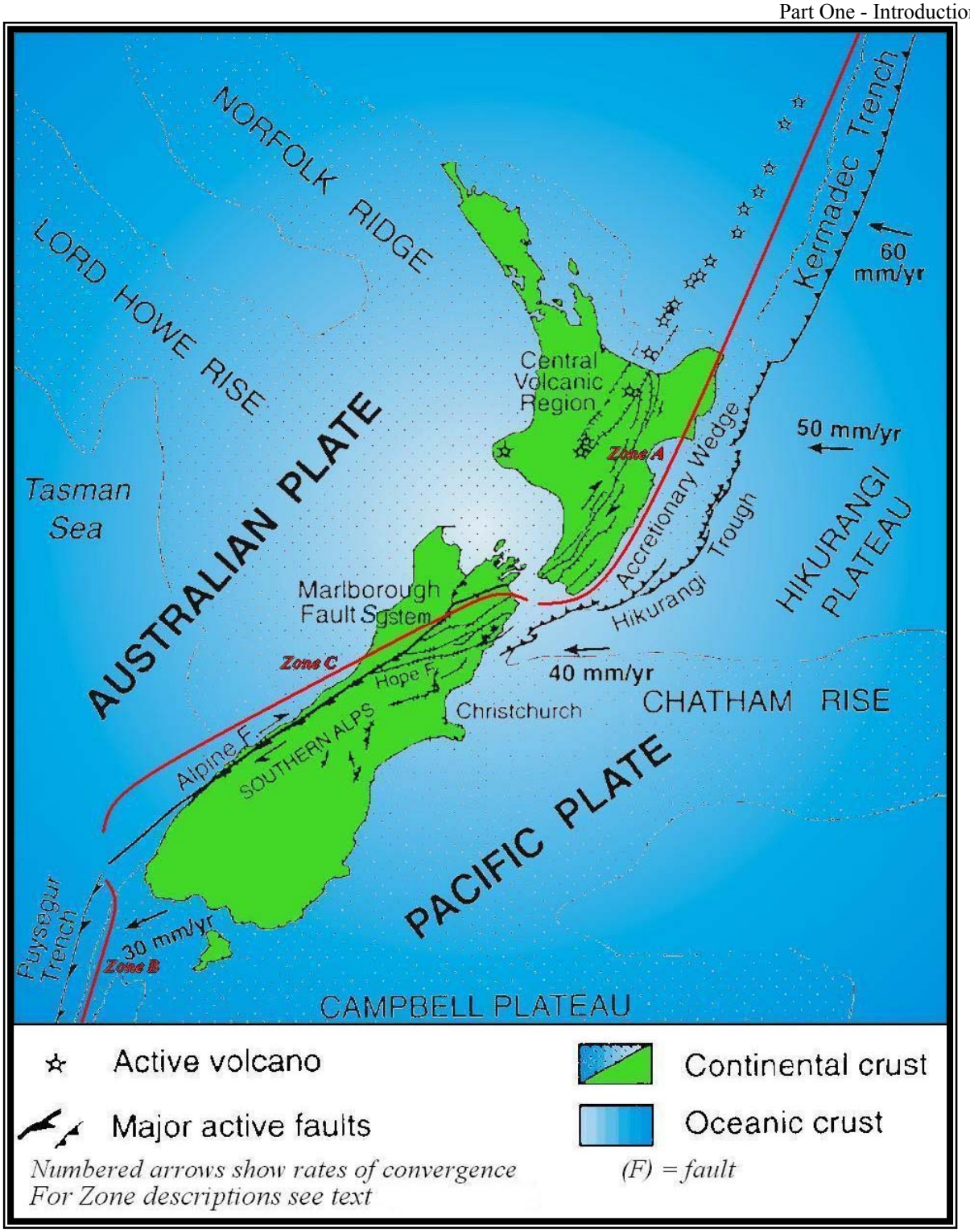

Figure 1.1 - *New Zealand Tectonic Setting.*
Selected elements of the plate boundary zone are illustrated. Movement along the opposite dipping subduction zones, the Puysegur Trench in the SW and the Hikurangi Subduction Zone in the NE, is accommodated by the Marlborough Fault System and the Alpine Fault. The Hope Fault is shown, currently considered to take up most of the motion between the Alpine Fault and Hikurangi Subduction Zone. Adapted from Pettinga et al. (2001).

Along the Hikurangi Subduction Margin, NW-SE contraction involves low-angle thrust rupturing along the subduction interface, reverse-dextral faulting in its immediate hanging wall, and a largely aseismic accretionary prism offshore (Sibson and Rowland, 2001).

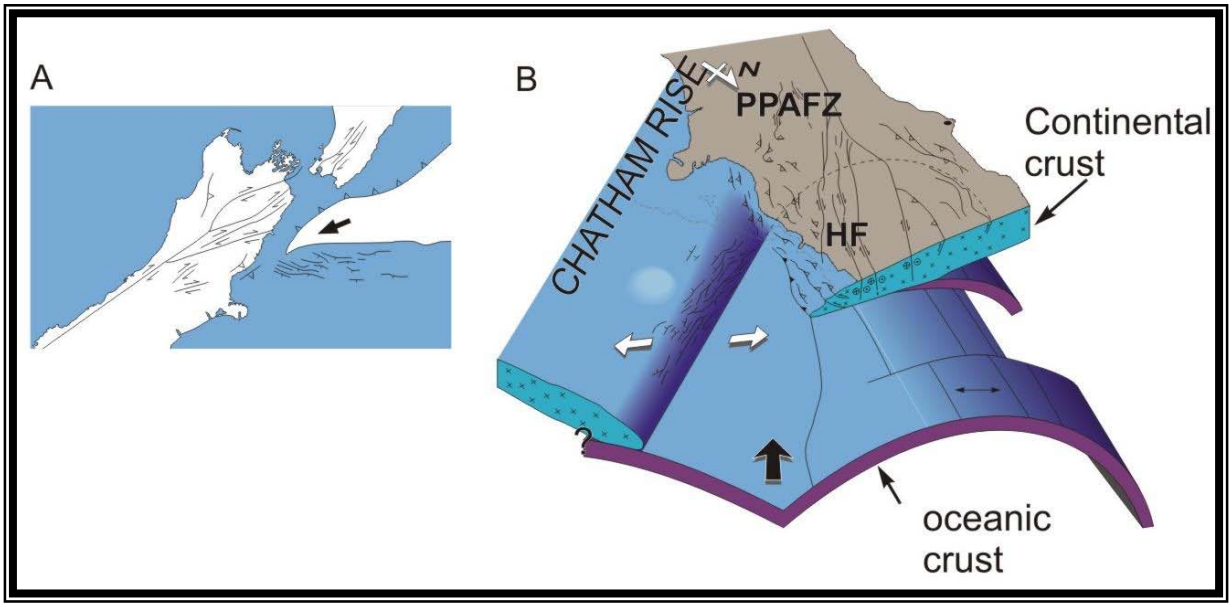

Figure 1.2 - *Subduction Zone example, the southern tip of the Hikurangi Subduction Zone. The view shows the subducting oceanic crust as it moves under the continental crust of the South Island. The Porters Pass Amberley Fault Zone (PPAFZ) and Hope Fault (HF) are also shown. For the Puysegur Trench to the southwest, this situation is reversed as the oceanic crust of the Australian Plate is being subducted by the Pacific Plate. Modified from Barnes (1994).*

Darby and Bevan (2001) suggest that convergence of the southern section of the Hikurangi Subduction margin is 39.4 mm/yr. This value increases dramatically further north, as the subduction zone becomes the Tonga-Kermadec Subduction Zone. Billen et al. (2003) suggest that over the last 5 million years the Tonga-Kermadec subduction zone has been characterised by very fast subduction at a rate of ~200 mm/yr total convergence.

In the southwest, (figure 1.1, Zone B) the Puysegur Trench is the dominant feature of the Pacific plate overriding the down-going Australian Plate, this is the reverse of the Hikurangi Subduction Zone to the northeast. Highly oblique convergence at a rate of 35 mm/yr is being partitioned between oblique subduction at the Puysegur trench, thrusting within the trench slope, strike-slip faulting on the Puysegur Bank,

and minor shortening within the Solander Basin (Melhuish et al., 1999). Here oceanic crust is being subducted, but at a slower rate than that of the Hikurangi Subduction Zone.

1.3.3 Transition Zone:

In the South Island, the Alpine Fault (figure 1.1, southern part of Zone C) was originally considered almost entirely in terms of a strike-slip zone, with the two plates sliding past each other (Suggate, 1963). Modern views hold that the Pacific and Australian plates are not sliding past each other without interaction. There is a significant amount of transpression involved in the fault, with a component of the shortening vector taken up directly as oblique-slip on the fault plane with convergence increasing towards the northern end, but deformation is also disseminated across a broad zone parallel to the plate boundary. In detail the fault is not a straight line, instead, it is a jagged series of strike-slip and thrust faults, and the more regional deformation also reflects a complex interaction of convergence and strike-slip dominated structures.

The Alpine Fault and the associated deformation are therefore currently considered part of a zone of highly oblique compression in its northern section, tending towards oblique-slip / strike-slip to the south. With the advent of plate tectonics, it has generally been viewed as a transform fault linking the west-directed subduction zone in the North Island with an east-directed oblique subduction zone in the southwest of the South Island (Norris et al., 1990).

1.4 North Canterbury Tectonic Setting:

1.4.1 Introduction:

The area between the Southern Alps and the Canterbury Plains constitutes a diffuse zone of deformation related to the oblique continental collision. Beneath the North Canterbury Plains, systems of thrust-fault related folds propagate southeastwards from the Alpine Fault. This broad zone of deformation has been interpreted as a part of a two-sided deforming wedge, associated with a mid to lower crustal detachment zone similar to the general model first proposed by Norris et al (1990), (see figure 1.3). The wedge in detail contains various backthrusts forming belts of deformation. Selected features of these belts such as the Springbank Fault are discussed in section 1.5.

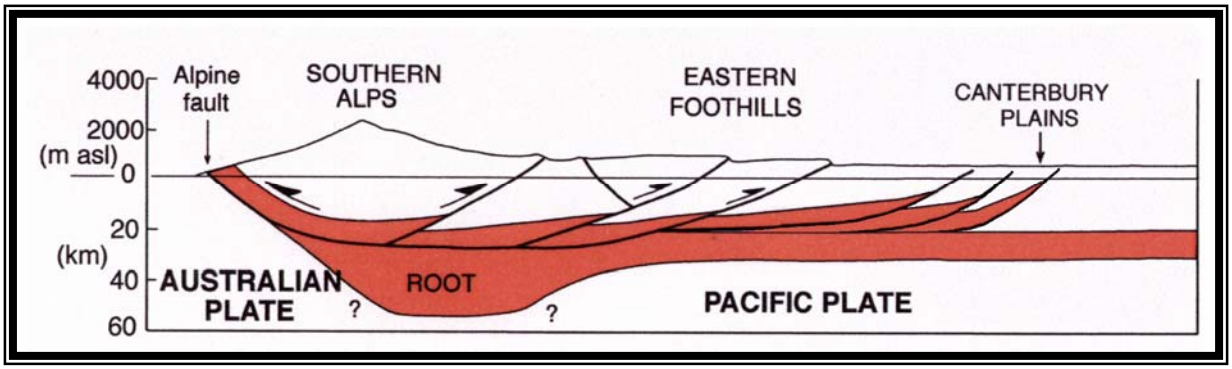

Figure 1.3 – *Schematic representation of the two-side deforming wedge model between the Southern Alps and the Canterbury Plains.*
Note the series of backthrusts situated throughout parts of North Canterbury forming belts of deformation. Modified from the adaptation of Norris et al. (1990) in Pettinga et al. (2001).

Between the Alpine Fault and the Hikurangi Subduction Zone to the north lies a complicated transfer zone of fault strands of the Marlborough Fault System feeding southwest to the northern sector of the Alpine fault. The area (figure 1.1, northern part of C, and figure 1.2) affected by this transition from subduction to more predominant strike-slip is wide, encompassing most of the North Canterbury and Marlborough regions. The zone is dominated by several major faults such as the Hope Fault with predominant strike-slip and some oblique-slip motion interconnected by cross-faults and an array of north to northeast striking thrust driven folds.

The regional stratigraphy and measurement of Quaternary slip rates suggests that activity on these faults has slowly migrated southward. As activity has decreased on a fault, the fault to the south has become more active, suggesting that the Marlborough Fault System and Hikurangi Subduction Zone is becoming realigned with a broad zone of deformation migrating into North Canterbury, see figure 1.4.

Field and Browne (1989) suggest that North Canterbury can be described in terms of a fold and fault belt consisting of a series of northeast trending anticlines and synclines typically bounded to the west by high-angle faults. This belt covers the area from Marlborough in the north to at least as far south as near Amberley. They describe the deformation as beginning in the Late Cenozoic from regional oblique plate-plate compression and continuing today, reflected in the rapid facies changes in the Late Cenozoic sediments.

Currently the Hope Fault is thought to take up most of the motion between the Hikurangi Subduction Zone and the Alpine Fault, with the juvenile Porters Pass-Amberley Fault Zone recently recognised as a significant zone for future tectonic activity. The activity on the major faults of the Marlborough Fault System is not as simple as the regional trend suggests. The faults themselves are more complex than figure 4 shows, with segmentation, step-overs and minor splays common on most of the faults, as well as further cross-faults between these, not all aligning with the regional trend of the major faults.

The Marlborough Fault System, connecting the Alpine Fault to the Hikurangi Margin, functions as a migrating duplex system. The theoretical expectation is that such a fault-bounded duplex will tend to be bypassed by the propagation of a new fault system to the south, preceded by compression and contraction strains. From recent mapping in North Canterbury, it is evident that no simple through going surface connection has yet been established (Campbell, 1991).

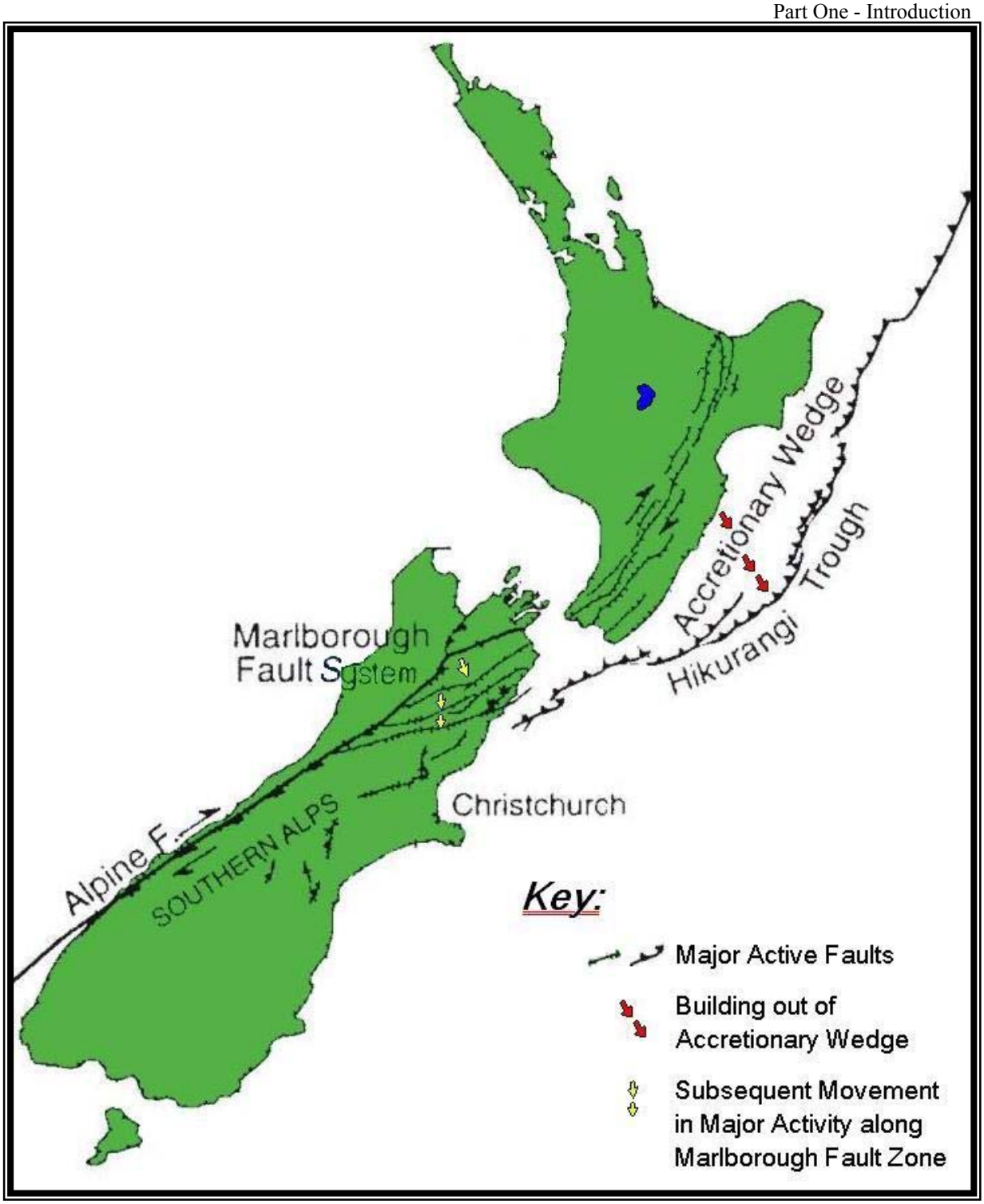

Figure 1.4 – *Alignment of the Marlborough Fault System with the Hikurangi Subduction Zone.*
As the Accretionary Wedge of the Hikurangi Subduction Zone has built out from the east coast of the North Island, the zone of major activity along the Marlborough Fault System has moved southeast to align. Fault outlines adapted from Pettinga et al. (2001).

1.4.2 Offshore Features:

The contractional deformation in North Canterbury extends 20 km offshore between central Pegasus Bay and Kaikoura. Barnes (1996) describes this deformation as including eleven major folds and numerous smaller-scale structures occurring beneath the shelf between Pegasus Bay and Kaikoura Peninsula. The major structures developed in the upper part of the sedimentary cover are gentle, asymmetric folds, approximately 10 – 32 km in length, and consistently merge to the northwest in accordance with major thrust faults and folds exposed in nearby coastal hills. The folds are inferred to overlie a system of southeast dipping thrust faults that are accommodating a small component of regional NW – SE crustal shortening in North Canterbury.

1.4.3 Canterbury Region Structural Domains:

A consequence of the interaction of the Marlborough Fault System with the deformation associated with the main length of the Alpine Fault has produced a complex pattern of locally dominant deformation styles. Pettinga et al. (1998; 2001) have divided the Canterbury Region into eight different structural domains. Each domain presents different tectonic characteristics related to fault style, geometry, and rates of deformation as shown in figures 1.5a and 1.5b.

This spatial picture of distinct structural domains is complicated by the fact that changes in the relative plate motion between the Pacific and Australian plates have caused strain partitioning to vary in both space and time (Jongens et al., 1999).

The focus areas of this study essentially lie within domain 7, the Canterbury Plains, however, the areas are in close proximity to the boundary between both domains 3 and 5.

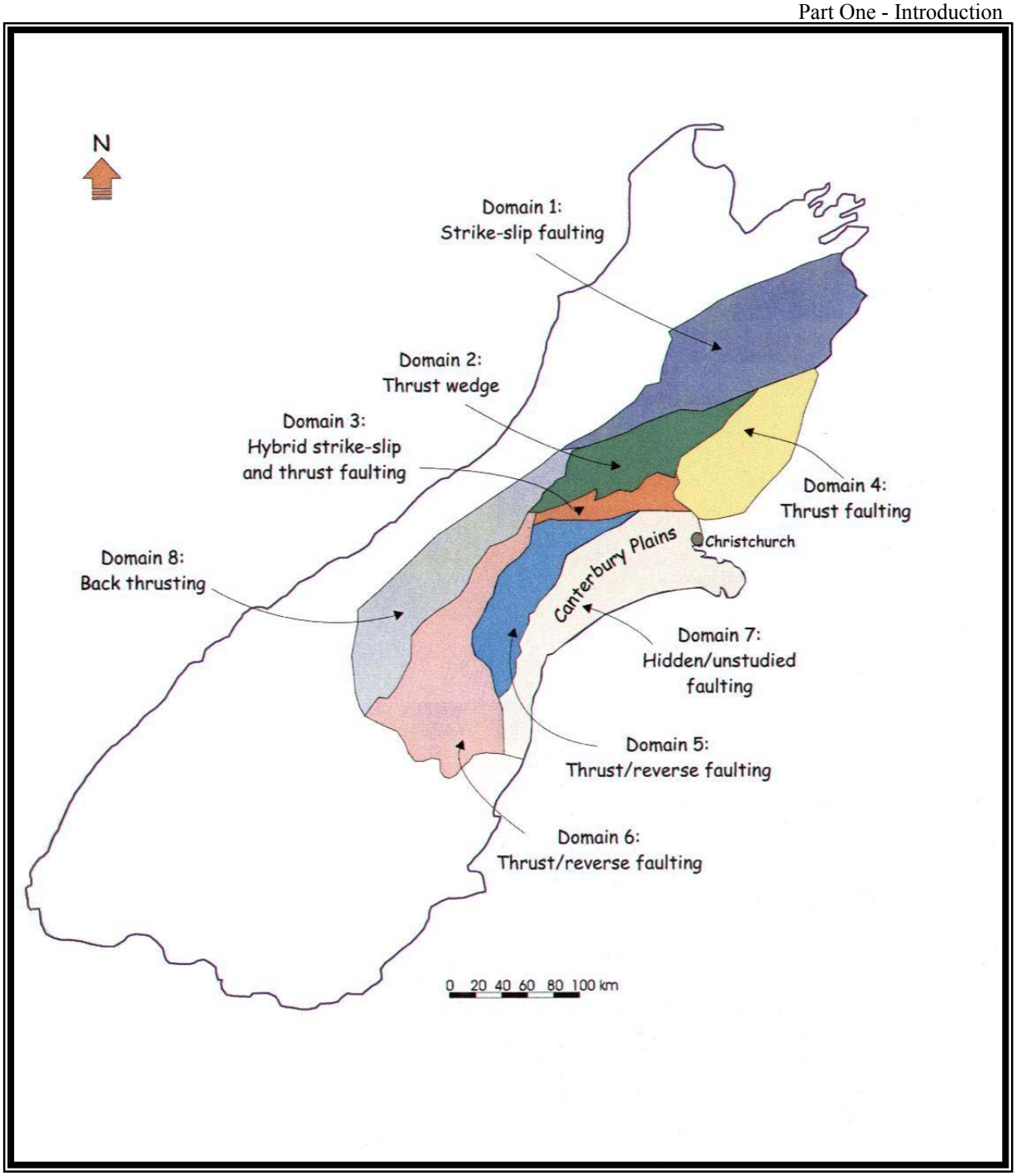

Figure 1.5a – *Structural Domains of the Canterbury Region.*
The areas of focus in this study essentially lie in domain 7, Canterbury Plains, but are close to the interaction at the boundary between domains 3 and 5. See Fig 5b over page for definitions of each of the structural domain. Modified in Estrada (2003) from Pettinga et al (1998, 2001).

DOMAIN	BRIEF DESCRIPTION
Domain 1: Marlborough Fault System	Major fault system of northeast trending strike-slip faults that transfer crustal shortening associated with subduction of the Pacific plate onto the west-facing Alpine Fault.
Domain 2: West Culverden Fault Zone	West dipping system of thrust/reverse faults and associated fault-propagation folds that represents the eastern margin of the wedge-shaped structural domain of the Southern Alps in north Canterbury. This fault system is interpreted as backthrusts to the east of the Alpine Fault zone and is inferred to extend to mid and lower crustal depths beneath the Southern Alps and Canterbury foothills.
Domain 3: Porter's Pass-Amberley Fault Zone	Juvenile hybrid system of interconnected east-northeast trending strike-slip transfer faults, oblique thrust and/or reverse faults with associated fault propagated folds that occur along the Southern Alps foothills and range-front at the west margin of the Canterbury Plains.
Domain 4: North Canterbury Fold and Fault Belt	Region of mainly east dipping thrust/reverse faults associated with strongly asymmetric folds that extend through the northeast part of the onshore Canterbury region, and offshore across the continental shelf and slope. The faults are well expressed as topographic ridges separated by fault-controlled synclinal valleys.
Domain 5: Central Canterbury Rangefront Fault Zone	Complex array of faults, folds, and associated warping along the west margin of the Canterbury Plains. This constitutes the eastern most expression of the double-sided wedge described by Norris et al. (1990).
Domain 6: South Canterbury Zone	This domain comprises the margin of the Southern Alps double-sided wedge style of thrust deformation.
Domain 7: Canterbury Plains	System of north and northeast trending active faults and folds are emerging from beneath the aggradation gravels of Pleistocene fluvio-glacial outwash in the Canterbury Plains. This system is the result of the tectonic shortening, crustal thickening and uplift taking place in the region.
Domain 8: Southern Alps Zone	The deformation here is dominated by oblique, reverse/thrust faulting, inferred to be driven by backthrusting off the dipping Alpine Fault.

Figure 1.5b – *Structural Domains of the Canterbury Region. Modified in Estrada (2003) from Pettinga et al. (1998, 2001).*

1.4.4 North Canterbury Region Fold Structures:

Complex fold structures found scattered throughout the North Cantebury region are described by Nicol (1991). He describes folding as the most widespread manifestation of late Cenozoic deformation. These folds are often non-cylindrical and reflect the interference of two fold sets to form irregular and non-classical basin and dome outcrop patterns. An example of this is the Cust Anticline, discussed in section 1.5.6, an irregularly shaped anticline.

Fold interference patterns develop where two sets of folds are superimposed on each other, either in succession or simultaneously (see figure 1.6). The resulting outcrop patterns are subtle and vary in character from area to area due to the effects of changing fold morphologies and topography.

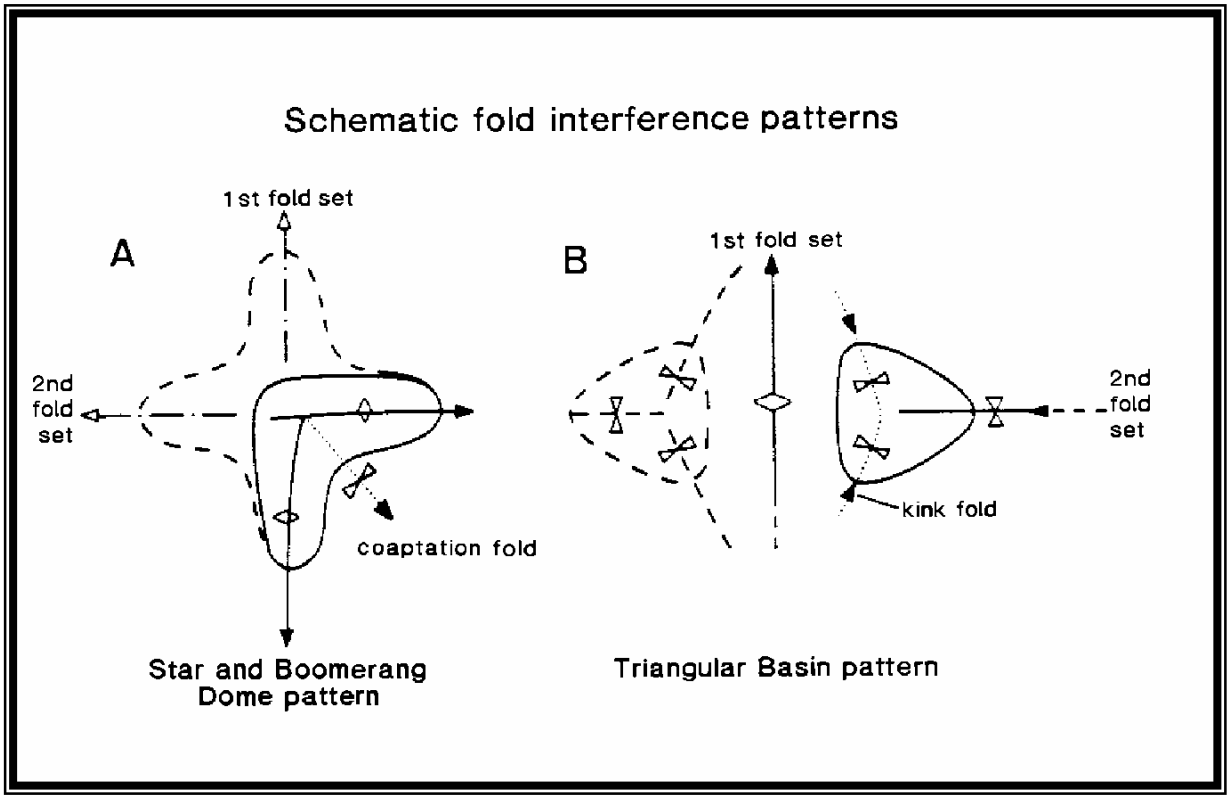

Figure 1.6 - *Fold Interference Patterns.*
Fold outcrop patterns developed in North Canterbury, represented by solid lines in (A) and (B) from Nicol (1991).

The preceding features of the North Canterbury tectonic setting imply that the tectonics contain a variety of patterns, however the way in which these patterns overlap causes multiple complexities not yet fully understood, both on the regional and individual feature scale.

1.5 Features of the Field Area: *(see figure 1.7)*

1.5.1 Springbank and Hororata Faults:

Located well out under the Plains, to the east of the study area, a zone of active deformation has been identified forming a belt extending from 7 km west of Rangiora, southwest to the eastern front of the Malvern Hills near Hororata, possibly crossing the Rakaia River to the south. This belt includes both the Springbank and Hororata Faults.

In her study of the Springbank Fault, Estrada (2003) concludes that the Springbank Fault is a blind thrust/reverse structure with an estimated strike of ~16 km and dip of ~60° to the northwest. She notes that the fault does not reach the surface, but instead, produces a broad anticline that was classified as a propagation fold with mainly the attributes of a trishear fold and successfully replicated by digital modelling using Trishear 4.5 (Allmendinger, 1998, 2000).

The study of the Springbank Fault also partially delineated two previously unrecognised faults, the Eyrewell Fault to the south and the Sefton Fault to the northeast. These two faults appear to be related to propagation folds with similar characteristics to the fold related to the Springbank Fault, and consequently, they appear to be associated with the same decollement beneath the Canterbury Plains, inferred to lie 12 to 14 km below the surface (Cowan, 1992). However, the surface expressions of the faults suggest they are not directly linked to each other, but are in close enough proximity that a seismic event on one may cause activity on another.

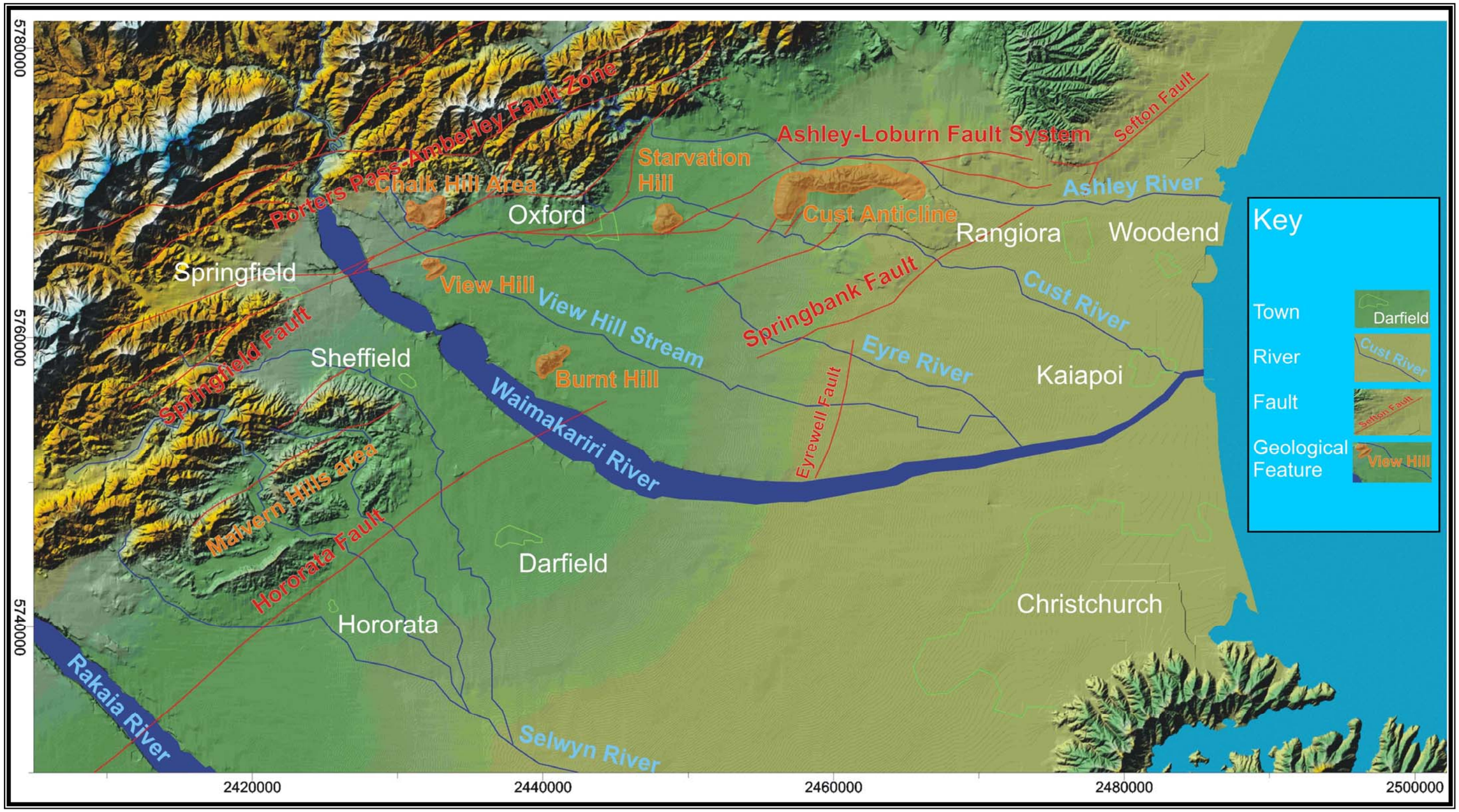

Figure 1.7 – *Selected Features of North Canterbury.*
Topographic data from New Zealand Digital Elevation Model (based on Terralink data of NZMS Topographic series 1:50,000). Town and River outline from Terralink. Fault outlines from North Canterbury Active Tectonics GIS. New Zealand Map Grid co-ordinates shown in meters.

The Hororata Fault has a similar strike and approximately aligns with the Springbank Fault. The Springbank and Hororata Faults are thought to be master faults to a series of backthrusts (Jongens et al., 1999). To this extent, the Springbank and Hororata faults may only be a small section of a wide zone of inter-linked activity as suggested by such authors as Pettinga et al. (2001), but is not fully understood in detail for the North Canterbury Plains area (see figure 1.3).

The Malvern Hills expose Torlesse Group basement and more of these potential backthrust structures and may serve as a model for the style of deformation underlying the deeper sedimentary cover to the north.

1.5.2 Ashley – Loburn Fault System:

In contrast to the northeast striking thrust system, an east-west fault zone, the Ashley - Loburn Fault System strikes westward across the northern Plains. It lies between the northern termination of the Springbank Fault and southern extent of the Sefton Fault, with a surface expression beginning approximately 7 km northwest of Rangiora.

The Ashley (southern) and Loburn (northern) Faults appear to converge to the west, somewhere along the axis of the current Ashley River. The plane of the Ashley Fault east of this convergence dips to the north, the Loburn Fault dips to the south. Both of these faults have demonstrably significant reverse-slip displacements which have uplifted the intervening area (Sisson et al., 2001).

The orientation sub-parallel to the Porters Pass - Amberley Fault Zone and elements of the fault morphology suggest that there may be significant oblique strike-slip. Thus the Ashley and Loburn Faults form splays of the Ashley - Loburn Fault System, where Sisson (2001) has shown the Ashley branch to be currently active and propagating eastward. The relationship with faults to the east is currently unclear due to the recent discovery of the Sefton Fault, which has yet to undergo significant investigation (see Springbank Fault section above).

The Ashley Fault System is inferred to project westward across the Plains, dipping south, to join the Springfield Fault and may function as the bounding transfer fault. This projection currently assumes a restraining bend or step-over, but lacks any significant surface expression over this more southern extension of the Ashley Fault System, between the Ashley - Loburn Fault System to the east and the Springfield Fault to the west. A significant part of this projection underlies the current course of the Eyre River. Two features, View Hill and Starvation Hill, are associated with this projection and are the subject of parts Two and Three respectively of this thesis.

1.5.3 Cust Anticline:

The Cust Anticline rises to ~100m above the surrounding plains. The structure is the hanging wall expression of oblique-reverse faulting on an E-W striking, south dipping fault plane projecting west along the axis of the Ashley River in line with the projected trace of the junction between the Ashley and Loburn Faults (Sisson, 1999).

The notable feature of this anticline is the strong curvature of the fold at its western end. Here deformation is accommodated both on the Cust Fault, a north - south striking, westward-dipping reverse fault, upthrown on the western side causing changes in drainage patterns (Cowan, 1992), and more cryptically on a west facing fold or fault suggested by Estrada (2003). The west facing fold or fault is suggested to be a backthrust related to fault bend folding initiated off the break up point where the Springbank Fault ramps up from the basal detachment. The result is an anticlinal trace with a marked right angle bend at the culmination of this periclinal structure. The Cust Anticline marks a position of which the east-west Ashley Fault System is thought to step through a restraining bend to continue further westward, problematically as noted above, under the Ashley – Loburn Fault System.

1.5.4 Starvation Hill:

Starvation Hill lies to the west of the Cust Anticline, east of the township of Oxford, and was originally inferred to be an opposing anticlinal structure associated with the same restraining bend of the westward projection of the Ashley - Loburn Fault System. The southward dip direction of the Ashley Fault and its originally inferred location to the south of Starvation Hill does not explain the formation of Starvation Hill as conventionally as the Cust Anticline because the hill appears to lie on the footwall side of the inferred fault. Starvation Hill is discussed in detail as the focus of Part Three and its relationship with the Ashley - Loburn Fault System is discussed further in sections 3.1.3 and 3.2.2.

1.5.5 View Hill:

View Hill lies to the west of the township of Oxford and is thought to be associated with tilting and warping on the hanging wall of a thrust fault expressed by a well developed surface scarp immediately to the west. The inferred bend of the fault from close alignment with the Springfield Fault to a more easterly alignment is a major factor in the projected linkage between the Ashley-Loburn Fault System and Springfield Fault. View Hill is discussed in detail as the focus of Part Two.

1.5.6 Springfield Fault:

It is evident that a zone of west facing, predominantly thrust faults runs along the western margin of the Canterbury Plains, parallel to the range front but separate from the major range boundary faults that dip back beneath the mountain front. This zone is not well documented but some preliminary studies (Evans, 2001; Powell, 2001) have demonstrated late Quaternary activity on these faults.

The Springfield Fault crosses the headwaters of the Hawkins River, west of Sheffield (Evans, 2001) where it deforms three Quaternary surfaces of uncertain age, increasing in scarp height to approximately 30 m on the oldest surface. A possible

continuation of this fault to the southwest offsets distinctive units of volcanics (Tappenden, 2003) suggesting that this zone extends at least to the Rakaia River.

Northeast the strike of the fault would extend beneath Springfield township although no aligning scarp has been identified. However, it is approximately on strike with the fault lying west of View Hill, included in this study area. The question arises as to whether the latter is strictly a continuation of the Springfield Fault, or that they are separate, segmented elements of the same system. For the purposes of this study, the segment adjacent to View Hill will be referred to as the View Hill Fault (see Part Two for more detail).

1.5.7 Porters Pass – Amberley Fault Zone (PPAFZ):

The PPAFZ extends from the Rakaia Valley in the Southern Alps through to near the township of Amberley, close to the east coast of North Canterbury. Cowan (1992) describes the PPAFZ as comprising anastomosing faults and block folded and faulted mountains, forming a complex system of interconnected faults and folds that is evolving in response to dextral transpression at depth. To this extent, he suggests three main structural sub-domains within the larger Domain 3 (see section 1.4.3):

1) strike-slip domain in the west
2) thrust and reverse domain in the northeast

These two domains pass into:

3) northwest verging folds on the Canterbury Plains to the southeast.

The PPAFZ is a broad and complex system where the strain between the Australian and Pacific Plates released in this zone is diverse and disseminated in its evolving manifestations, not all visible from the surface. It is within close proximity to the boundary point of all three sub-domains that the main study areas of this thesis, View Hill and Starvation Hill, lie. This produces the possibility of a complex tectonic setting for the study areas.

1.5.8 Burnt Hill:

Other exposures of the Pre Quaternary Sequence above the Plains level occur north of the Waimakariri River, the two largest being Burnt Hill and the Chalk Hill area. Others are exposed in the river banks.

Located 9 km south of Oxford, Burnt Hill protrudes 100 m above the surrounding plains. The hill is formed from various sandstone units, a volcaniclastite unit, and capped by basalt flows of the Burnt Hill Group (see section 1.6.2.5) forming a prominent escarpment. The escarpment dips approximately 10° east-southeast.

Browns Rock, 3.5 km to the west, forms a basalt promontory on the north bank of the Waimakariri River. Chemical affinities suggest the rock is related to volcanics at Burnt Hill (McLennan, 1981). Extensive exposure of Torlesse basement forms the walls of the Waimakariri Gorge at the Waimakariri Gorge Road bridge. The close proximity of these three localities implies a thin gravel cover over the uplifted basement.

1.5.9 Chalk Hill Area:

A heart-shaped remnant of outcrops, 12 km west of Oxford, occurs between basement of the Torlesse Supergroup to the north and Quaternary gravels of the plains to the south. The sequence contains various sedimentary units including Broken River Coal measures and Oxford Chalk, the site of a chalk quarry. The sequence dips gently southwards with early and middle Tertiary basalt flows forming resistant ridges (McLennan, 1981). The basalts are of View Hill Formation, of the Eyre Group (see section 1.6.2.2)

1.6 Geology:

1.6.1 Basement:

The basement rock of the entire Canterbury Region, and extending into Marlborough and North Otago, comprises predominantly the Torlesse Supergroup. This Supergroup forms the Torlesse Terrane and is comprised dominantly of quartzo-feldspathic sandstones and argillite, informally referred to as greywacke.

The Torlesse Terrane contains three major belts of rocks, the Rakaia and Pahau subterranes separated by the Esk Head Melange, with ages ranging between Permian to Jurassic and late Jurassic to early Cretaceous respectively (Bradshaw, 1989).

The 8 – 10 km wide Esk Head Melange separates the Rakaia and Pahau subterranes, trending approximately north-northwest inland through North Canterbury, projecting under the Plains from the Okuku Valley just to the north of the study area.

1.6.2 Late Cretaceous to Early Quaternary Cover Sequence:

1.6.2.1 Introduction:

The following is a selected list of the major stratigraphic lithological groups in the North Canterbury region, (based on Browne & Field, 1985; Wilson, 1989; and Field et al., 1989) particularly those that are likely to be found in, or nearby the field area.

1.6.2.2 Eyre Group:

The oldest group is the Eyre Group which comprises a thick Upper Cretaceous to Upper Eocene sedimentary sequence. The majority of the sequence is a generally poorly-exposed, transgressive suite of sediments consisting predominantly of soft,

easily eroded sandstone. The remainder of the sequence consists of a variety of subordinate lithologies including conglomerate, siltstone, mudstone, greensand and interbedded basic volcanics. The Eyre Group unconformably overlies the Torlesse Supergroup.

It is within the Eyre Group that the View Hill Volcanics lie. The View Hill Volcanics crop out at and around View Hill, the focus of Section Two and in the Chalk Hill area. The volcanics consist predominantly of alkaline basalt flows, sills and pillow lava and are of Early Eocene Age. For further detail, see section 2.3.3.

1.6.2.3 Amuri Limestone:

Widely distributed throughout Marlborough and North Canterbury, the Amuri Limestone is the most widespread formation in Canterbury. Early to Mid Eocene in the north and younging to Mid Oligocene age to the south, it is distinctive white to pale green-grey, indurated, thin-bedded (centimetre to decimetre), fine-grained and bioturbated, however does not occur in the immediate study area.

1.6.2.4 Motunau Group:

The Motunau Group is widespread in North Canterbury, but predominantly in the east. The group was formed during a marine regression which took place between the Mid Oligocene to Early Quaternary. Limestones, greensands, siltstones and conglomerates represent the group which unconformably overlies the Amuri Limestone and interdigitates with the Burnt Hill Group.

1.6.2.5 Burnt Hill Group:

Found at Burnt Hill (see figure 1.7) and Miocene in age, the sequence consists largely of volcaniclastic and flow rocks, with subsidiary interbedded detrital formations. Depending on location, the group interdigitates with the Motunau Group

or lies unconformably on Amuri Limestone, and is unconformably overlain by late Quaternary outwash or Motunau Group.

1.6.3 Late Quaternary Deposits:

1.6.3.1 Introduction:

"The Canterbury Plains are a series of coalescing low-angle alluvial fans built by major rivers during successive Quaternary glaciations when huge quantities of gravel were poured into the river systems by glaciers that filled the main valleys in the Southern Alps" (Wilson, 1989).

Late Quaternary sediments related to glacial and interglacial periods overlie the Cretaceous to early Quaternary cover sequence. Climatic changes resulted in cycles of coastal transgression and regression affecting what is now approximately the eastern third of the plains in North Canterbury, causing an accumulation of swamp, estuarine, lagoonal and beach deposits intermingled with the alluvial fans.

Further inland, the younger four cycles of glaciation are assumed to be associated with the aggradation events that have been mapped in the study area (Wilson, 1989). Traditionally the nomenclature of these gravel units has been applied both to the contained gravels as a formational unit and to the overlying surface. These are described below, based on Brown & Wilson (1988) and the map of Wilson (1989), shown in part in figure 1.8.

1.6.3.2 Woodlands Formation:

It forms the highest aggradation surface on the north bank of the Waimakariri River, extending intermittently to the Eyre River. The surface is gently undulating, with poorly drained depressions and is commonly blanketed by loess deposits up to 6 m thick. The formation is thought to be greater than 100 m thick in places and deposited around 150,000 years ago.

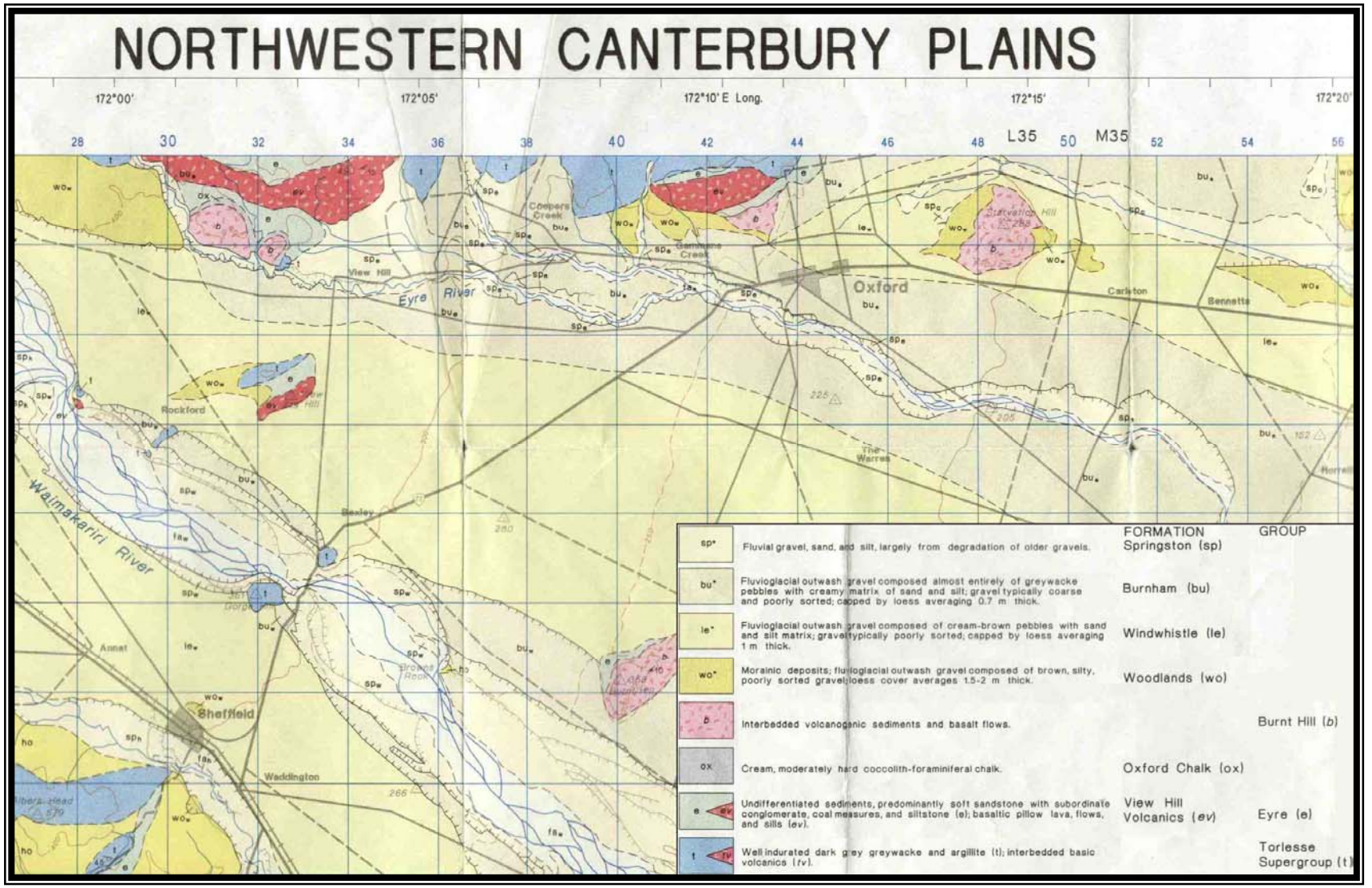

Figure 1.8 – *Selected area & key of the Wilson (1989) map: Quaternary geology of Northwestern Canterbury Plains. Grid = 1 km^2.*

1.6.3.3 Windwhistle Formation:

It is slightly undulating due to the presence of faint ancestral drainage patterns. The surface is covered by loess deposits of 0 to 4 m thick, averaging 1 m and tending to be thickest on the banks of major rivers. The formation is thought to be locally greater than 80 m thick and deposited about 70,000 to 40,000 years ago.

1.6.3.4 Burnham Formation:

The identification of the formation is extremely difficult as its superposition on the Windwhistle Formation is rarely seen. The formation occupies large areas of the central Canterbury Plains, however there are no simple diagnostic features to help separate Burnham Formation from either the later Springston deposits or older Windwhistle deposits.

The Windwhistle-Burnham interval would seem small compared to the Woodlands-Windwhistle interval, and the total volume of Burnham deposits, despite covering a large area, is much smaller than the volume of earlier sets of outwash. Loess thickness ranges from 0 to 3 m and the Burnham Formation is thought to have been deposited between 27,000 to 15,000 years ago.

1.6.3.5 Springston Formation:

Comprising a thin veneer of gravels and silts that cap all post-Burnham degradational terraces, the Springston Formation represents fluvial deposition that followed glacial retreat at the end of the deposition of the Burnham Formation. It includes all postglacial deposits, excluding those of present-day river channel and flood plains. The formation is thought to have deposited in the last 14,000 years.

1.6.4 Volcanics:

The stratigraphic relationships and age of various isolated volcanic units exposed in outliers across the Canterbury Plains and foothills presents some correlation problems, notably on Starvation Hill, and the available stratigraphic information is singled out and summarised below. In many places throughout Canterbury, localised volcanics are coeval with lateral sedimentary units, frequently limestones, which they may replace in the sequence and may not be distinguishable as reflectors in seismic profiles.

McLennan's (1981) Cretaceous – Tertiary study included nearby Burnt Hill, View Hill and outcrops around Chalk Hill. These three areas contain igneous outcrop, predominantly extrusive although intrusive bodies do occur. Of note these include:

- View Hill Basalt Member containing pillow lavas, of late Paleocene to early Eocene age, found at View Hill.
- Oxford Basalt of Oligocene age found in the Chalk Hill area.
- Bluff Basalt and Harper Hills Basalt, both of late Miocene age and found at Burnt Hill.
- Also various tuff and volcaniclastite units have been mapped in these areas.

McLennan (1981) concludes the late Cretaceous – Miocene period in inland Canterbury, particularly at Chalk Hill and Burnt Hill, appears to be characterised by a sequence which broadly represents a transgression – regression cycle but in detail contains many, often local, unconformities and volcanic phases.

1.7 Geomorphology of the North Canterbury Plains:

Loess stratigraphy provides a means for regional correlation of present and buried geomorphic surfaces (Tonkin and Almond, 1998). The Plains of North Canterbury contain extensive river systems and a variety of topographical features. These topographic features and margins of river boundaries are often sites of substantial

loess accumulation of several meters thickness. The production of loess occurs from and during periods of fluvial aggradation and degradation and is predominantly wind blown silts, sourced from overbank sediments on the floodplain.

Loess is still accumulating in the Canterbury Region, and typically forms a loess wedge on the south side of the major rivers, as a consequence of the prevailing northwesterly winds (Ives 1973). This loess has an estimated basal age of 13±2 ka (Berger et al. 2001). In North Canterbury commonly three loess units have been recognised on the basis of a soil stratigraphy including the surface and buried soils (Trangmar, 1987).

1.7.1 Geomorphic Surface Definition:

A surface is a two-dimensional plane. It has width and length, but no thickness. A geomorphic surface is a part of the land's surface defined in space and time (Ruhe 1969); a landform or group of landforms that represent an episode of landscape development (Balster and Parsons, 1968); a part [of the Earth's surface] that has been studied and mapped (Daniels et al., 1971). A geomorphic surface is either constructional, or erosional, or both. All erosional surfaces during their formation grade to a constructional surface (Daniels and Hammer, 1992).

Unstated but implied in these definitions is the concept that pedogenic features occur in materials immediately underlying a geomorphic surface (Gile et al., 1981).

1.7.2 Late Pleistocene Loess Chronology:

A loess section in North Canterbury containing three Late Pleistocene loesses has been TL dated (see figure 3.14) and appear to correlate with a single loess unit at dated Akaroa sites on Banks Peninsula and near Timaru (Berger et al. 2001). This may reflect a proximal – distal relationship. Loess stratigraphy is currently being studied on both Banks Peninsula and North Canterbury (P. Tonkin, pers. comm.).

1.7.3 Evolution of a Loess Landscape:

The evolution of a loess landscape as shown in figure 1.9 is a model illustrating the evolution of a loess downland landscape through successive episodes of loess deposition and erosion. The episodes of loess deposition are considered to relate to major episodes of fluvial aggradation that are apparently synchronous with climatic events resulting in glaciation in the mountains of the South Island (Suggate 1990).

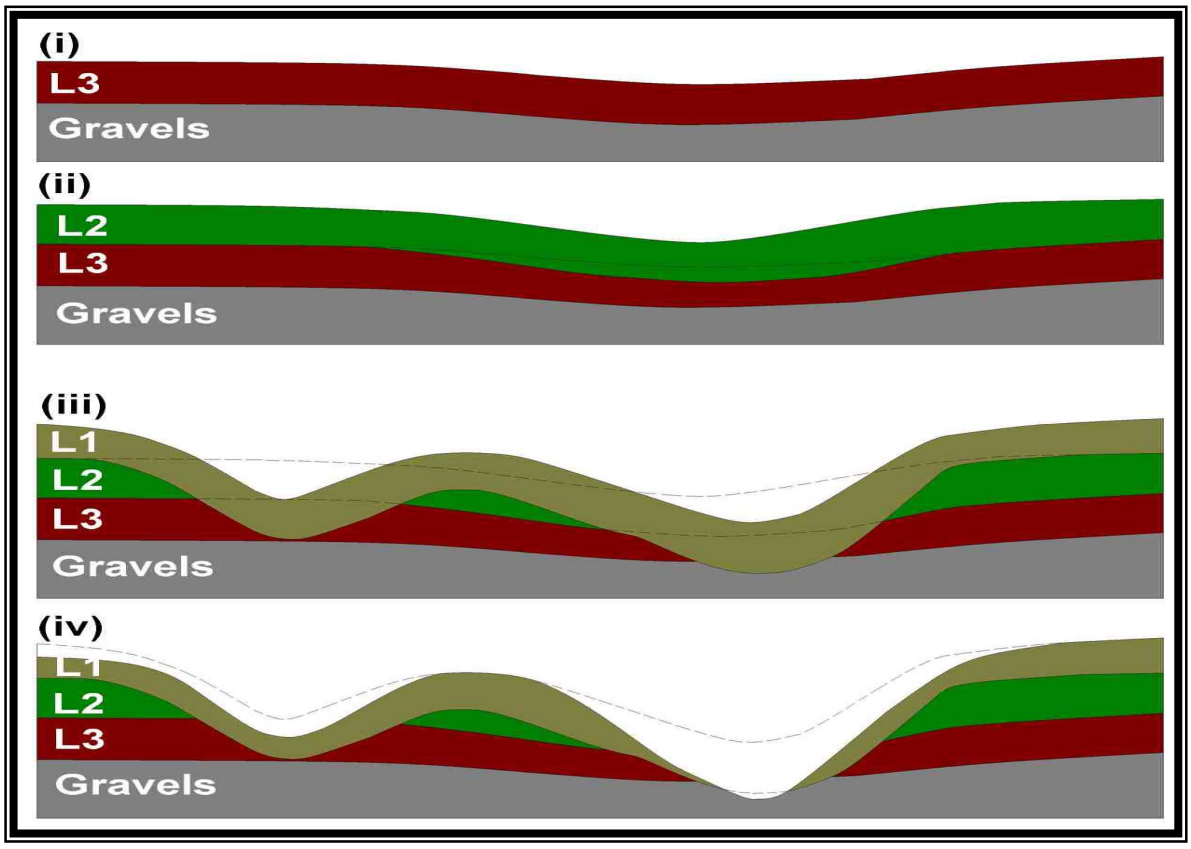

Figure 1.9 – *Hypothetical Evolution of a Loess Downland Landscape.*
Original deposition of the oldest loess unit (L3) blanketing gravels of little relief (i). Deposition of the second loess unit (L2) following an interval of channel incision into L3 (ii). Deposition of the youngest loess unit (L1) after further channel incision into L2 & L3 (iii). Continued erosion of the loess to form the Downland landscape (iv). Fluves are assumed to approximately stay at same location and elevation, while interfluves build up.

Between periods of aggradation, the rivers have responded to the regional tectonic setting, which in the inner parts of the plains is one of net tectonic uplift, and this has resulted in the formation of flights of aggradational and degradational terraces.

There is a general relationship between the age of the terrace surface on the alluvial gravels (Quaternary Formations Woodlands - Wd; Windwhistle - Ws; Burnham - B; and Springston - Sp) and the thickness and the number of loess units as illustrated in figure 1.10. The relationship of the underlying alluvial gravels is unclear and the vertical scale is exaggerated.

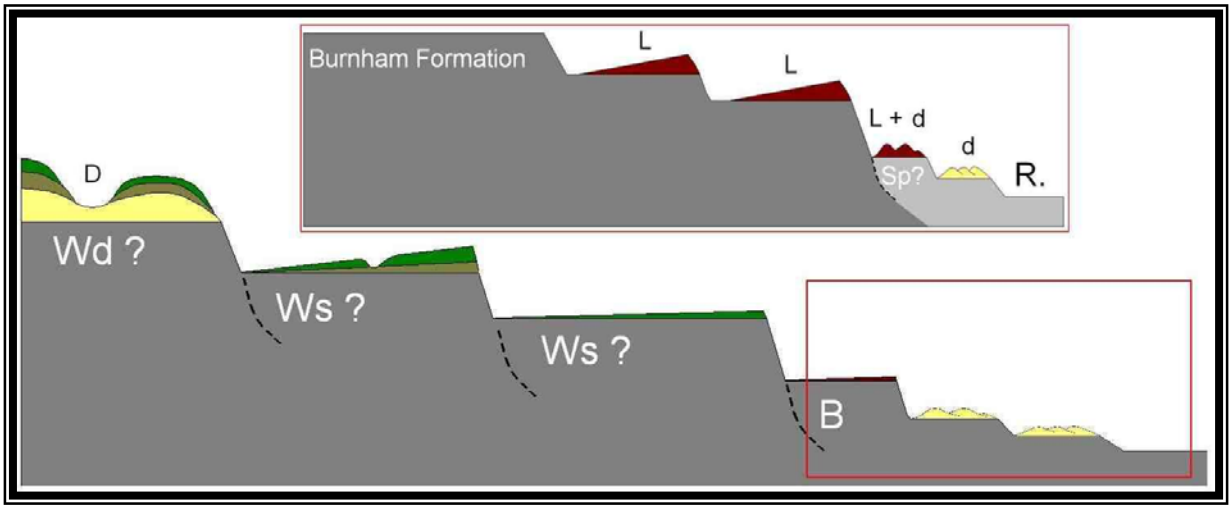

Figure 1.10 - *Loess stratigraphy on a flight of terraces and older downland landscapes. Riverbed (R) Dune Deposits (d) Loess deposits (L) & Downlands (D). Formations likely in the study area include Woodlands (Wd) Windwhistle (Ws) Burnham (B) and Springston (Sp). This situation is an approximation of the current North Canterbury Rivers such as the Waimakariri, where the river is currently deeply incised, due to a current degradational episode, and a series of higher terraces remain, of which some have significant loess cover where not eroded. The relationship of the underlying gravels is unclear.*

1.7.4 Use of Loess Stratigraphy in Determining Tectonic Deformation of a Landscape:

The soil and loess deposits can be used to assign relative ages to geomorphic surfaces and buried geomorphic surfaces. The latter may include the surface of the underlying gravel formation. With correlations of ages of loess dated elsewhere, and those currently under study, the potential exists for approximate ages to be assigned to geomorphic surfaces and therefore the tectonic deformation of landscapes in North Canterbury.

1.8 Modern Soils and Soil Patterns:

The soil map of North Canterbury (Kear et al., 1967) shows a complex pattern, shown in part in figure 1.11a & b. This pattern of soils reflects the depositional history of the Canterbury Plains and the associated sequence of fluvial landforms, from the Pleistocene to Present. The soils are divided into subhumid and humid groups, reflecting the climatic gradient from east the west across the plains, related to the rainfall evaporation-transpiration. The soils on the Downlands, are commonly developed in quartzose-feldspathic loess, and there maybe one to three loess units which are typically underlain by older fluvial gravels or by bedrock. The Downlands underlain by gravels are the remnants of older fluvial aggradation gravels and their associated dissected terrace landforms (see figure 1.9).

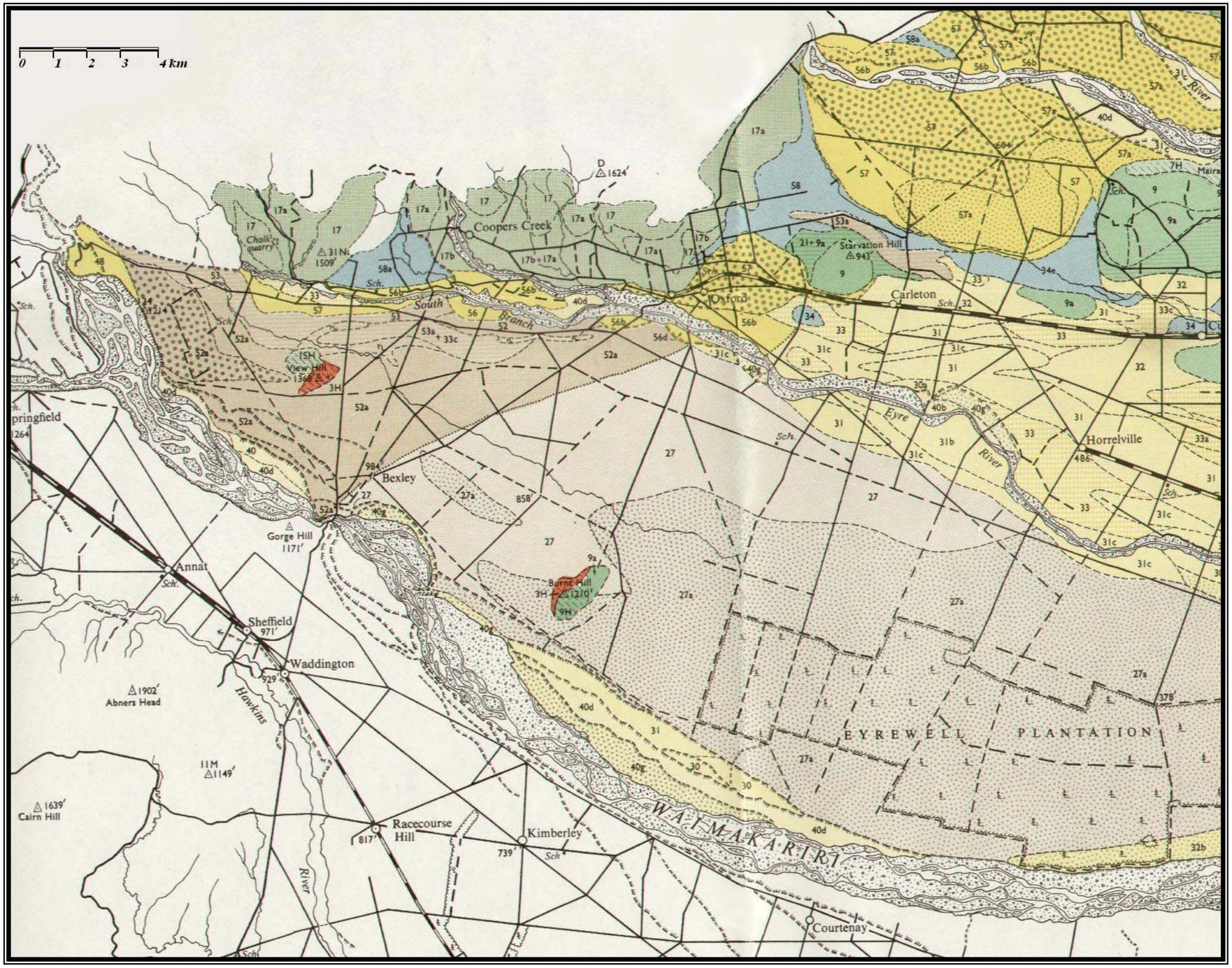

Figure 1.11a – *Soil Map of North Canterbury.*
Section of "Soils of the Downs and Plains, Canterbury and North Otago, New Zealand" modified from Kear et al. (1967), see figure 1.11b over page for key.

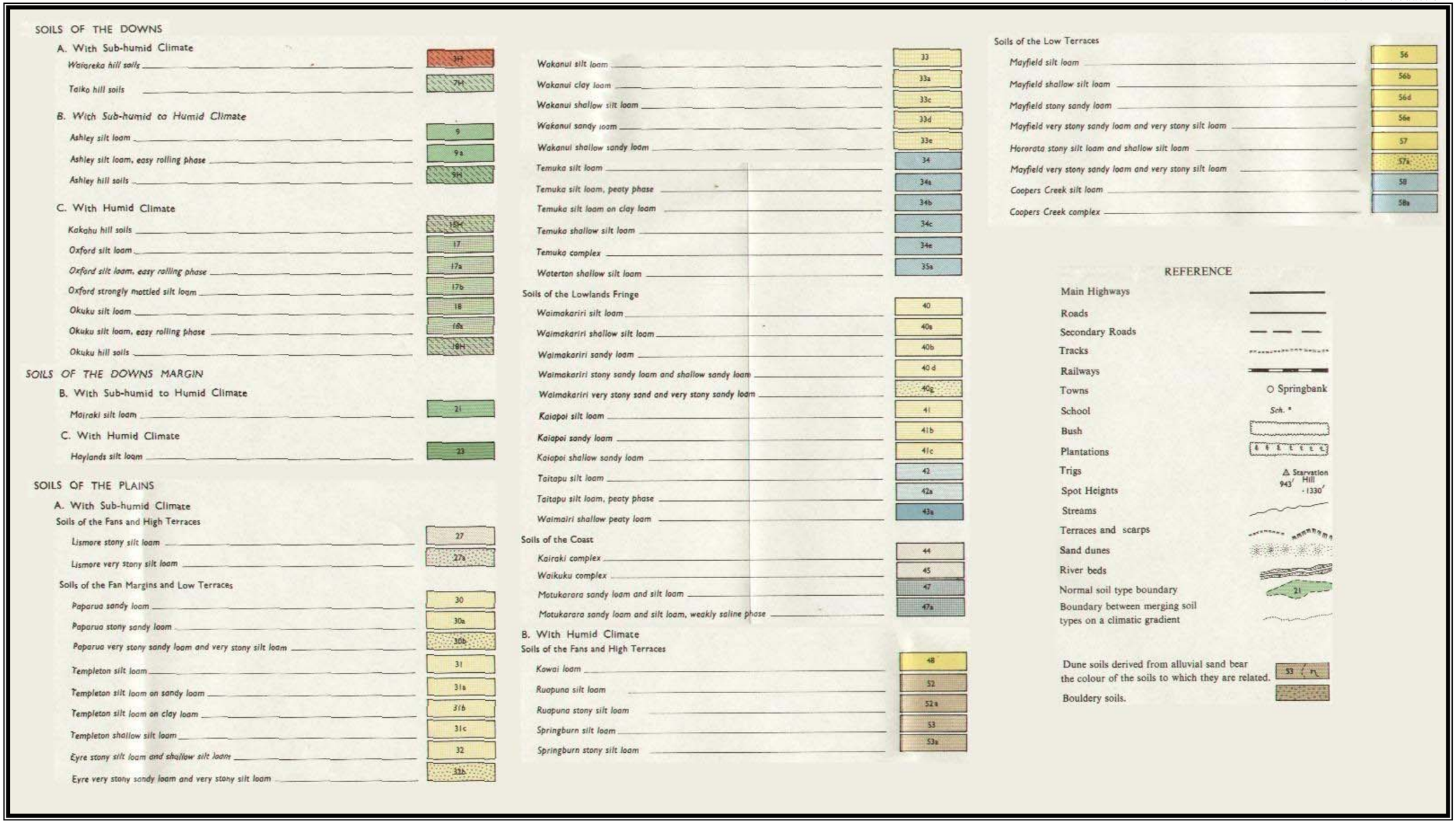

Figure 1.11b – *Key of Soil Map of North Canterbury.*
Section of "Soils of the Downs and Plains, Canterbury and North Otago, New Zealand" map key modified from Kear et al. (1967).

1.9 River Systems in North Canterbury:

1.9.1 Introduction:

The field area is located between two major rivers, the Waimakariri to the south and the Ashley to the north. Between these lie smaller rivers and streams (see figure 1.7 for river locations). A brief description of the various significant waterways is given below:

1.9.2 Waimakariri River:

The Waimakariri is one of the larger braided rivers in New Zealand. Its flows are controlled by the weather in its upper basin (Waimakariri Irrigation Ltd, 2000). In the field area, the river flows from west to east, heading across the plains, to its mouth north of Christchurch. The river has always been a flood menace to Christchurch, control measures have been emplaced in the lower reaches to restrain it within acceptable lateral limits (Wilson, 1989).

Inland, the river is incised and a significant feature of the river landscape is the Waimakariri Gorge, at the site of the Waimakariri Gorge Road bridge, where the river cuts through uplifted Torlesse basement rock. Upstream of the gorge bridge, the river is incised into Burnham or older gravels leaving a flight of terraces predominantly on the north bank and in general the evidence points to slip-off and southward migration of the river.

1.9.3 Ashley River:

The Ashley is the second major river in the field area, located to the north of the Cust Anticline, however this was not always the case. The river formed the channel through which the Cust River now flows, prior to the growth of the Cust Anticline, during which, it was diverted north to its current position (Wilson, 1988; Cowan, 1992; Sisson et al., 2001; Estrada, 2003) where it now flows out to the coast, north

of Rangiora and Woodend. The river flow depends greatly on snowmelt of the nearby hills, subsequently it regularly dries up over summer above the Ashley bridge at Rangiora (Waimakariri Irrigation Ltd, 2000).

1.9.4 Cust River:

The Cust River runs from the foothills behind Oxford, north of Starvation Hill, through the Cust valley and then into the Cust Main Drain. This drain was built in 1862 to drain the Rangiora Swamp. When the drain was enlarged in 1868, it accidentally captured the Cust River and the drain is now this river's main course (Waimakariri Irrigation Ltd, 2000). The Cust flows through part of an ancestral channel of the Ashley, active approximately 20,000 years ago (Cowan, 1992), to the south of the Cust Anticline and flows into the Waimakariri River near the coast.

1.9.5 Eyre River:

The Eyre is an intermittently flowing river with much of its flow seeping into the resorted gravels (Wilson 1988). Dry for much of the summer, its beds and banks are covered with gorse and broom (Waimakariri Irrigation Ltd, 2000). The Eyre extends from the eastern foothills of the Southern Alps to the west of Oxford, passing south of Starvation Hill, where it flows across the plains and into the Waimakariri River.

"The significant difference between these three rivers, the Ashley, Cust and Eyre, and the Waimakariri River, are their east coast catchments. While hot north-westerly winds are drying out the Waimakariri Plains, the Waimakariri River is often swollen by nor-west rain or snow-melt from its mountainous catchment" (Waimakariri Irrigation Ltd, 2000).

1.9.6 View Hill Stream:

View Hill Stream is a minor stream running to the north of View Hill and flowing east where it becomes diverted into an irrigation scheme, flowing close to its original path, and eventually making its way into the Eyre River.

PART TWO – VIEW HILL:

2.1 View Hill Introduction:

The View Hill structure lies approximately 12 km west of the township of Oxford, which is ~45 km northwest of Christchurch. Here two topographically prominent ridges emerge from the Canterbury Plains, see figure 2.1 and figure 1.7. The northwest ridge rises ~70 m above the Canterbury Plains to a height of 409 m and the southeast ridge rises ~90 m to a height of 419 m with a lower saddle between them. The entire elevated topography covers an area of approximately 1.2 km^2.

2.2 Geology and Tectonic Setting Overview:

The View Hill structure is a prominent feature of the region. The structure consists of Torlesse Super Group basement rock to the northwest forming a ridge, and to its southeast, a View Hill Basalt ridge dipping moderately southeast. A saddle-like area of softer but unexposed lithology, considered to be undifferentiated sedimentary rock of the Eyre Group separates the two ridges (McLennan 1981), see figure 2.1.

There is a distinctive geomorphic feature inferred to be a fault scarp, located around the northwest of the hill, striking northeast and uplifted on the southeast side. The scarp is inferred to be the result of a southeast dipping thrust fault, responsible for the occurrence of the Torlesse basement rock protruding from the surrounding plains to form the northwest ridge of View Hill. For the purposes of this study, the fault segment adjacent to View Hill will be referred to as the View Hill Fault.

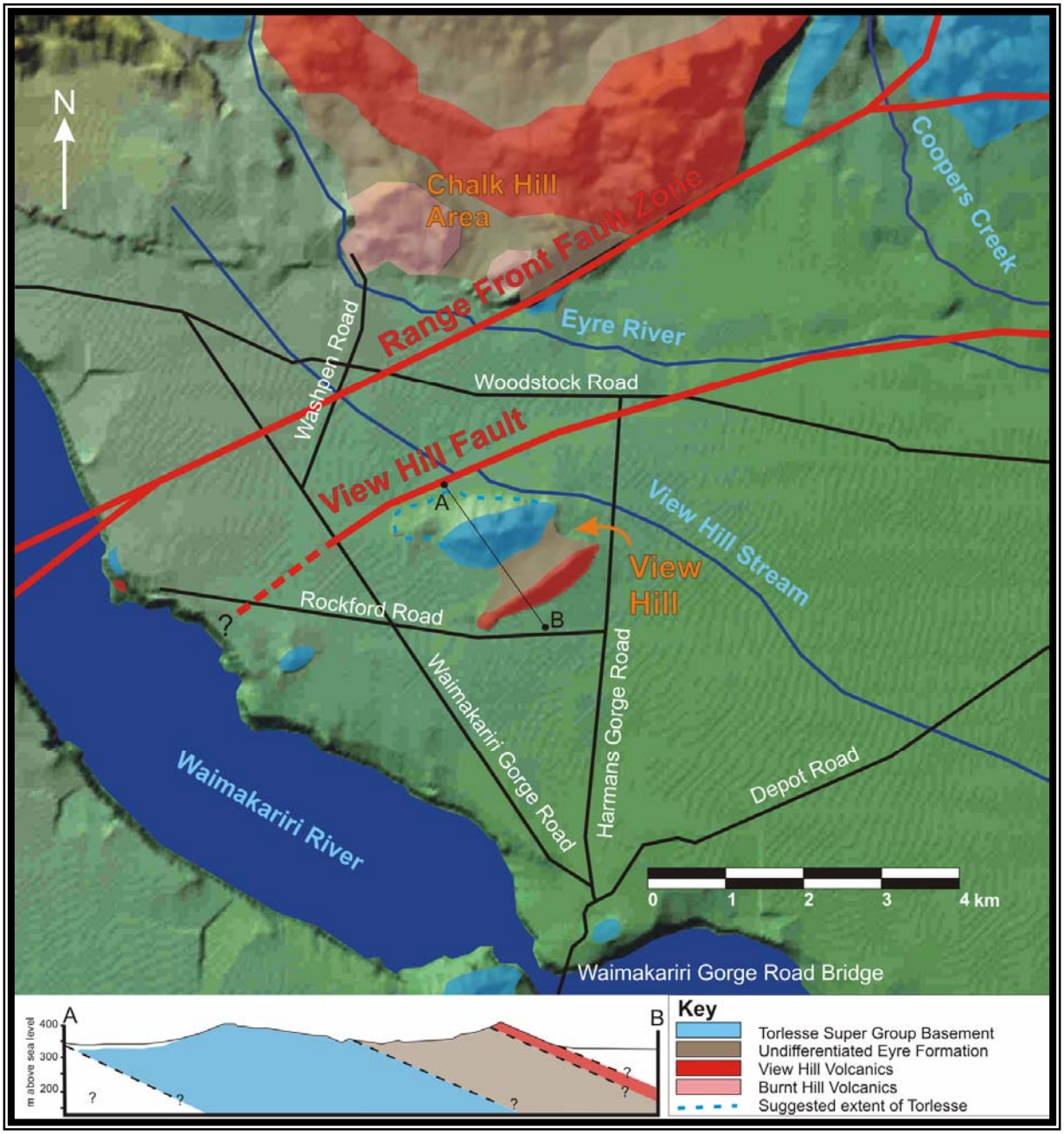

Figure 2.1 – *View Hill and surrounding tectonic setting.*
View Hill comprises two ridges (see text). Significant and main roads are shown. View Hill geological boundaries and cross-section modified from McLennan (1981). Other selected Geological outcrops from Wilson (1989). Location of fault lines are approximate only. Southeast dip of View Hill Fault in cross section approximate only. Dip of Range Front fault inferred to be to the northwest.

The Torlesse crops out again along strike, approximately 2.5 km southwest on the north bank of the Waimakariri River. To the southeast, Torlesse is again uplifted above the level of the plains to form a gorge at the site of the Waimakariri Gorge

Road bridge. The only other exposure of note is an isolated outcrop in the bed of the Waimakariri River, upstream of the southwest projection of the View Hill Fault.

Simple tilting and uplift of basement and cover may account for the basalt ridge, although the space occupied by the assumed, approximately 200 m thickness of the Eyre Group sequence is relatively thin (see figure 2.1 – cross section) and could be condensed by the presence of a second thrust splay.

Patchy outcrops of the Cretaceous-Tertiary cover rocks occur adjacent to the study area at Coopers Creek, a tributary of the Eyre River to the northeast of the Chalk Hill area (north of figure 2.1), and along the range front in the Chalk Hill area, caught up in the range front fault complex. The only other exposure of note is an isolated outcrop of basalt in the bed of the Waimakariri River, upstream of the projection of the View Hill Fault, at a lower elevation than the nearby Torlesse outcrop.

Further to the northwest of View Hill, a second fault is inferred, forming the southwest projection of the of the main range front system. In general the elements of this system are assumed to dip northwest under the steep-range front scarps and are uplifted on the west side. The interaction of this and the View Hill Fault as they appear to converge to the south is poorly understood, but there is some indication of subtle differential elevation of the topography along the inferred strike of this system.

To the southwest, the View Hill Fault appears to align with the Springfield Fault (see figure 1.7 and section 1.5.2). However, the scarps of both faults die out, leaving a sizable distance between, such that inferences as to whether or not the View Hill Fault is strictly a continuation of the Springfield Fault, or is a separate, segmented element of the same system, becomes ambiguous.

To the east, the fault is projected to connect with the Ashley-Loburn Fault System, however the Starvation Hill Structure lies approximately between the two and its tectonic setting and likely connection with the View Hill Fault is examined further in Part Three.

2.3 Structure of the View Hill Fault and Subsurface Geology:

2.3.1 View Hill Fault Structure, Swiss Seismic Line Expectation and Constraints:

During August of 2003, a Swiss research group from ETH Zurich undertook a seismic survey along Waimakariri Gorge Road, from near Washpen Road to past the intersection with Rockford Road (see figure 2.1). The results of the survey would hopefully show the structure underlying the fault scarp and warping or back-tilting to the southeast, potentially from backthrust structures.

As an arrangement for helping them with the surveying, there was an agreement that results of the survey, including processed seismic data would be passed along for inclusion in this study. The assumption that this data would be available was a factor in including View Hill as part of this project. Unfortunately, the group have been unable to find time and/or resources to process this line, subsequently it is not included in this study, and has limited the quantification which might have been attempted from topographic analysis of the ground deformation, if the subsurface structure were better constrained.

The seismic line would have allowed significant insight into the characteristics of the fault shaping View Hill and producing the scarp on its northwest side. In particular allowing for some control on the dip and shape of the fault plane, to allow for the conversion of throw into net slip, and modelling hanging wall deformation.

Connection of the View Hill Fault with the Springfield Fault to the south (see section 1.5.2) is currently ambiguous due to the significant distance between surface fault traces. A second seismic survey was undertaken on the south side of the Waimakariri River, parallel to the survey on the north side, with the intention of assisting in the projection of the View Hill Fault. However results of this survey have also not been provided by the group for inclusion in this study.

2.3.2 Torlesse Basement and Cover Rocks:

The Torlesse basement exposed at View Hill suggests that fault displacement is significant, as the basement rock is typically overlain by a significant thickness of Cretaceous and Tertiary cover sequence. Although the undisturbed thickness is not known conclusively for the inner areas of this part of the basin, it would also include a variable thickness of gravels of glacial outwash in this area of the North Canterbury Plains.

McLennan (1981) acquired a strike and dip of the Torlesse basement, shown on her map to be striking northwest and dipping 53° to the southwest, but his would not be of significance because of the major unconformity between the basement and cover rocks.

McLennan (1981) defines the saddle-like area between the Torlesse ridge and the Basalt ridge as undifferentiated sedimentary rock of the Eyre Group. Her cross section assumes parallelism of the basal unconformity with the dip of the basalts. At the time of her study, the View Hill fault was not recognised and presumably the dip was attributed either to folding or more distant faulting. At some stage there may have been an anticline on the hanging wall, but at this level of exposure, it is evident that there is no space for preservation of a northwestern limb between basement outcrop and the fault scarp.

During the activity of the river, at the time the surrounding gravels of the View Hill area were emplaced, it is evident that the western side of the preceding scarp of the View Hill Fault was eroded. This erosion occurred well behind (southeast of) the fault outcrop to cut back into Torlesse rocks exposed close to the scarp along the front of View Hill and along strike near the north bank of the Waimakariri River. The present structure is therefore a simple backtilted sequence on the hanging wall of the View Hill Fault.

2.3.3 Basalts:

McLennan (1981) describes the basalt ridge as comprising part of the White Stream Formation of the Eyre Group (see section 1.6.2.2). The formation is divided into two members, the first is the View Hill Basalt member found at View Hill. The second is the Wharfedale member comprising sediments of shallow marine strata which are interbedded with the View Hill Basalt member in outcrops in the Chalk Hill area approximately 2 km north of View Hill (see figure 2.1).

The View Hill Basalt consists of dark-grey to medium brownish grey basalts of variable petrology and chemistry. There is a variety of structures within the member with pillows being the most common, although columnar jointing is also widespread. Where basalt overlies Wharfedale member sediment, baking of the top margin of the sediment has occurred.

The variable thickness of the View Hill Basalt member as a whole and the abundance of rubbly bases, glassy tops and lenticular units show it is dominantly of extrusive rather than intrusive origin. Pillow structures indicate extrusion was submarine and this is supported by the thin sandy lenses and fossils incorporated between flows.

The age of the View Hill Basalt member is inferred to be late Cretaceous, although outcrops of flows found in the Eyre River indicate some residual volcanism carried on into the Eocene. The flow-banded columnar jointing of these outcrops also suggests, either that locally water depths were very shallow (possibly receding) with submarine basalts being overlain by subaerial ones, or that late stage sill intrusion occurred. The fossiliferous components of the limestones of the Wharfedale member generally indicate shallow marine conditions with relatively clear, well-oxygenated warm waters, thus an inner shelf environment below wave base is envisioned.

The scarcity of fossils and the abundance and coarseness of the tuffs in the east of the Chalk Hill area, compared to those to the west indicate that the west was much less affected by volcanism and is thus inferred to have been further from the main volcanic vents, possibly in the direction of Starvation Hill.

2.3.4 Implications:

Some constraint as to subsurface structure can be made on the basis of available outcrop. The relative elevations of the basalt outcrops low on the bank of the Waimakariri River at ~300 m and on View Hill at ~419 m infer a minimum total throw of ~120 m.

Downstream the pattern is repeated with cover rocks exposed again at Burnt Hill ~10 km to the east and Torlesse basement rock exposed at an elevation of ~300 m near the Waimakariri Gorge Road bridge. It therefore seems likely that these thrust faults are not steep and may flatten at depth. This throw would translate into a net slip substantially larger than the elevation difference, but cannot be quantified further without subsurface data. Any indication of the fault dip, and if it flattens, would constrain the thrust model and require some sort of termination at each end.

The thickness of the Eyre Group at View Hill is significantly less than inferred at other locations around the Canterbury Plains. The Eyre Group unconformably overlies the Torlesse Supergroup, potentially explaining the relatively thin deposit as resulting from the Torlesse having been uplifted prior to deposition of the Eyre Group.

Two other possible explanations for the comparatively thin sequence of Eyre Group include this area being the edge of Eyre Group deposition, which was thinner than elsewhere on the plains. Alternatively, tectonic thinning of the Eyre Group by overthrusting of the basalt unit on a second splay of the View Hill Fault may have occurred.

2.4 Geomorphology:

2.4.1 View Hill – Two Ridges:

The basalt ridge (figure 2.2) is scattered with vegetation of gorse, brush and occasional cabbage trees, making observations of detail difficult. The ridge is approximately linear, trending SW – NE and the basalt forms a dip slope to the southeast. The northeast end of the ridge slopes steeply down to the surrounding plains, compared with the gentle termination of the southwest end.

Figure 2.2 - *Views of View Hill.*
Looking northwest up the dip slope of the the basalt ridge (a). Looking northeast, along the west side of the basalt ridge with air gap (b). Looking southwest at the basalt ridge (c). Looking north at the saddle-like area between the Torlesse hill (left) and basalt ridge (d).

The Torlesse ridge (figure 2.2d, left side) is more sparsely vegetated, steeper sided and more rounded in topography and expanse than the basalt ridge. The Torlesse ridge is more bulbous than the basalt ridge with erosional gullies having cut into the northwest face.

2.4.2 Terrace Sequence of the Waimakariri River:

Figure 2.3 shows the terrace sequence of the Waimakariri River to the southwest of View Hill. The terraces suggest the river once flowed around the base of View Hill, as it avulsed over the Plains. The river is the largest to affect the North Canterbury Plains, currently lying ~3 km southwest of View Hill.

The river is responsible for the prominent series of terraces on its north bank. There are also a series of less prominent features between these terraces and View Hill. These are possibly younger drainage channel features, but have the appearance of relicts of older channels of the Waimakariri River, and of a less prominent flight of terraces, indicating the onset of abandonment and degradation of this upper surface.

The topography formed by the river during the time it occupied the high surface is distinguished by a faintly preserved, braided channel pattern, that is not evident where the surface has been degraded by younger stream activity north of View Hill. This is shown in figure 2.3 inset, where former river channels crossing the scarp of the View Hill Fault have not been diverted significantly by the scarp. This suggests the scarp formed after the channels, and no notable lateral movement occurred. The channels appear to be truncated by the approximately east – west lying terrace, which, when followed east, cuts in towards View Hill, then curves south around the southern end of the basalt exposure.

The highest surface of gravel against the southwest corner of View Hill was interpreted by Wilson (1989) as a remnant older Woodlands surface, but an alternative interpretation will be discussed in section 2.5.2.

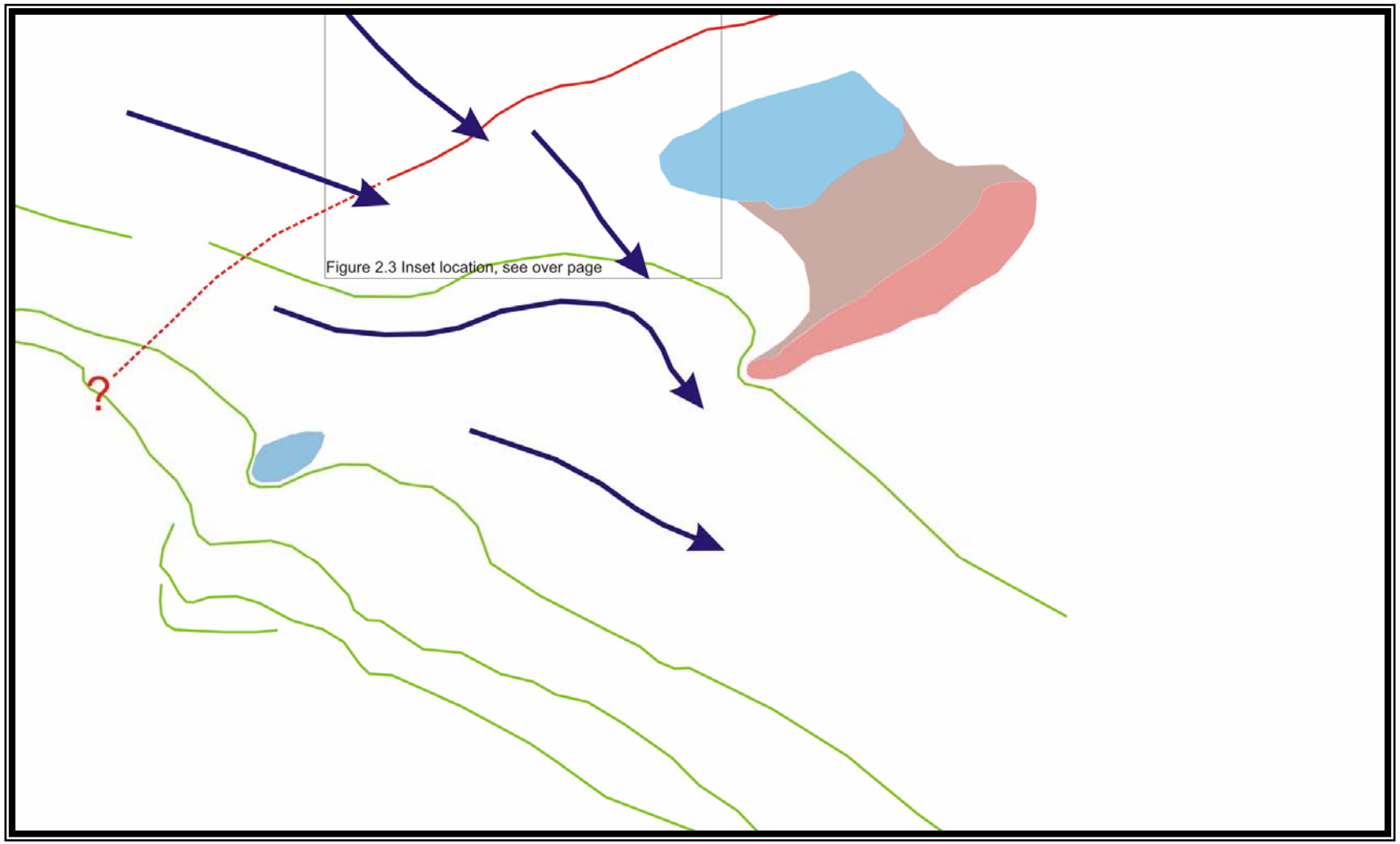
Figure 2.3 Inset location, see over page
?

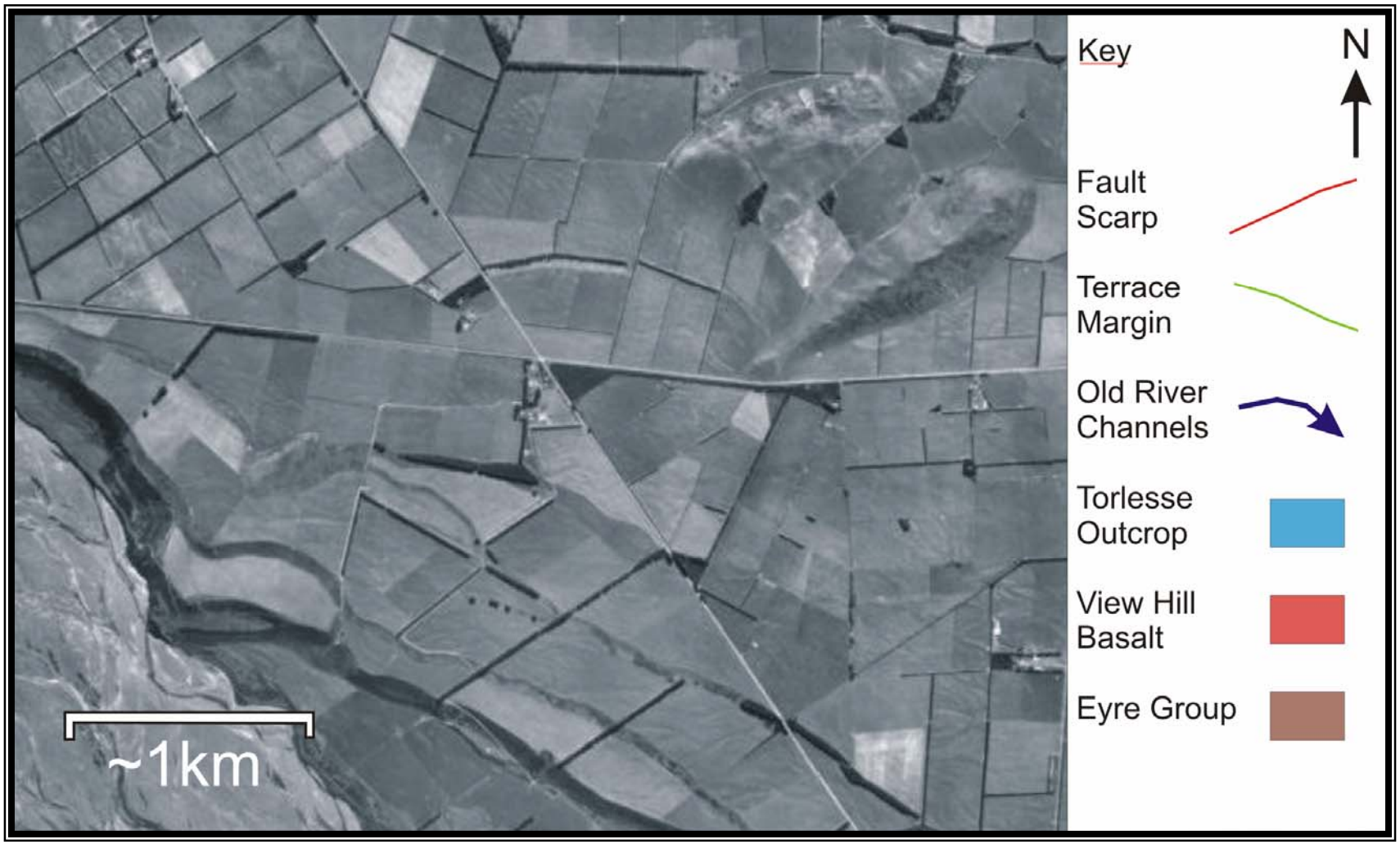

Figure 2.3 – *Waimakariri River Terrace Sequence.*
Note the terraces' predominance on the north side implying channel location slipping off southward in 'recent' times, possibly a result of growth of View Hill or more regional tilting. Note pattern of old braided channels south of View Hill.

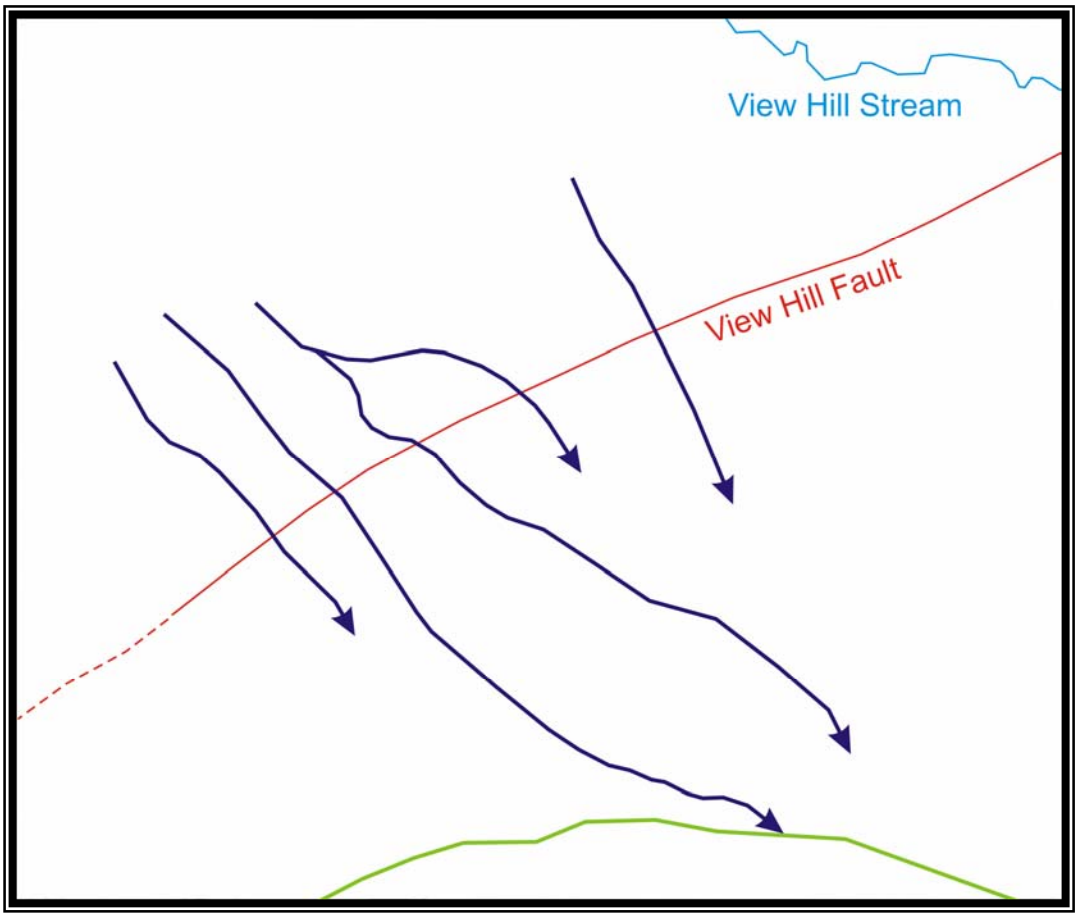
View Hill Stream
View Hill Fault

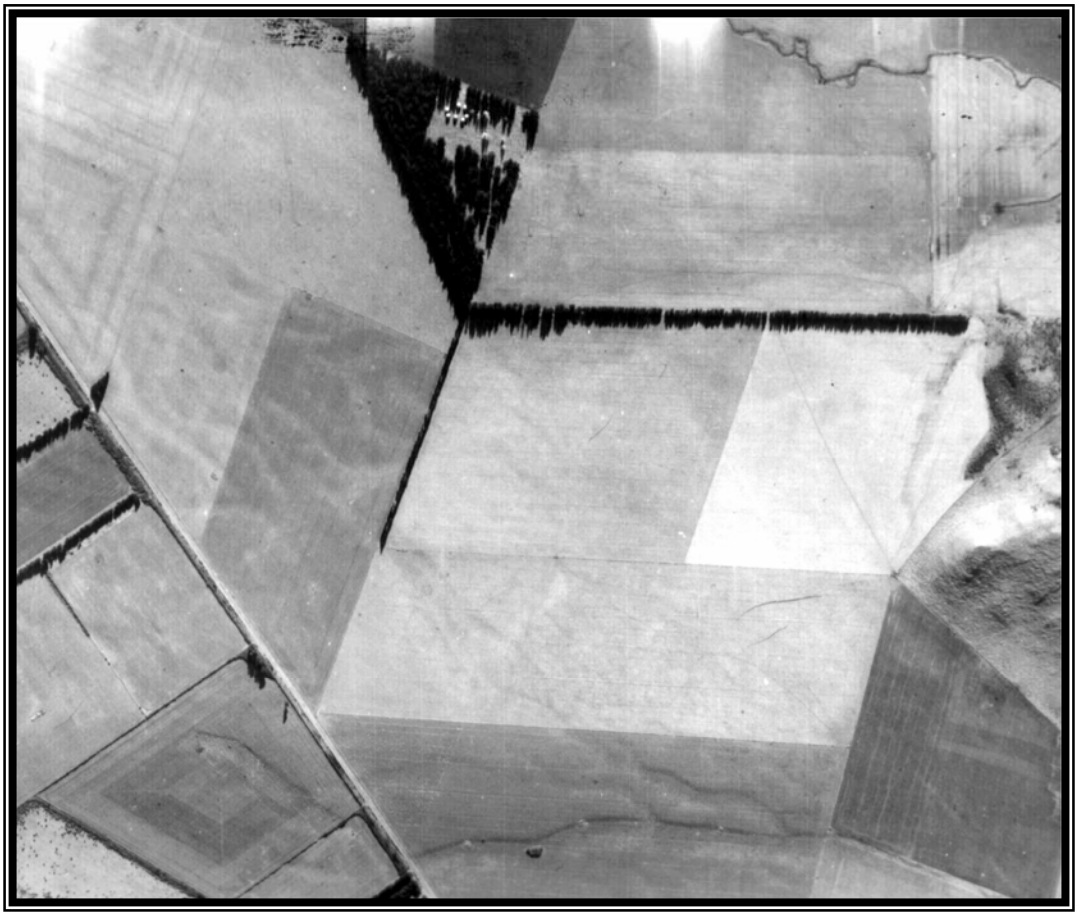

Figure 2.3 inset – *Close up view of old river channels crossing the View Hill Fault Scarp (See Figure 2.3 for location). Photo is from an older set of Aerial Photographs.*

2.4.3 Degradation of Burnham Formation Surfaces and Downcutting by View Hill Stream and Eyre River:

At the height of the last glacial maximum, aggradation of the Waimakariri River was assumed to be building a substantial fan over the entire area surrounding View Hill, to be joined by coalescing fans from other rivers out of the range front. However, as the Waimakariri River became entrenched to the south of View Hill (see section 2.2.2 above), the Eyre River remained as a more locally sourced, minor river perched on the surface. The Eyre has not been able to maintain the same rate of downcutting as the larger Waimakariri River, but has worked across the surface, apparently slipping off northward (see figure 2.4), while the Waimakariri River was migrating south, suggesting that uplift was occurring centred on the View Hill structure.

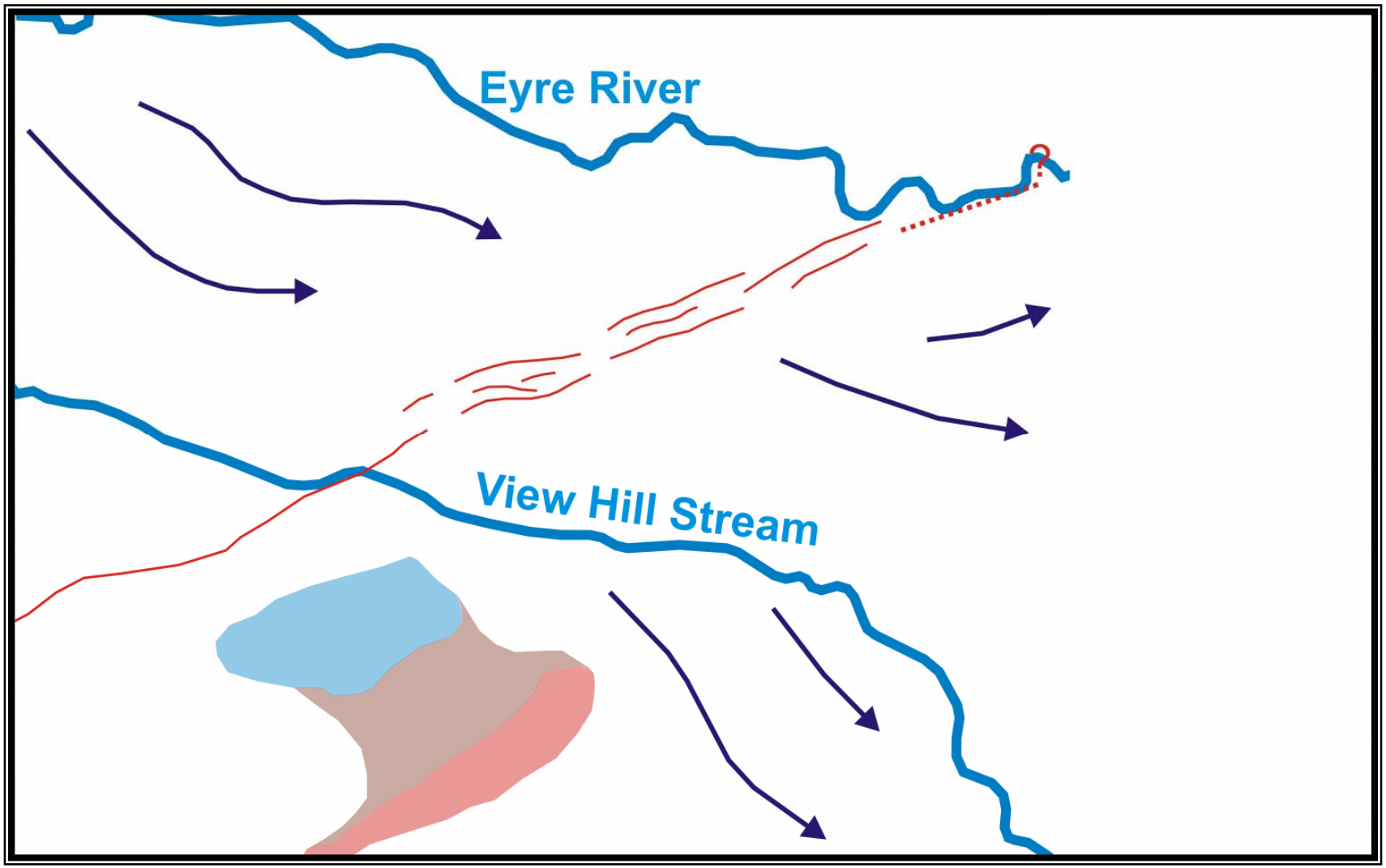
Eyre River
View Hill Stream

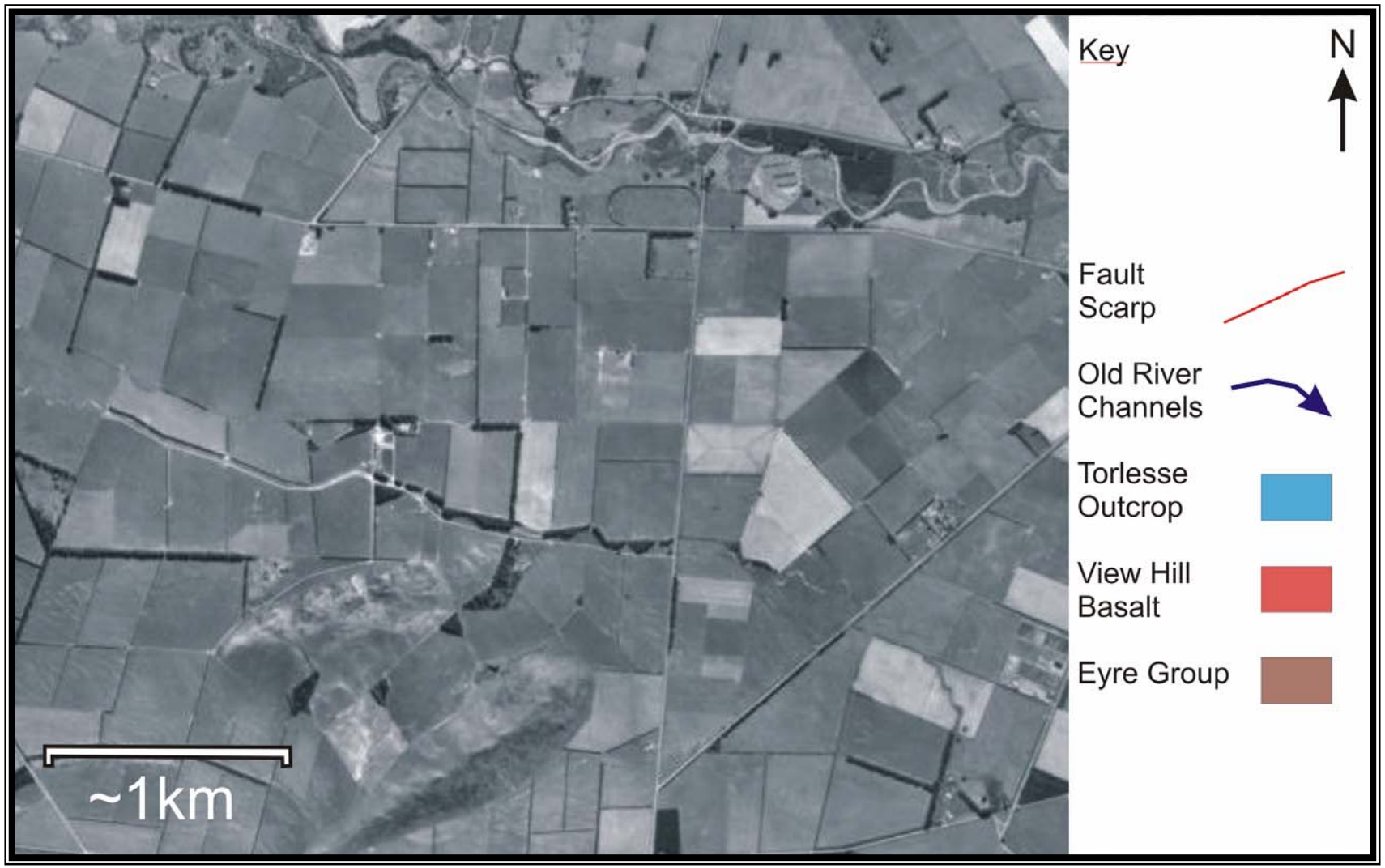

Figure 2.4 – *Eyre River and View Hill Stream.*
Arrows represent flow direction on former channels, red lines represents the View Hill Fault, note splays (see section 2.5.1).

The Eyre River is a small, intermittently flowing river (see section 1.9.5) with much of its flow seeping into re-sorted gravels, but it has had a significant impact on the surfaces surrounding the north side of View Hill. Originating from the foothills to the northwest (further north, with a significantly larger catchment area than View Hill Stream), the river is currently flowing nearly 2 km north of View Hill, but previously may have been much closer. This is implied by the inferred ancient river channels from within a few 100 m of View Hill, gradually descending north to the present course, leaving scalloped relicts of low terrace fragments and shallow, meandering channels, particularly evident north of the fault trace. Downstream of the fault trace the river is more deeply incised. View Hill stream currently may be flowing through part of one of these ancient Eyre River channels.

View Hill Stream is a small stream flowing on the north side of View Hill (see section 1.9.6). Its influence on the landscape is thought to be minor compared to that of the Eyre and Waimakariri Rivers. It originates from the foothills to the northwest, where it flows past the hill, within 300 m. The Stream appears to have migrated north, and has produced a meandering course culminating in an area of flats, upstream of the fault scarp. These represent some ponding along the approximate line of the fault scarp, suggesting the scarp has influenced channel location. However, despite the small size of the stream, it has maintained an antecedent channel across the fault scarp into which it has incised steeply.

2.5 View Hill Fault:

The View Hill Fault is located around the north and west sides of View Hill (see figure 2.1). It appears to be a restraining bend of a thrust fault dipping to the southeast, inferred to have thrust up the View Hill structure.

2.5.1 Scarp Morphology:

The View Hill fault scarp rapidly changes morphology around the View Hill structure. On the northern side of the hill, the scarp is inferred to be a complex belt of inter-fingered scarp splays. This belt becomes a single, prominent scarp to the west of View Hill.

Examination and surveying of the scarp profile suggests that on the west side of View Hill the scarp is ~4 m high, and appears to have a wide back tilt zone, more than 500 m back to the southeast from the scarp. A notable feature of the scarp observed in aerial photographs is that, while the base of the scarp is marked by a faint lineament at possibly the last surface break, the braided surface pattern is preserved on the scarp indicating a monoclinally rolled and little degraded underlying morphology. This surface becomes Wilson's "Woodlands surface" but is clearly a continuation of the same braided surface onto the uplifted side of the fault seen in figure 2.3 Inset.

On the north side of the hill, the scarp appears as a less distinct feature. Unlike the prominent scarp on the west side of View Hill, on this side, the scarp appears as a zone of multiple, smaller scale scarps, possibly inter-fingering, such as suggested by Lin et al. (2003) for sections of scarp from the 1999 Chi-Chi, Taiwan, Earthquake fault rupture, shown in figure 2.5 (G). This figure shows a selection of variations in scarp morphology possible along the extent of a thrust fault line (surveys of the topographical changes across the fault scarp at three locations are discussed in section 2.7). Alternatively, the soil map of Kear et al. (1967) shows these ridges as dues (see figure 2.8).

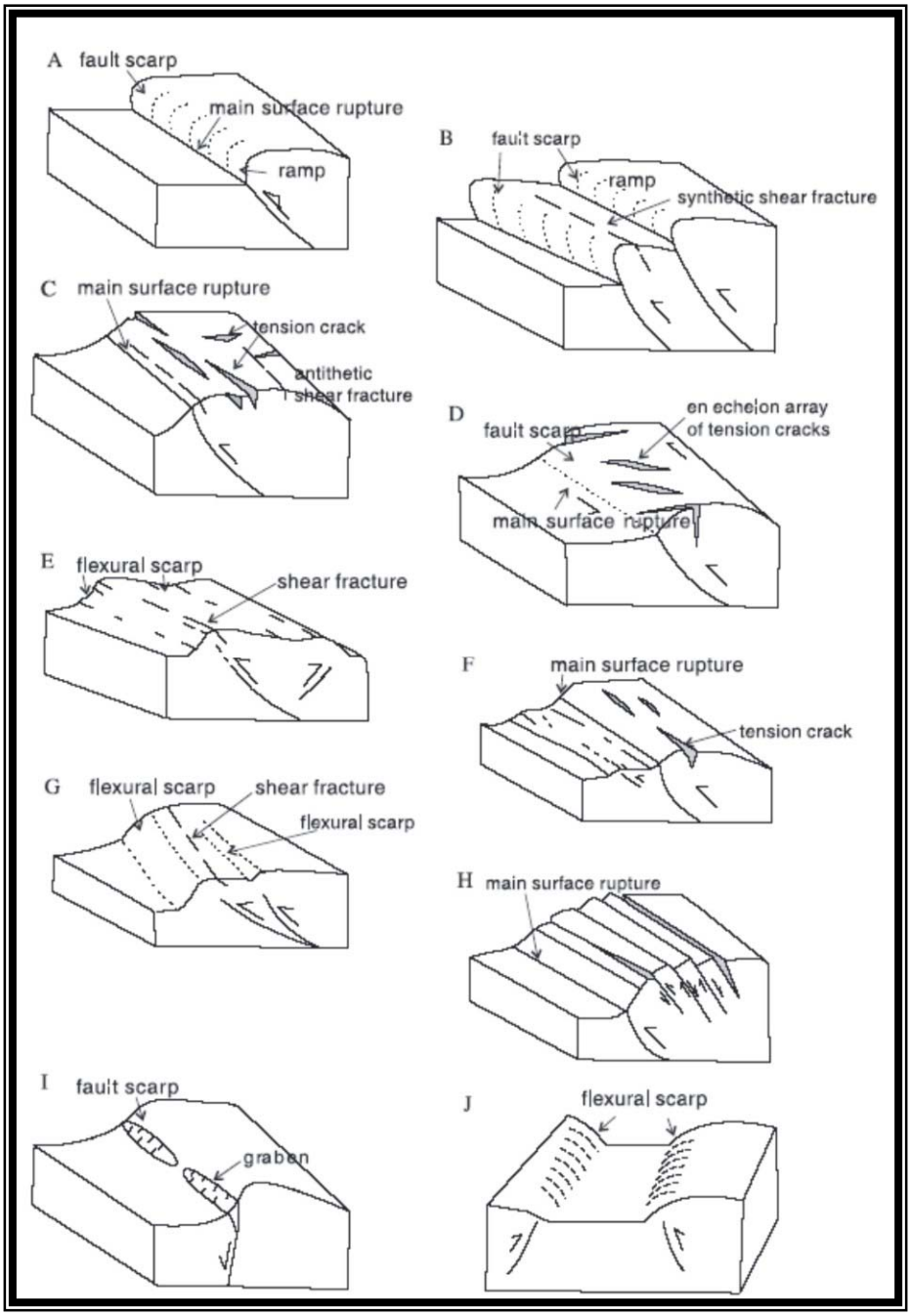

Figure 2.5 – *Variations in fault scarp morphology.*
From Lin et al. (2003) examining variations in the fault scarp of the Chi-Chi Earthquake, Taiwan, 1999. Although relatively degraded in detail, the View Hill scarp retains morphological features suggestive of splays controlling lengths of rolls in the topography resembling figures B, G and less probably E to the north and northeast of View Hill and of A to the west and southwest.

2.5.2 Fault Exposure in the Eyre River:

Tracing the fault scarp to the Eyre River, due to geomorphic modification from river degradation and road infrastructure, the scarp becomes difficult to define. Upon examining the (dry) Eyre River bed, an anomalous section in gravels showing evidence of faulting was exposed in the south side of the bank (see figure 2.6 & 2.7).

The fault dips to the southeast, but displacement is uncertain. A marker horizon S2, (Fig 2.6 (ii)) consisting of a distinctive yellow-brown silt horizon was only located immediately below the shear plane on the footwall of the fault, and not unequivocally duplicated on the hanging wall. There is a similar silt horizon S1 (Fig 2.6 (i)) exposed 4 – 5 m away on the hanging wall with a low, down-stream dip. This is overlain by a few centimetres of gravel and these units are truncated by an unconformity with a dark soil horizon and a further sequence of gravely silts. These underlie the modern soil immediately under the degradation terrace forming the top of the ~2 m high bank.

If S1 and S2 are correlatives then projection of S1 up the dip of the hanging wall requires a throw of the order of 2m. Upstream, the point at which the fault reaches the surface is obscured, making the exposure of the fault plane incomplete. Therefore, the net displacement cannot be determined, but must be substantially larger than the throw at this low angle. A small-scale fold in the gravels marks the ramped, fault-bend step up onto the low-angle, leading tip of the fault propagating through the gravel.

The location of this outcrop is approximately 50 m northwest of the riser on the road which marks the main fault scarp (see Fig 2.7). At the scarp the river has cut a meander into the upthrown side forming a steep, but heavily vegetated bank where little of the internal structure is exposed. Upstream the scarp has clearly formed a barrier causing the river to form a series of degradation terraces, dropping down to the terrace overlying the fault exposure.

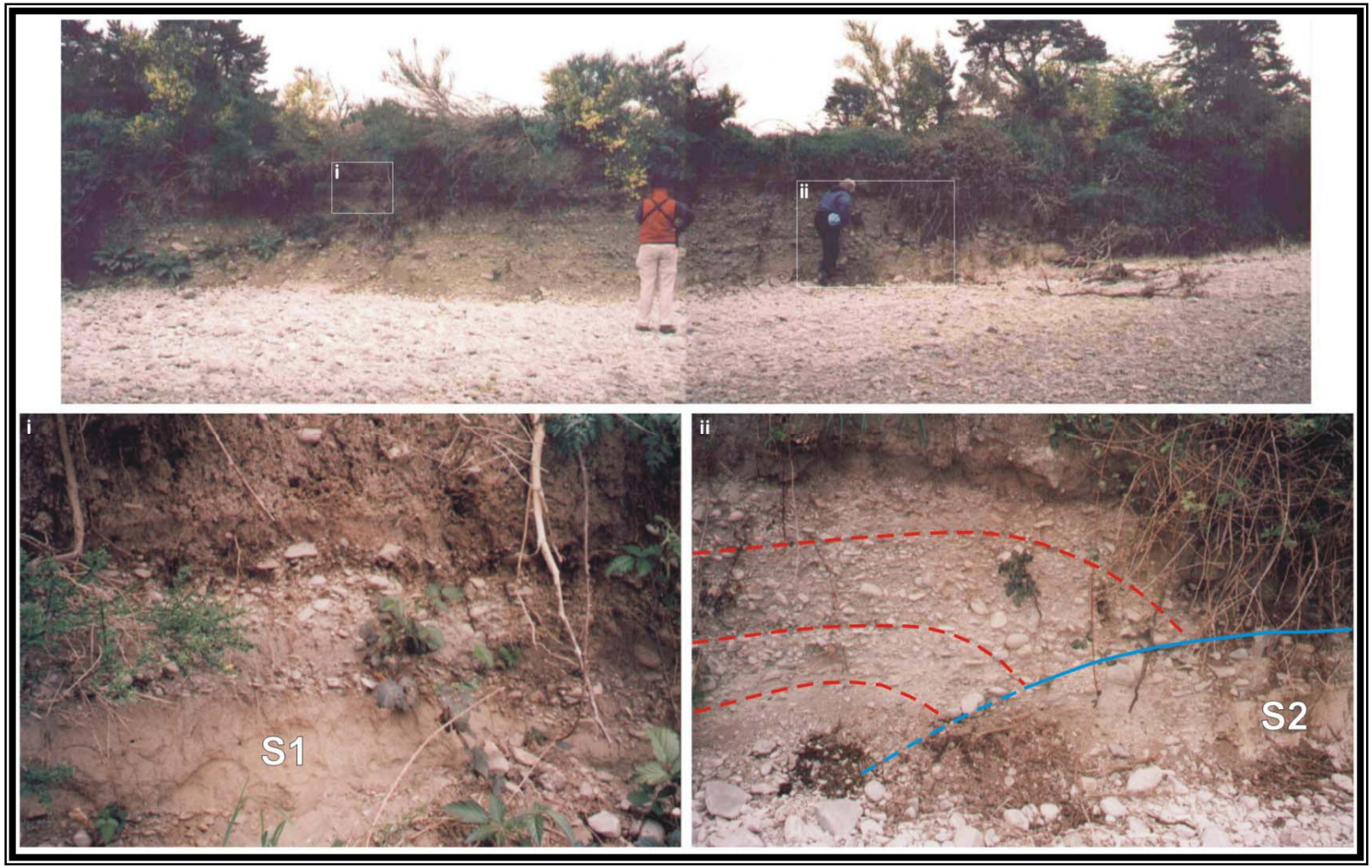

Figure 2.6 – *Photo of fault in Eyre River riverbed*
Inset (i) shows detail of beds. Inset (ii) shows detail of the fault suggesting folding of beds, and as the fault is traced to the right (northwest, upstream) it appears to be horizontal, suggesting a decollment. For location of fault, see figure 2.7.

It seems likely then, that there is a tendency for the fault to propagate along the base of the scarp with the youngest ruptures to be found on the downthrown side. This exposure is therefore likely to be related to the youngest event and the relative timing of this event in the context of the river terrace sequence presents some problems.

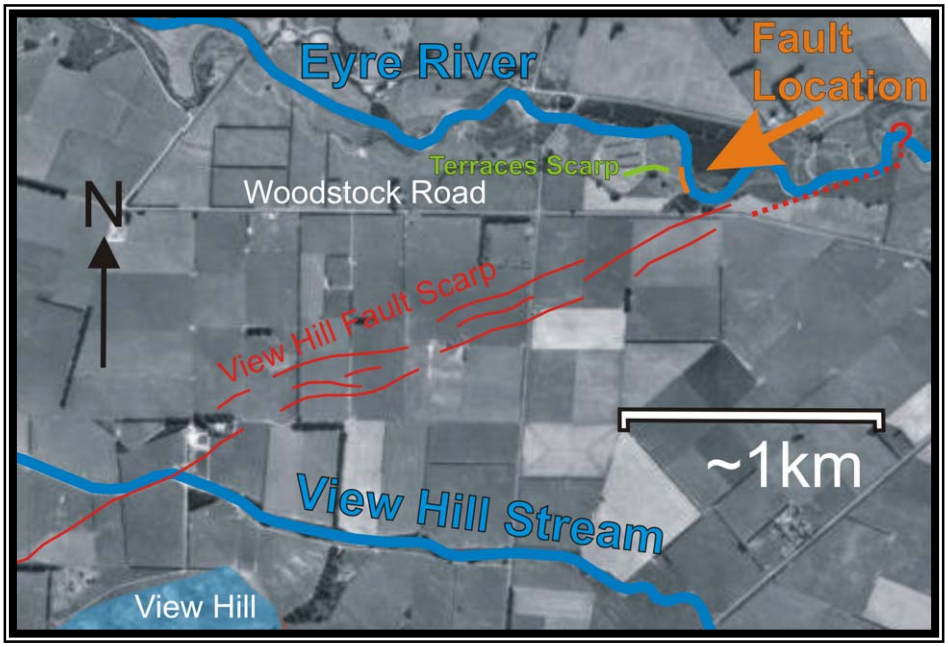

Figure 2.7 – *Fault exposure location and its tectonic setting.*

Clearly, the tilted gravels on the hanging wall are eroded and have a paleosol buried beneath more gravels and soil. Therefore the terrace surface post-dates part, or all of the thrust activity. Conversely, there does seem to be a small scarp on the terrace surface itself and the terrace is back tilted relative to the present river gradient (marked in green in figure 2.7). Predictably a rupture event upthrown across the flow of an active river bed would produce short-term rapid aggradation before general, rapid downcutting, and could account for the gravel veneer over the buried soil.

On balance the evidence points to establishment of this fault strand through older aggradation gravels, trimmed during terrace degradation and abandoned by the active bed for sufficient time to form a thin soil. Less clear is the evidence pointing

to a displacement event when the river was still at, or about that level, causing deformation of the terrace surface, with possible short-term reoccupation of the terrace marked by a flush of debris before final incision. If so, this appears to be a late Holocene event, but is difficult to date by any material seen in the exposure.

When revisiting the site of the fault exposure, it was found to have been obscured by bulldozed gravels pushed against the back to the height of the top of the exposure, thus preventing any further investigation.

2.6 Cover Sequence of the View Hill Area:

2.6.1 Modern Soil:

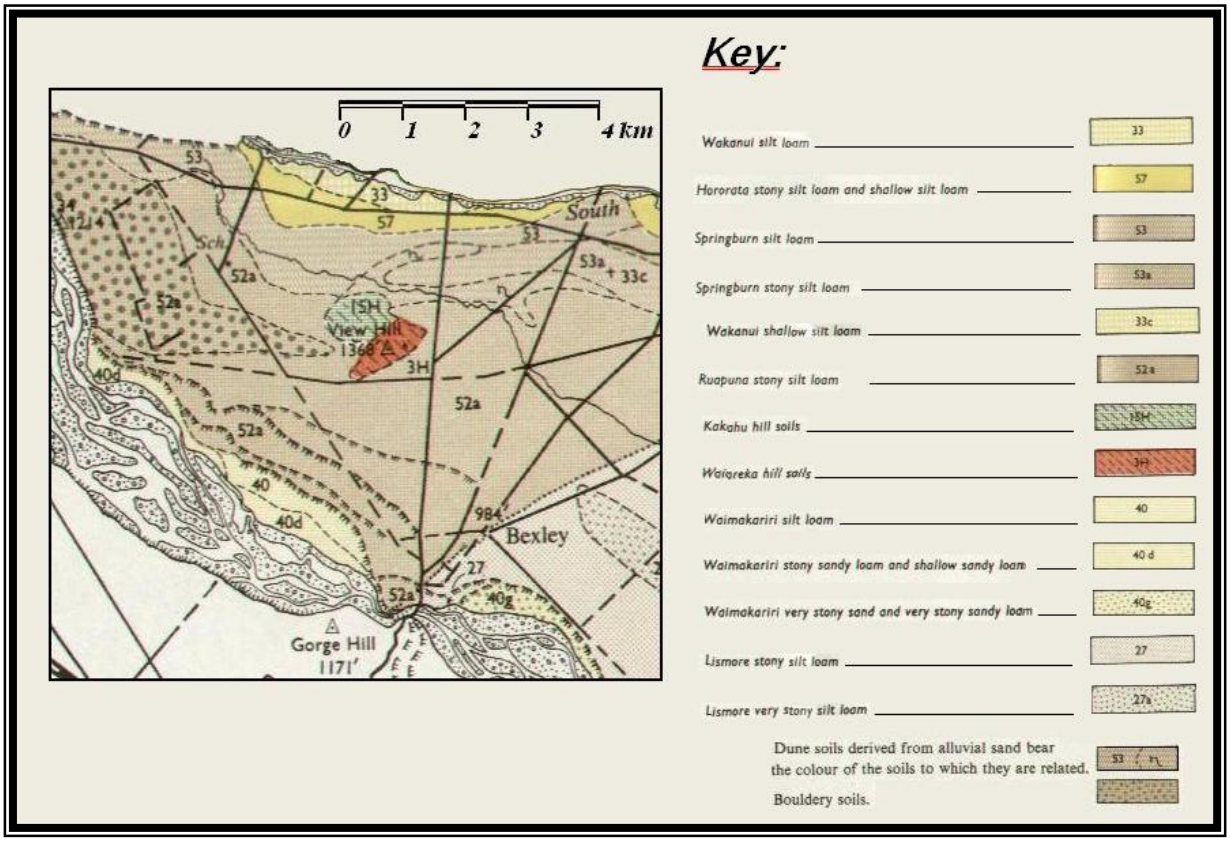

Figure 2.8 – *Soil map of View Hill area. Modified from Kear et al. 1967.*

As shown in figure 2.8, View Hill and the surrounding area contains a wide variety of soils. This is a reflection of the changes in river system channels of the various rivers in the area. The soils range from silt loams predominant around View Hill, to very stony sandy loams on the lower terraces of the Waimakariri River. Also of note is the dune soil extending to the northeast of View Hill, as this area is the approximate location of a distinctive style of scarp morphology, different from the scarp to the west of the hill.

The Springburn Silt Loam (53) and Stony Silt Loam (53a) suggests the extent of the degraded surface produced by the slip off of the Eyre River while the Ruapuna Stony Silt Loam (52a) is inferred to reflect the surface of the original Waimakariri River aggradation surface.

2.6.2 Late Quaternary:

As shown in sections 2.4.2 and 2.4.3, View Hill is surrounded by a variety of terraces from the Waimakariri and Eyre Rivers. The late Quaternary deposits have been degraded by rivers avulsing across the plains, creating the current topography of terrace systems.

The Wilson (1989) map of the area (shown in part in figure 2.9), suggests the surfaces surrounding View Hill comprise a section of Woodlands Formation extending to the west and Windwhistle Formation surrounding the remaining section.

The continuation of the braided pattern (as shown in figure 2.3 inset) across both the “Woodlands” and “Windwhistle” surfaces to the west of View Hill precludes them from being different and the north boundary of the “Woodlands” surface appears to follow the elevation difference coinciding with the fault uplift. The degree of preservation and lack of regolith cover makes correlation with the Windwhistle Formation doubtful. Also, there is no corresponding aggradation at any intervening level in the Eyre river and further downstream at Starvation Hill (see section 3.8) substantial soil exists only on gravel at the highest terrace left by the Eyre River.

If the Windwhistle Formation surface has no or minimal loess cover, the soils formed should be able to be distinguished from the Lismore soils developed on the Burnham Formation as there is going to be 15 to 20 ka difference in soil age. As shown in figures 2.8 and 2.9, the soils map does not support the geologic map. The only complication that could arise is if the Windwhistle Formation had an aeolian cover of 1+ m of sands or loess that has subsequently eroded to re-expose the gravels. Therefore the entire area surrounding View Hill is inferred to be Burnham Formation.

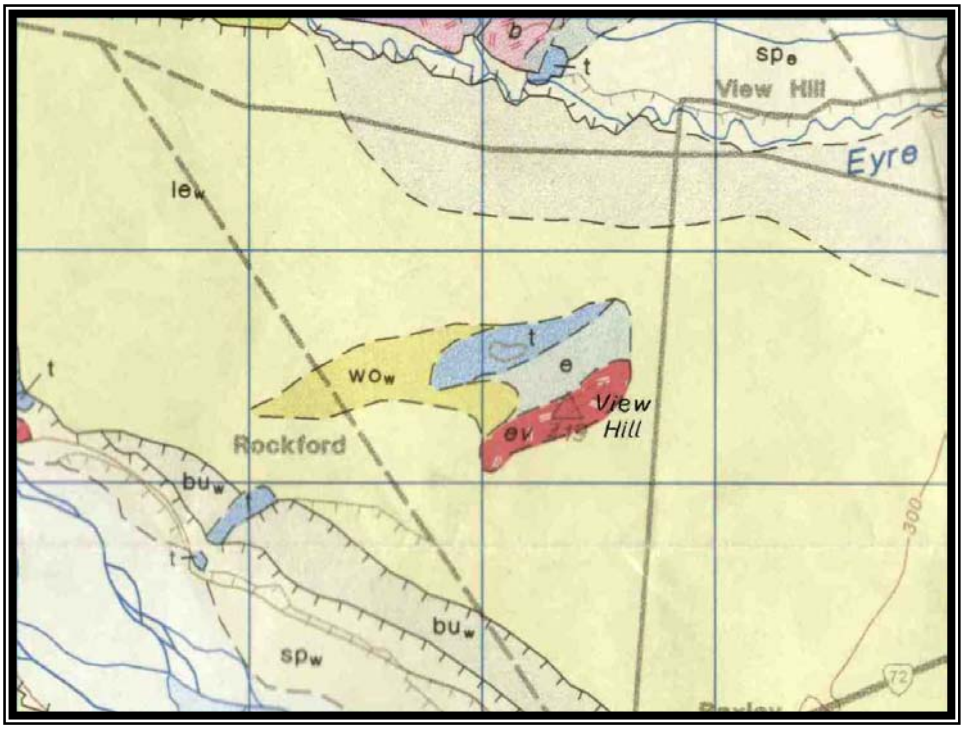

Figure 2.9 – *View Hill section of the geologic map of Wilson (1989). Woodlands Formation* (wo)*, Whindwhistle Formation* (le)*, Burnham Formation* (bu)*, and Springston Formation* (sp)*, Torlesse* (t)*, Eyre Group* (e)*, Eyre Group Volcanics* (ev)*, and Burnt Hill Group basalts* (b)*. Subscript letter represents suggested river catchment (Eyre* ($_e$)*, and Waimakariri* ($_w$) *Rivers). Blue grid equals 1 km*^{2}.

The precise locations of the Torlesse and Eyre Group Volcanics shown in the banks of the Waimakariri River (figure 2.9, middle-left) are unclear, as is the relationship between these units, due to the volcanics appearing to outcrop lower in elevation in the riverbed than the Torlesse basement rock. This does not conform to the pattern shown at View Hill. These outcrops were not investigated due to their location on the riverbed and steep side of the river.

2.6.3 Soil Profiles:

Two soil profiles were described to the northeast of View Hill and three in the saddle-like area. The primary purpose of these surveys was to determine if loess cover was present and what lay under the loess. Details of the soil profile procedure can be found in section 3.7 and the data of the profiles in Appendix I. The location of the profiles are shown in figure 2.10.

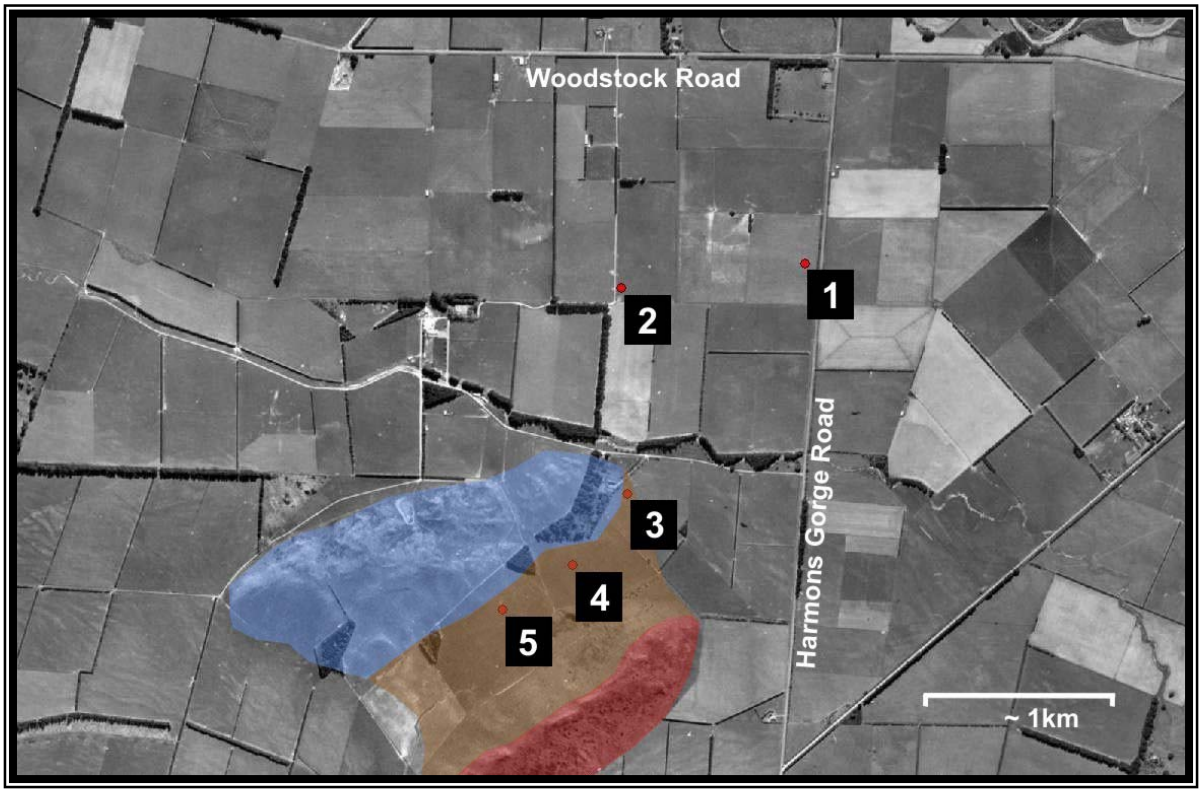

Figure 2.10 – *Soil profile location map.*
Brown area represents the saddle area between the Torlesse (blue) and View Hill Basalt (red) of the View Hill structure.

The two profiles to the northeast of View Hill were located within the zone termed dune soils by Kear et al. (1967) shown on the soils map (see figure 2.8). The profiles were located on topographic highs of elongated ridges, and the profiles showed a thin cover of loess grading down into sandy units at a depth of 50 and 70 cm. The sandy units appear to conform to the mapping of dune formations. These dune formations are discussed in further detail in section 2.7.1.

The three profiles in the saddle showed an underlying sandy unit. These sandy sediments may be aeolian in origin or represent unexposed deposits derived from the Eyre Group. The saddle appeared to be a suitable location for loess accumulation, however it was not present, resolving in an unanswered question.

2.7 Fault Scarp Survey:

2.7.1 Methodology:

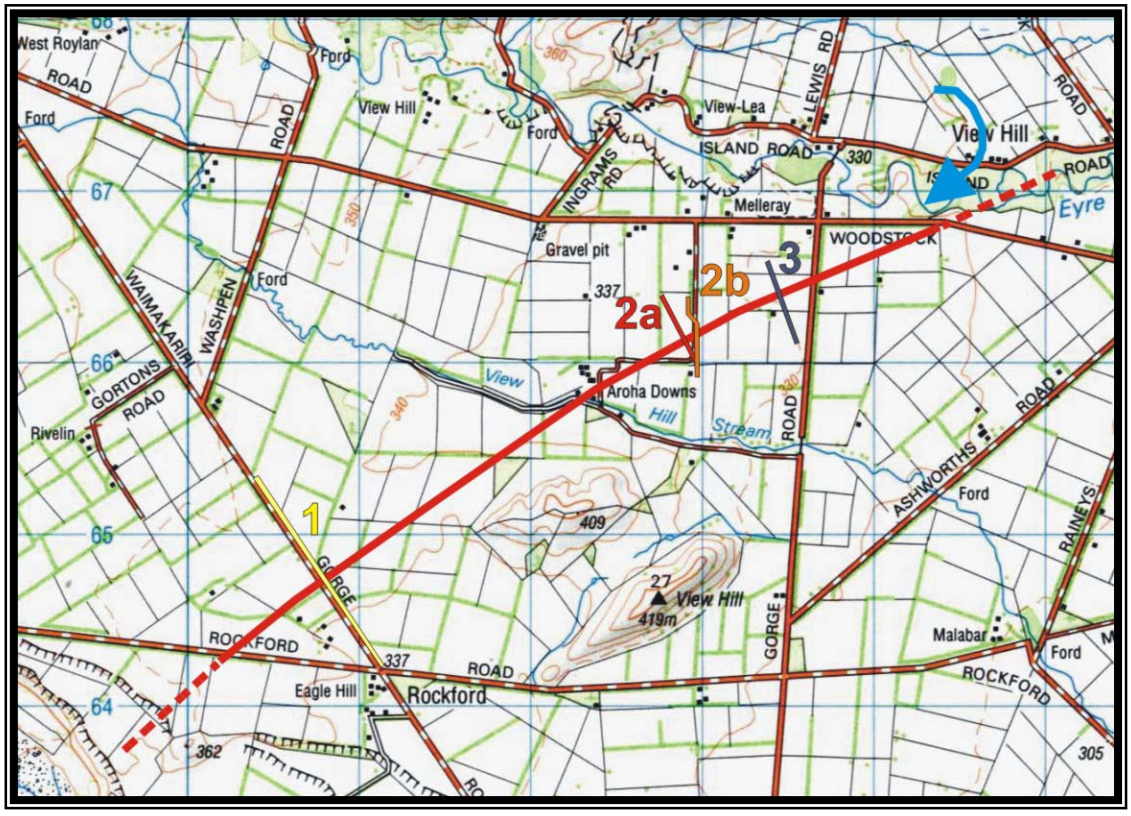

Figure 2.11 – *Location of fault scarp surveys.*
The survey lines were located approximately perpendicular to the scarp, constrained by line of sight through such features as large hedges and changing topography. Blue grid represents 1 km^2. Blue arrow indicates location of Eyre River fault exposure.

A total station (integrated theodolite and electronic distance measurement instrument) was used to survey changes in topography across selected sections of the fault scarp. Figure 2.11 shows the location of the four surveys. Surveys were conducted approximately perpendicular to the scarp, where line of sight allowed. Tall hedges, trees and livestock affected the choice of locations for the profiles.

2.7.2 Character of Profiles:

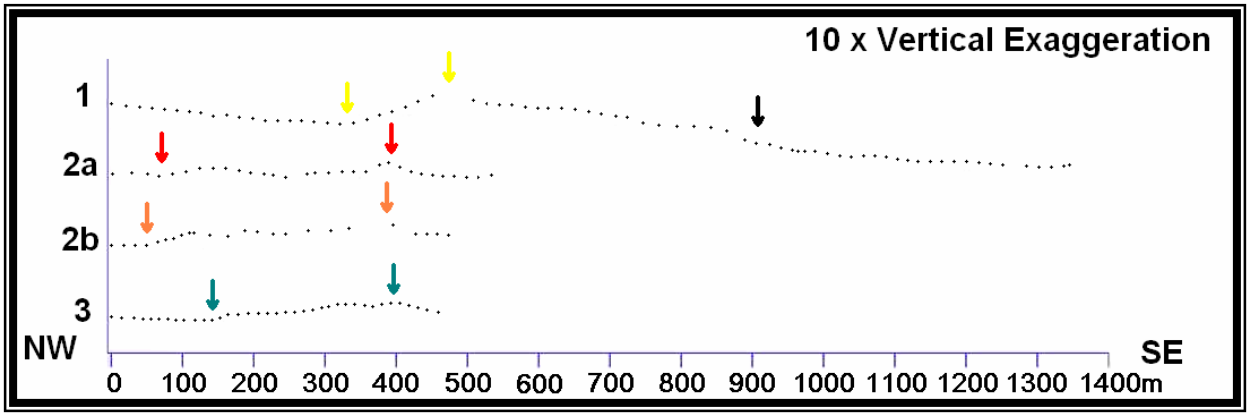

Figure 2.12 – *Profile sections of the scarp surveys looking NE. Coloured arrows indicate the extent of the fault scarp at each site. Black arrow (Profile 1) indicates river terrace location.*

Profile 1 shows a distinct, ~4 m high, ~150 m wide scarp with a ~500 m back tilt zone. Note that the east facing scarp (black arrow) thought of as a possible backthrust, can be traced as an obvious river terrace in a curved arc, projecting westward across the fault trace and marks the first degradation surface.

Profile 2a and 2b show a zone of deformation, comprising three steps and a divergence of these structures between the closely adjacent lines, reflecting strands as described in section 2.5.1. Profile 2a was located approximately perpendicular to the scarp, and shows a ~160 m wide zone, ~1.8 m high. Profile 2b was located along the road, crossing back into the paddock to cross the scarp, avoiding the hedge further along the side of the road. This has produced a slightly elongated profile, but shows similar changes in height to Profile 2a.

Profile 3 shows the least change in altitude comparing one edge of the scarp to the other of ~1.2 m. The profile also shows a separation of fault strands, manifesting in further isolated scarp features. The surface expression suggests either the fault is propagating towards the surface at a slightly steeper angle than at the location of Profile 2, or that the surface expression is less degraded.

2.8 Discussion of Results:

2.8.1 Dunes:

The area around profiles 2a, 2b and 3 have been termed dune deposits based on the soils map (figure 2.8) and soil profiling (section 2.6.3). The existence of these dunes is suggested as resulting from two possibilities:

1) The uplift of the hanging wall side of the fault raised the dunes above the level of river erosion, preserving them, or
2) The fault scarp formed a sediment trap for dune formation which may have modified both the height and morphology of the scarp.

However, the nature of neither the formation of the dunes, nor their extent can currently be answered.

2.8.2 Changes in Scarp Style:

The scarp has been shown to change significantly across the View Hill area. Currently only evident north of the terraces of the Waimakariri River, it becomes a distinct, ~4m high single scarp to the west of View Hill. As the scarp is tracked northeast, to the north side of View Hill, it becomes a comparatively flat and wide belt of deformation with a net accumulation of only ~1.2 m in height. The potential exists for this area of the scarp to have been modified or influenced by the presence of dune formations, affecting the height of the scarp. Further east, the scarp becomes intersected by the Eyre River.

At Woodstock Road the scarp is still relatively prominent. The Eyre River is incised quite deeply into a meander cutting back against the surface which the road runs across. Terraces and present river location shows the persistent history of strong meanders on the upstream side of the fault as the riverbed gradient is affected by fault uplift.

The close correlation of decrease in scarp height with inferred decrease in surface age makes it probable that the scarp represents the accumulated throw of several events at its maximum elevation, rather than loss of displacement along strike during a single event.

2.8.3 Minimum Slip Rate:

To determine the minimum slip rate, several assumptions are made including:

- The rate of minimum vertical uplift is based on the ~4 m of vertical offset distance from Scarp Profile 1.
- An estimated dip angle of the thrust is taken as 25° based on the McLennan map (figure 2.1) and the low angle of thrust required to have Torlesse rocks outcropping along the Waimakariri River in the several places noted in section 2.3.4.
- The oldest surface ruptured is of the age of the Burnham Formation, giving an estimated age range of 27,000 to 15,000 years based on ages from Wilson (1989).

Therefore 4000 mm / 27000 to 15,000 yrs = 0.148 to 0.267 mm per year of vertical uplift (**v**).

Slip Rate equals **v**/ Sin 25°
Slip Rate = 0.148/0.423 = 0.350 mm per year
to 0.267/0.423 = 0.631 mm per year

This would convert this to around 0.5 mm per year for a 20,000 year old surface, an age approximating the timing of the last Glacial Maximum, after which post-glacial downcutting is assumed to permanently abandon Burnham age aggradation.

2.8.4 Interpretation:

The prominent and distinct scarp on the west side of View Hill becomes a dispersed and topographically smaller feature on the north side. This could be the result of:

- Change in strike of the fault. As the fault potentially changes strike from northeast, in approximate alignment with the Springfield Fault, to a more eastward strike, heading towards Starvation Hill, the morphology of the fault scarp may change. The change to overlapping scarplets could reflect an increasing component of oblique motion.

- Change in near surface dip of the fault. The exposure in the Eyre River suggests that the surface rupture of the fault propagates and breaks to the surface at a very low angle, with a fault propagation fold on the hanging wall creating much of the scarp topography. This interpretation of folding rather than a steep break through the ground surface is supported by the continuity of preservation of the detailed channel morphology preserved over the scarp on to the southwest of View Hill (see figure 2.3 Inset). The youngest displacement takes place at the base of the scarp, making it likely that where the morphology splits the northern scarplet is the most recent splay. Towards the west side, the near surface dip of the fault may be steeper, accounting for the single, more prominent scarp, but still appears to break out of the scarp base beneath a rolled over hanging wall fold.

- Variations in surface lithology properties. As discussed in section 2.6, there is a wide variety of cover sequences. These variations may significantly affect the rate and amount of erosion of the fault scarp, or accumulation of soil against it. The presence of dune formations is discussed in section 2.8.1.

- Variation in thickness of surface lithologies. The depth to basement rock in the surrounding area is not known and may be significantly asymmetric when comparing one side of View Hill to the other, but is clearly near the surface at View Hill and along strike southwest towards further Torlesse outcrops at the Waimakariri River. Variations in thickness of gravels, or the presents of the Cretaceous – Tertiary cover sequence, could be manifesting as variation in scarp morphology.

2.9 View Hill Summary and Conclusions:

- View Hill is an isolated feature, rising out of the North Canterbury Plains, set in the back drop of the range front faults and a complex tectonic setting. The hill structure comprises a Torlesse ridge and View Hill Basalt ridge separated by a saddle-like area of undifferentiated sedimentary rock of the Eyre Group with no loess cover found on the saddle.

- The View Hill structure is inferred to be the result of activity on the View Hill Fault. The fault is located to the northwest side of View Hill as it curves around the structure. The relationship of the View Hill Fault with those faults to the southwest and east is not easy to interpret due to the significant distance between surface expressions of propagating tectonic features.

- Simple tilting and uplift of basement and cover may account for the basalt ridge, however the presence of a second thrust splay may explain why the space occupied by the assumed, approximately 200 m thickness of the Eyre Group sequence is relatively thin, by comparison with corresponding stratigraphy elsewhere.

- At least two, and probably more, uplift events, post-dating deposition of a surface argued to be of late Pleistocene age, are needed to account for variations in scarp height.

- Broad constraints on fault dip and the age of the displacement surface suggest that slip-rates are in the order of 0.5 mm/year.

Part Three – Starvation Hill:

3.1 Starvation Hill Introduction:

3.1.1 Setting:

The Starvation Hill structure lies approximately 3 km east of the township of Oxford, which is ~45 km northwest of Christchurch. The hill has a structure and tectonic setting only inferred from reconnaissance mapping and projection of structures observed in seismic reflection lines passing to the northeast. This setting is of interest due to the seismic hazard to Christchurch and North Canterbury posed by the tectonic forces shaping the landscape northwest of Christchurch towards the Southern Alps, acting on structures hidden beneath the Plains.

Prior to this study, there was little documentation about the formation of Starvation Hill and its relevance to seismic hazard, or how it fits into the regional tectonic setting. The hill was initially inferred to be formed primarily due to a fault line suggested to be located approximately along the southern side of the hill connecting the Ashley-Loburn Fault System in the northeast to the Springfield fault in the west (Jongens et al. 1999). The Hill was also inferred to be an anticlinal structure, the anticline running approximately north-northeast and thought of as a possible restraining bend related structure. This study is based on an analysis of the surface morphology with very little exposure of the underlying rocks from which the structure could be determined, and uncertainties remain. It is clear that the geometry and evolution of this structure is not simple.

3.1.2 General Topography and Character:

Starvation Hill lies approximately 3 km east of the township of Oxford. The hill appears to rise out of the surrounding relatively flat plains (see figure 3.1), separate from the nearby foothills and Cust Anticline. The hill rises to a height of 288.9 m, ~85 m above the surrounding Canterbury Plains.

Figure 3.1 – *View of Starvation Hill looking south-southeast.*

The hill is not a regular shape, instead appearing to be a dual-hinged anticline, possibly reflecting two directions of folding (see figure 3.2). Starvation Hill is a broadly rounded feature, etched into by distinctive surfaces formed at a range of elevations and dissected by steep gullies, most with running water only immediately following high rainfall.

The grass (and gorse) covered hill is predominantly used for farming, with a wide variety of stock ranging from sheep, dairy cows and deer, to occasional emus, lamas, bulls and two very large rotweilers. There are also small areas of pine plantations, a council pit and seasonal crops ranging from stock feed to exported flowers.

The Cust and Ashley rivers flow past Starvation Hill approximately 1 and 5 km respectively to the north, and the Eyre River approximately 4 km to the south (see figure 3.3). In previous times, these and the Waimakariri River have modified the basal surfaces and terraces that were surrounding Starvation Hill.

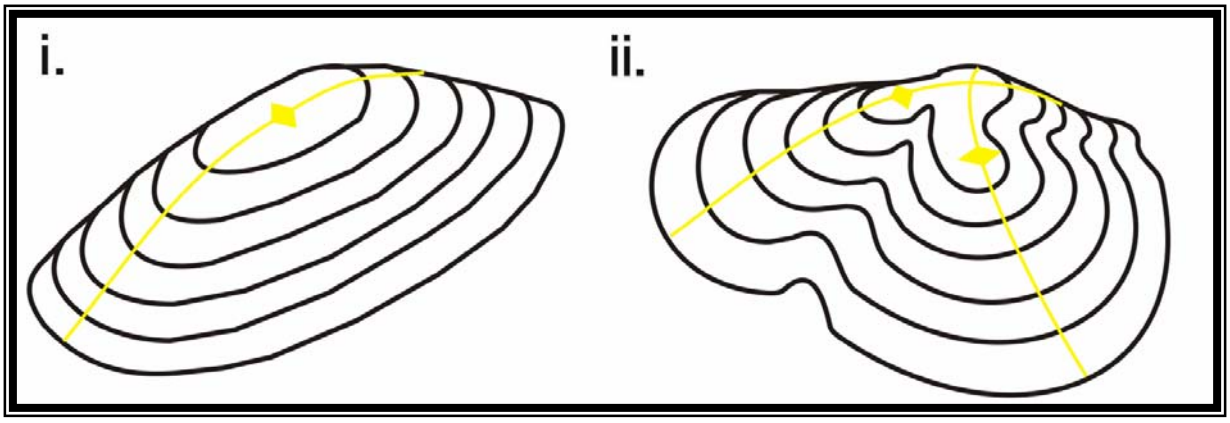

Figure 3.2 – *Comparison of Starvation Hill with a 'typical' anticlinal structure. A stylised view of a 'typical' antiform (i) compared with the crudely triangular approximation of the shape of Starvation Hill looking south (ii).*

The hill comprises parts of eight different farms, making toll calls for access both time-consuming and somewhat expensive, but access was never a problem and the farmers were all friendly and supportive of the study.

3.1.3 Current Tectonic and Geological View of Starvation Hill:

Prior to this study, Starvation Hill was interpreted to be the result of an oblique strike-slip fault to the southeast of Starvation Hill, running between Oxford township and Cust Anticline (Jongens et al. 1999). The fault was thought to form a restraining bend (Campbell et al. 2000), causing the uplift of Starvation Hill (see figure 3.3).

The geology of Starvation Hill is mainly inferred from information on geological maps (Gregg, 1964; Wilson, 1989). There is no outcrop of pre-Quaternary rocks other than a capping of volcanics which crop out at scattered localities and a range of elevations. These volcanics have variously been correlated with those of View Hill or of Burnt Hill. Otherwise, the maps distinguish the surrounding surfaces as a range of Burnham, Windwhistle, Woodlands and Springston Formations.

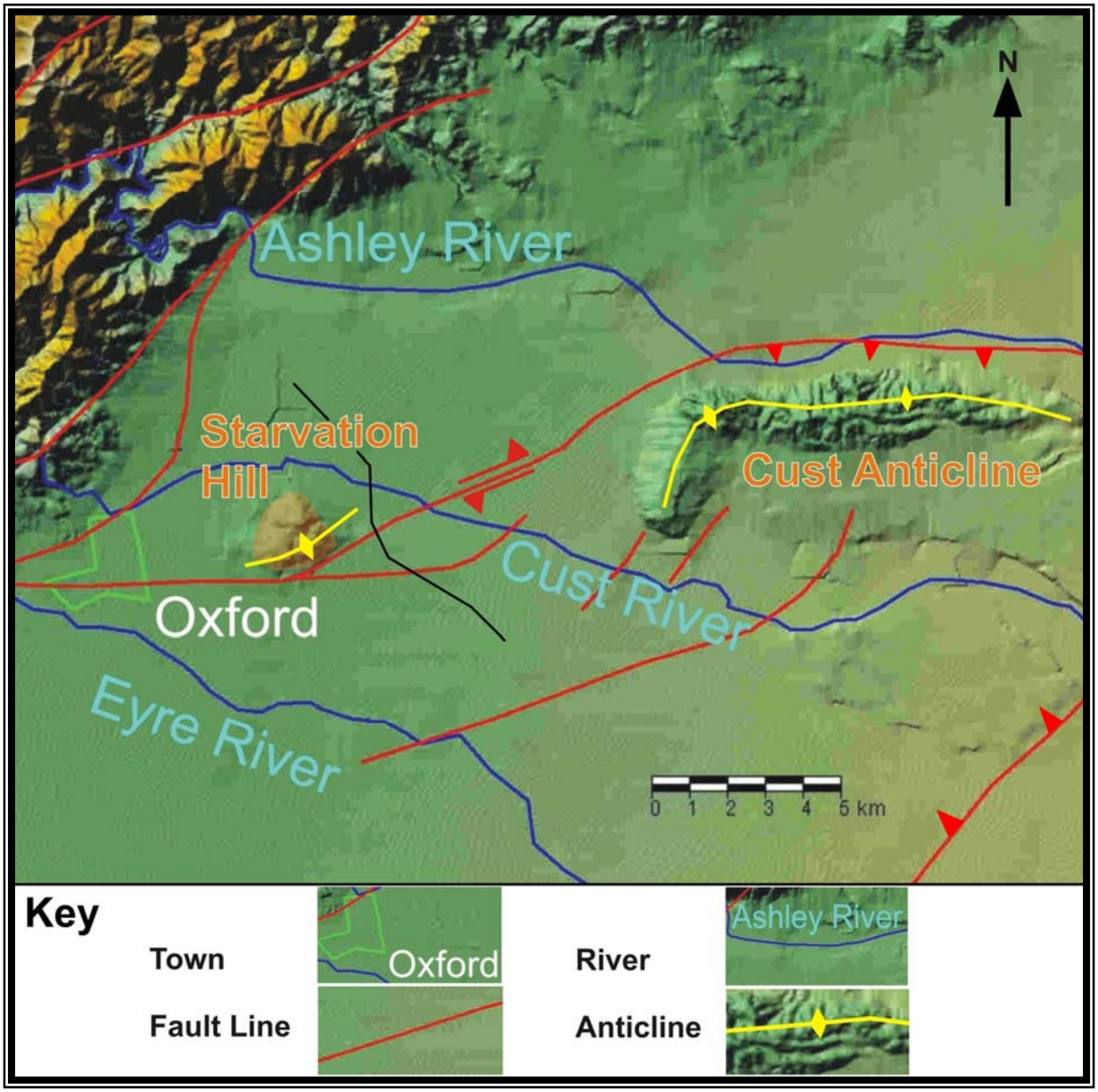

Figure 3.3 - *Tectonic Setting of Starvation Hill based on Jongens et al. (1999). Starvation Hill was inferred to be a pop-up structure related to a restraining bend of the fault to south of the hill. The fault (based on a fault observed in the Indo-Pacific Ltd 'Line 002' which is located as the black line in this figure, and discussed in section 3.2) was inferred to connect the Ashley-Loburn Fault Zone in the east to the Springfield Fault in the west, past View Hill (Jongens et al., 1999; Campbell et al., 2000).*

There is no clear evidence of surface faulting at Starvation Hill. There is no scarp evident, nor one marked on previous geological maps, other than the unpublished map of Jongens et al. (1999) which suggested that a small terrace on the south side might be fault related. This poses the question of the extent to which folding may reflect both fault geometry and fault activity.

3.2 Seismic Line:

3.2.1 Indo-Pacific Ltd Line 002 Location:

Indo-Pacific Ltd (1998) conducted a seismic survey (Line 002) along the northeast side of Starvation Hill, located in figure 3.4.

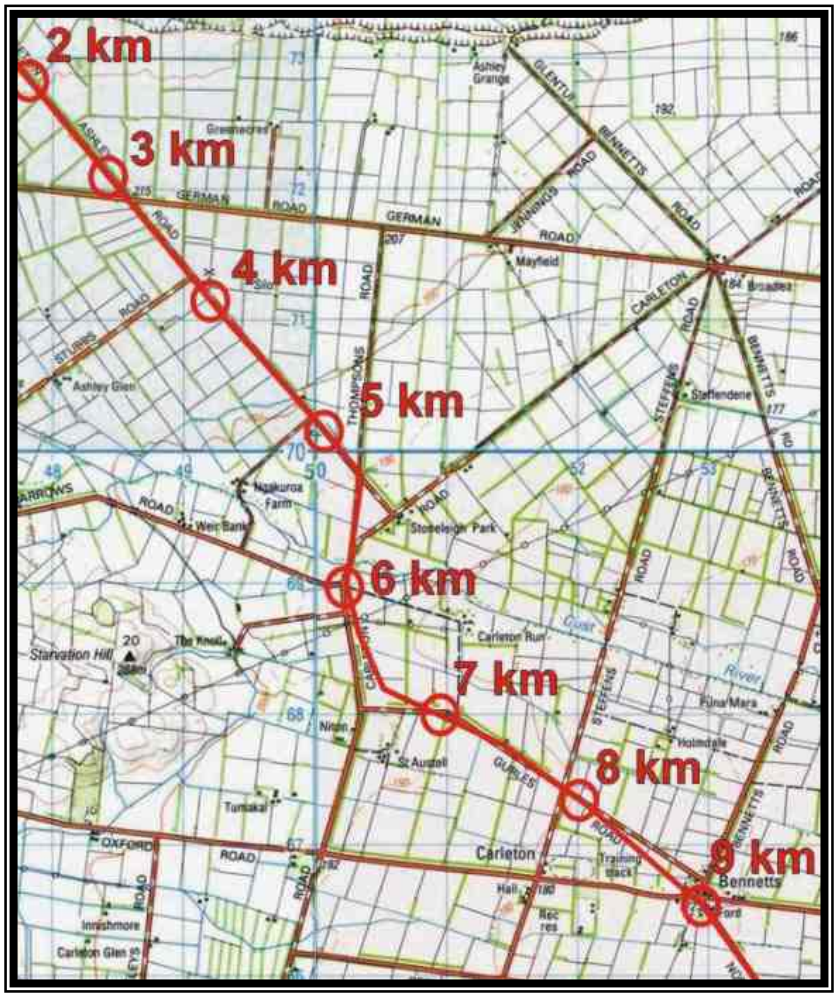

Figure 3.4 – *Location of section of the Indo Pacific Ltd Seismic Line near Starvation Hill. See Figures 3.5a & 3.5b for seismic data, grid of topographic map at 1 km. Approximate location of this section of the seismic line also shown in figure 3.3.*

The seismic line extends to the southeast where it crossed the Springbank Fault, allowing that fault to be first recognised. The southern end of this seismic line has been the focus of recent investigation (Estrada, 2003), however little interpretation of the area around Starvation Hill has been published.

The following two figures (3.5a & 3.5b) show overlapping sections of the Indo Pacific Ltd seismic line. The two figures extend the length of seismic line from 2500 m to 10,000 m, covering the length assumed to contain features affecting Starvation Hill.

3.2.2 Indo-Pacific Line – Interpretation & Inferences for Starvation Hill:

The sections of seismic line data appear to show the following features:

- ~3500 m – possible thrust fault
- ~5000 m – upwarping reflector units
- ~6500 m – a south dipping thrust fault
- ~8000 m – upwarping reflector units

The break in reflectors at ~3500 m does not appear to propagate closer than ~1 km in depth however may continue west as a decollment before thrusting upwards again. This feature is almost due north of Starvation Hill, and is thought to project past to the northwest, having little affect on the hill structure based on a southwest – northeast alignment.

The upwarping of reflectors at ~5000 m may be the result of a southward dipping fault as shown. This upwarping may be an extension of the Starvation Hill structure. The upwarping correlates to approximately 50 m of vertical uplift, potentially accounting for the uplifted hill structure.

The thrust fault at ~6500 m is an approximation only of the main fault responsible for the Starvation Hill structure inferred by Jongens et al. (1999). This fault dips to the south at a moderate angle and is the evidence for projecting a linking fault from the Cust Anticline structure towards Starvation Hill. Tectonic features in the area located through which the main thrust fault is shown are not obvious. The distinct units directly under the near horizontal section of the thrust are thought to be Mt Summers Volcanics, which provide strong reflectors but the volcanics themselves are not continuous over long periods (M. Finnemore, pers. comm.).This suggests the apparent break in the reflectors marked by the thrust fault increasing in dip at

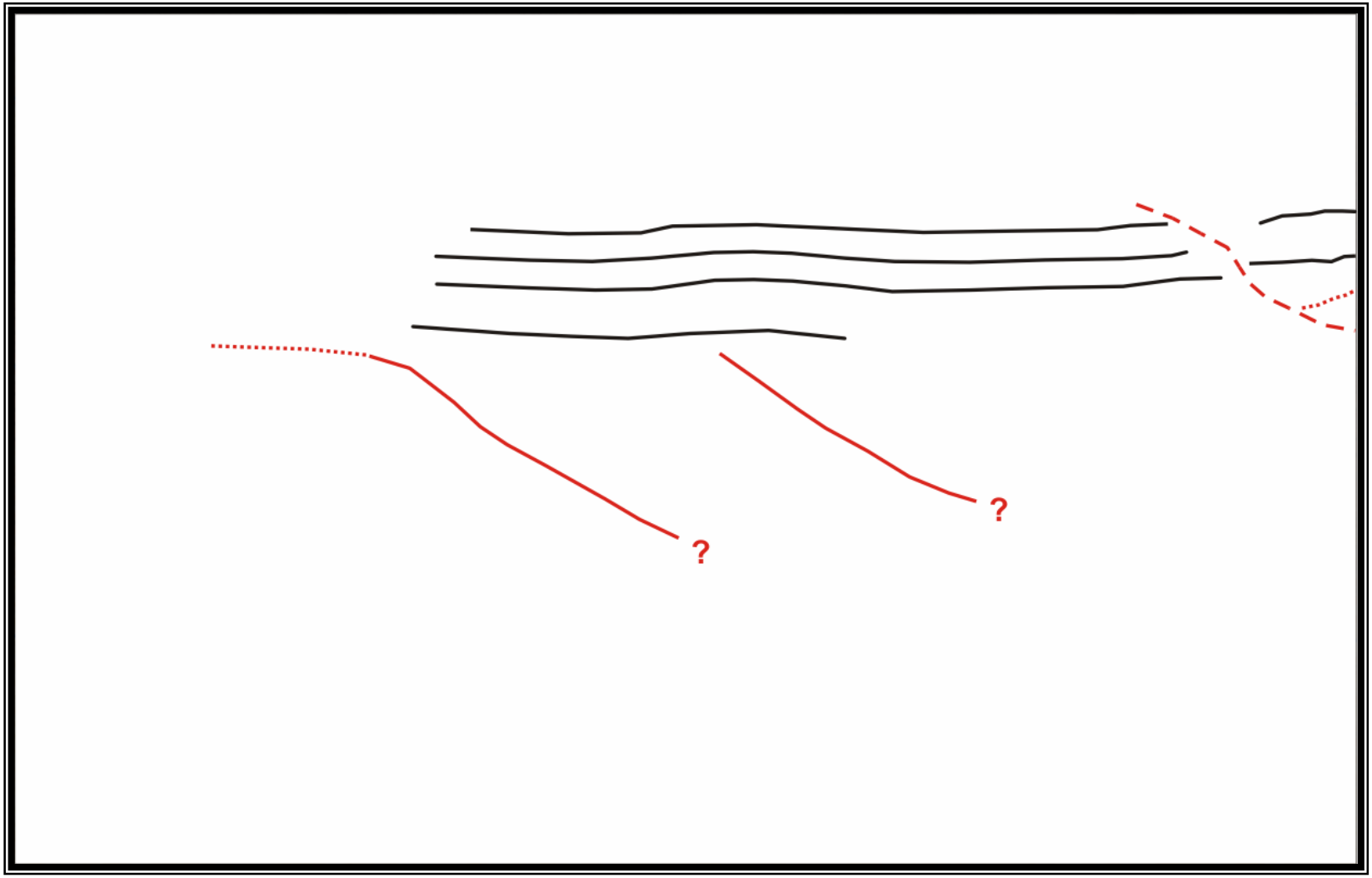

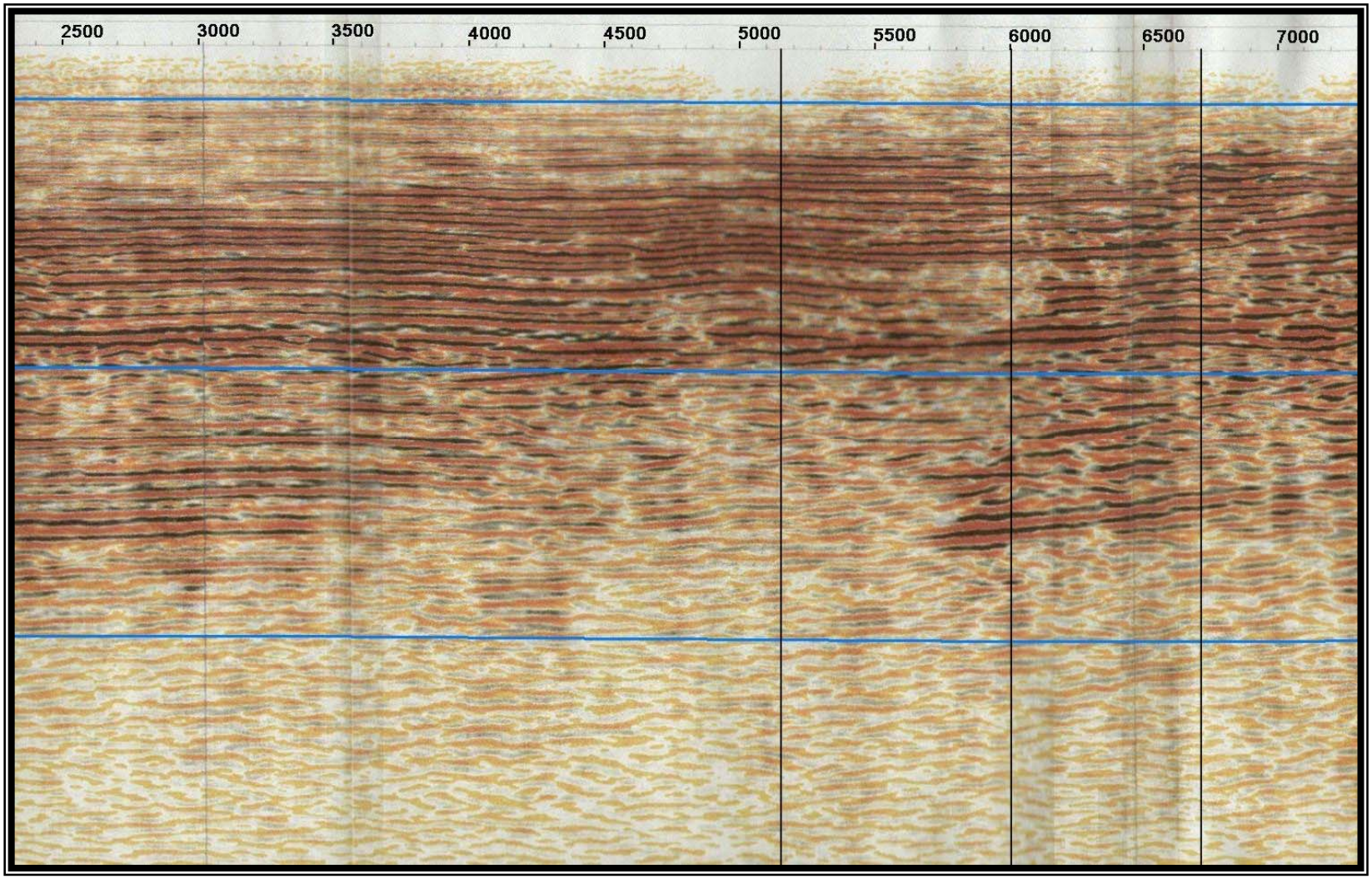

Figure 3.5a – *Seismic Line.*
See figure 3.4 for location of line. Blue lines are 1 second two-way travel times, approximately equivalent to 1 km depth (0, 1 & 2 km.) Black lines denote change in orientation of seismic line. Interpretation of tectonic features shown on overlay, see text for details.

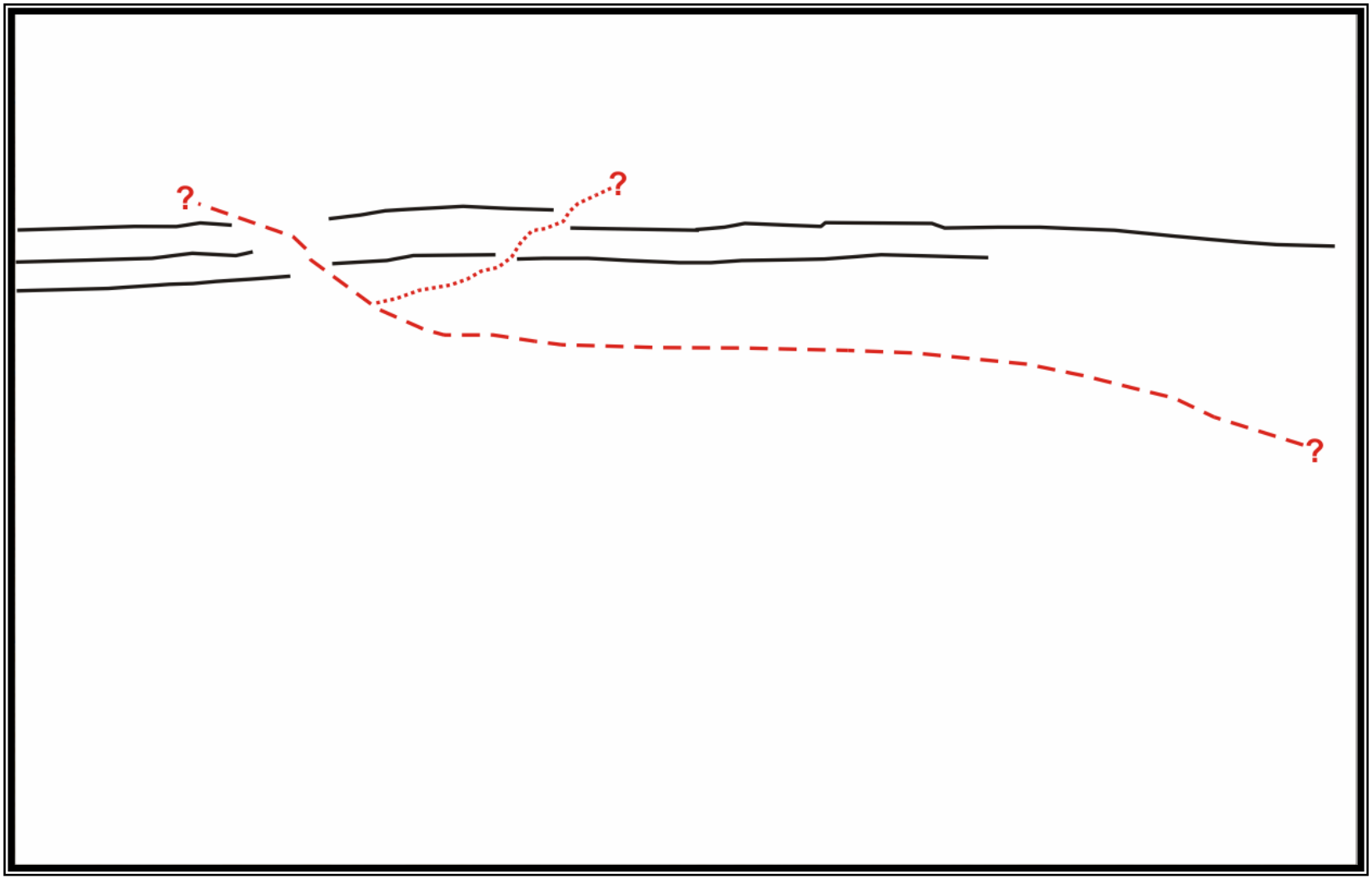

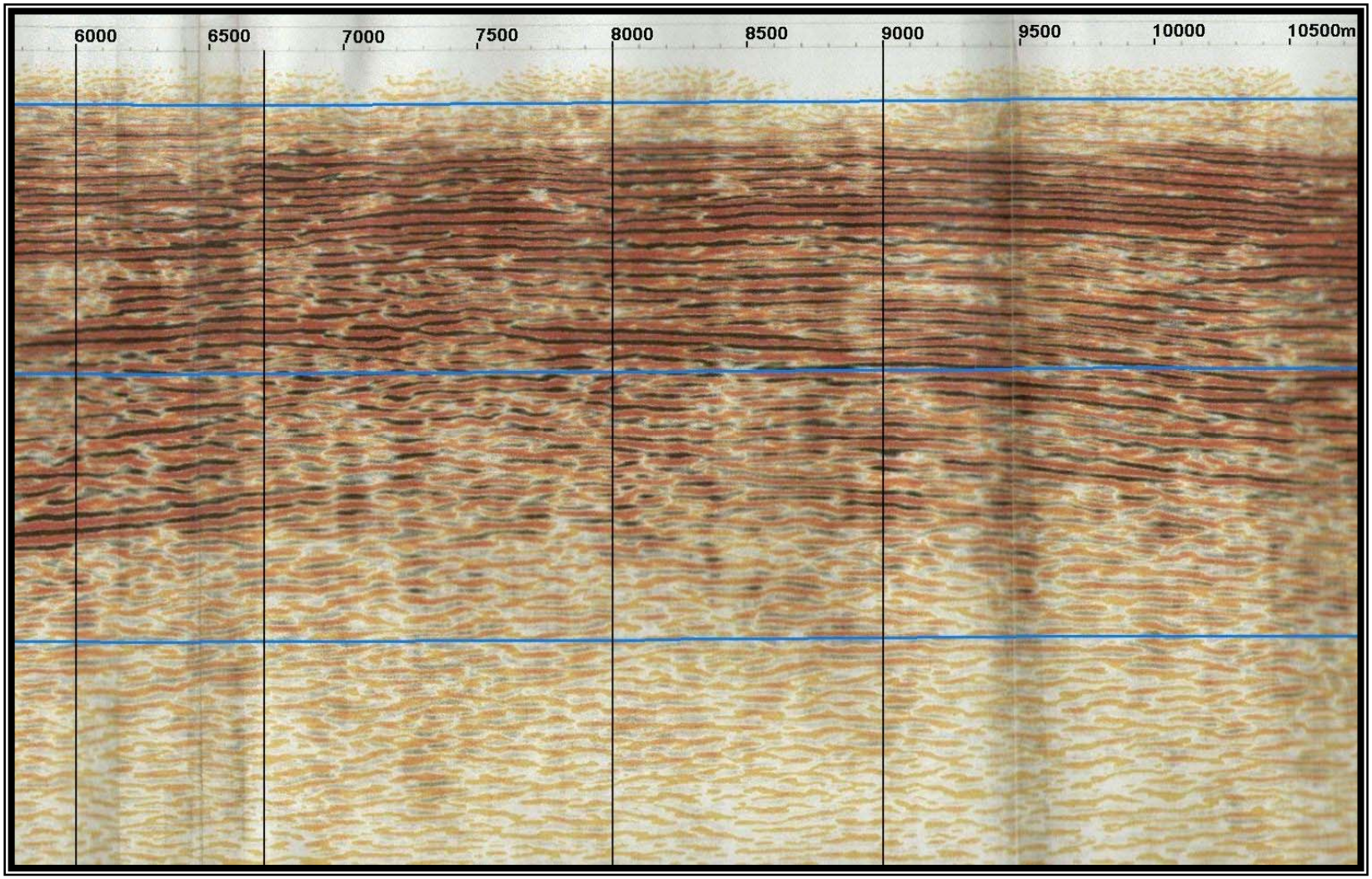

Figure 3.5b – *Seismic Line.*
See figure 3.4 for location of line. Blue lines are 1 second two-way travel times, approximately equivalent to 1 km depth (0, 1 & 2 km.) Black lines denote change in orientation of seismic line. Interpretation of tectonic features shown on overlay, see text for details.

~10,000 m may only be the edge of the volcanics. This fault may have caused the anticlinal shape of the hill but would require a complex linkage to the predominantly strike-slip sections of the Ashley-Loburn Fault System in the east, and an equally complex linkage westwards to create the opposing uplift of both the Cust and Starvation Hill folds as a restraining bend mechanism.

The three thrust faults shown may form splays connected at depth, or separate segments, of a complex system of tectonic activity between the Ashley-Loburn Fault System and the View Hill Fault. A result of this complex fault system is the apparent uplift of the Starvation Hill structure, possibly on more than one axis of tilt due to the multiple tectonic features.

The feature at ~8000 m is potentially a backthrust of the main thrust fault. This is likely to be too far south to have any significant influence on the Starvation Hill structure, and like all the features mentioned above, does not appear to rupture the current surface of the region.

3.2.3 Tectonic Summary for Starvation Hill:

The tectonic setting inferred from the seismic line, and an inferred tectonic linkage trending southwest – northeast, is one of a series of approximately south to southeast dipping thrust faults. These could only in part explain the triangular, dual-hinged anticlinal shape of the hill (see figure 3.2) as there appears to be two divergent hinges to the structure, one on the north and one on the east , only one of which conforms to the apparent tectonic setting.

The steepness of the south and southeast sides of the easterly trending section of the hill reflecting one hinge, along with the initial interpretation of a restraining bend to the southeast of the hill, would suggest an asymmetrical anticline on a northwest dipping fold. However, northwest dipping structures were not observed in the seismic lines. The tectonic setting appears more complex than initial inferences suggest, based on the seismic line and the general shape of the hill structure.

The connection of the fault system at Starvation Hill with the Ashley-Loburn Fault System to the east can only be inferred as complex and unclear. There appears to be no obvious model allowing for both the south dipping Ashley-Loburn Fault System, its role with respect to the Cust Anticline, and the apparent two directional folding of Starvation Hill to produce the dual-hinged anticline. The hill lies on what should be the footwall side of the initial fault projection, for a simple restraining bend model based on south dipping faults.

3.3 Geology and Bedrock Control of Morphology of Starvation Hill:

There is little exposure of rock on Starvation Hill except boulders and a few outcrops of basalt cap rock. Basalt clearly caps the hill and crops out near the highest point by the trig station at 289 m. Extensive outcrops occur at 230 m on the isolated knob to the east-southeast (see frontispiece). Other exposures of basalt crop out on the edges of surfaces N3 and N4, but as boulders are clearly embedded in the loess cover in many places, it is not clear which of the smaller outcrops are in situ. The outcrop of basalt capping therefore is enigmatic as it varies in elevation and may be interpreted in a variety of ways.

The distribution of the basalt may be entirely a product of folding, in which case it appears to form a broadly domal cap on the hill. Alternatively, there may be duplication by faulting, or stratigraphic duplication involving more than one flow and forming quite a thick sequence. The part played by the presence of this resistant unit in the preservation and shape of the hill is currently uncertain. No good exposures of units under the basalt make the stratigraphic position uncertain, but sand at the base of some of the stratigraphic profiles (see section 3.7) suggest that greensand may lie beneath and this would favour a correlation with Oligocene Burnt Hill Volcanics.

The lack of exposure is now known to be the result of a thick loess layer, blanketing the hill with up to more than 6m of loess (see section 3.7). Because of this, there is

therefore little bedrock control on the superficial morphology and further data on the underlying structure of Starvation Hill is not possible by surface mapping.

3.4 Semi-Planar Surfaces:

3.4.1 Relevance of Starvation Hill:

The focus on Starvation Hill evolved around the presence of a series of distinctive, smooth, semi-planar surfaces, lapping across the Hill at a range of elevations and gradients. These surfaces appeared to be clearly steeper than normal fluvial gradients and are thought to be indicative of tilting and warping (see figure 3.6).

These surfaces must be remnants representative of some combination of aggradational or degradational fluvial surfaces imposed around both sides of a growing structure. If this was the case, there is potential for a detailed study of these surface remnants to allow a partial 3D reconstruction of the growth of the Starvation Hill structure. This would require correlation of the surface remnants surrounding the hill into their former surfaces, and for them to be able to be rebuilt in a digital model and possibly retro-restored, back to suggest their original shape, extent and orientation, prior to growth of Starvation Hill.

The initial expectation was that the apparent surface remnants around the flanks of Starvation Hill were remnants of old river terraces. The higher terraces would therefore be older and would be more tilted than the lower/younger terraces if active growth was contemporaneous with downcutting. Surficial deposits on the surface remnants were initially expected to provide some control on their relative age, on the assumption that emergence of the structure would preserve a succession of thicker and more complex cover over fluvial gravels on the higher surface remnants, becoming systematically progressively thinner and simpler down the flight of terraces. Detail of the cover sequence is given in sections 3.6 to 3.9.

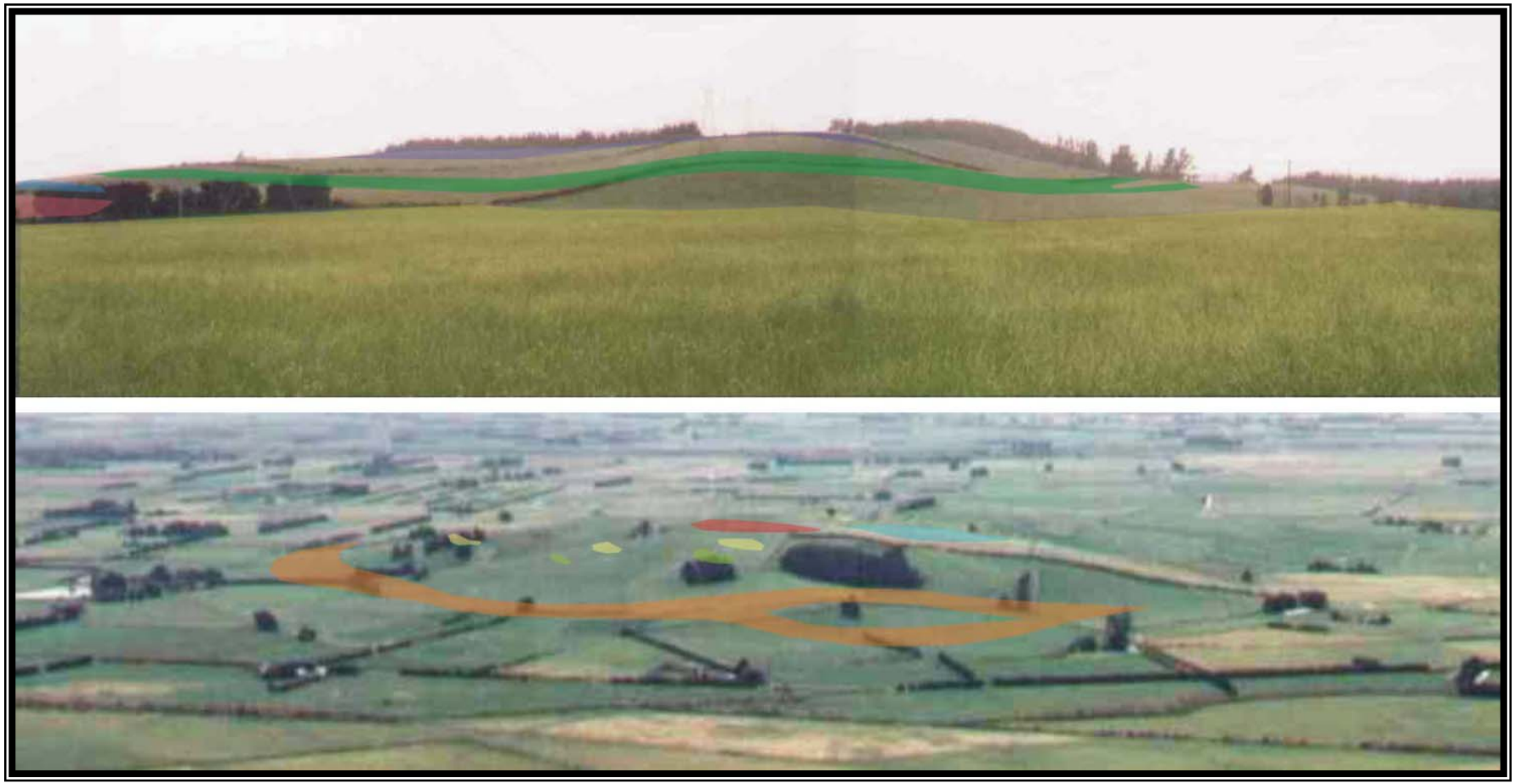

Figure 3.6 *– View of surfaces on Starvation Hill – looking northeast from near the corner of Starvation Hill Road and Oxford Road (a), and looking south-southeast (b). Note the surfaces appear to warp upwards across the middle sections of both (a) and (b), surfaces are numbered and described in section 3.5. and the remnants making up these surfaces are shown in figure 3.8.*

3.4.2 Alternatives for the formation of semi-planar surfaces around the hill:

The morphology of Starvation Hill could be representative of resistant beds, especially the underlying volcanics. The volcanics, in the form of tabular or lensoid masses of basalt, could be constraining the landform of the hill. However, some of the semi-planar surfaces are formed below the level of outcrops of basalt, and other surfaces above, appear to project below the basalt. Therefore, it is unlikely the basalt is responsible for the formation of the semi-planar surfaces on and around the Starvation Hill structure.

3.4.3 Climatic Versus Tectonic Input:

The Canterbury Plains have widely been regarded as forming through a series of aggradational and degradational episodes (Gage, 1958; Browne et al., 1988; Suggate, 1990). As such, the lithologies found on the plains represent scattered preservations of sections of the entire depositional history of the area.

The preservation of deposition from an aggradational period may be insignificant, deposits being partially or completely eroded by the following degradational period. In this regard, the gravel unit is unlikely to represent original thicknesses of material deposited on the plains in many areas.

Adding to this complication, the effects of tectonic activity on accumulation thicknesses can be significant. Tectonic uplift may raise part of an aggradational deposit above the reach of the following degradational period. Thus it is possible to preserve minor episodes of aggradation that may not be coeval with the major episodes. Any uplifted deposits can then be eroded either as a consequence of subsequent tectonic activity or other climatically driven erosional episode, potentially being redeposited, incorporating clasts of anomalous size, or degree of weathering into younger deposits.

The emergence of a growing structure across a drainage system potentially results in riverbeds which may be aggrading on either side of the structure, but actively eroding the riverbed section crossing the crest of the structure. The resulting riverbed therefore forms a continuous surface which may be correlated with an aggradation event, but is not everywhere underlain by thick gravel deposits.

When such a surface is preserved, but is uplifted and warped, possibly partially eroded, or on-lapped by subsequent cycles of aggradation, a succession of complex surfaces may be preserved across the emerging structure. These are of fluvial origin, but may neither preserve much gravel, nor necessarily correlate chronologically with the successions observed in less active parts of the catchment.

3.4.4 Requirements:

In order to determine the original extent and alignment of the apparent river terraces on the flanks of Starvation Hill, significant fieldwork was required. This work included the following components:

i. Geomorphic mapping – This mapping defines the boundaries of each remnant of surfaces, and separates out the steep erosional gullies that have cut down the hill slopes dissecting them. During the mapping, correlation of the remnants was made visually, by sighting along the gradient of each surface to the adjoining segments. This correlation provides the basis for extrapolation and rejoining of the remnants to recreate the undissected surface, after input into a digital elevation model, allowing reconstruction of possible original complete shapes (further detail is given in section 3.5).

ii. Stratigraphy profile surveys of surfical deposits – The intention was to provide stratigraphic control on the minimum age of the underlying surface, plus depth of cover material and consequential altitude corrections to the alignment of the underlying orientation of the surfaces (further detail is given in section 3.7).

iii. Provision of good topographic control – This would provide correlation, reconstruction and projection of the remnants, vital to determining the amount of tilting occurring. For this a substantial GPS survey was undertaken, incorporated into 3D computer modelling software (further detail is given in section 3.10).

3.5 Geomorphology of Starvation Hill:

3.5.1 Description of Major Surfaces:

The following is a description of the semi-planar surfaces shown in figure 3.7. The surfaces are comprised of surface remnants mapped in the field, and correlated both by field observation and with the aid of digital elevation data (see section 3.4 and 3.10). Many of these surfaces have had auger cores drilled on them, profiling their stratigraphy (see section 3.7). These remnants have been correlated across erosion channels (shown in figure 3.8) and around the flanks of the Starvation Hill structure.

The surfaces are separated and described firstly into the series of surfaces occupying the north side of the hill (N1 to N5), secondly those that can not easily be traced to the north or south, but are primarily on the eastern side (E1 to E4), and thirdly, those to the southwest side of the hill (S1 to S5). This is due to the likelihood that the north and south surfaces were formed either by separate rivers (ancestral Cust, Ashley and Eyre catchments) on either side of Starvation Hill, or by channels migrating across the hill structure, therefore it cannot be assumed that surfaces on the north and south(west) sides can be closely correlated.

The dashed yellow line in figure 3.7 shows the inferred extent of significant loess cover on the SH structure. On surfaces below this line, loess cover was found to be less than 0.8 m. Above this line, loess cover is considerably thicker, increasing rapidly to over 6.45 m, as shown in the stratigraphy profiles of section 3.7. The northwest corner of Starvation Hill was not studied in any detail, hence the ending of surfaces and loess cover lines prior to this area, however likely scenarios of this are

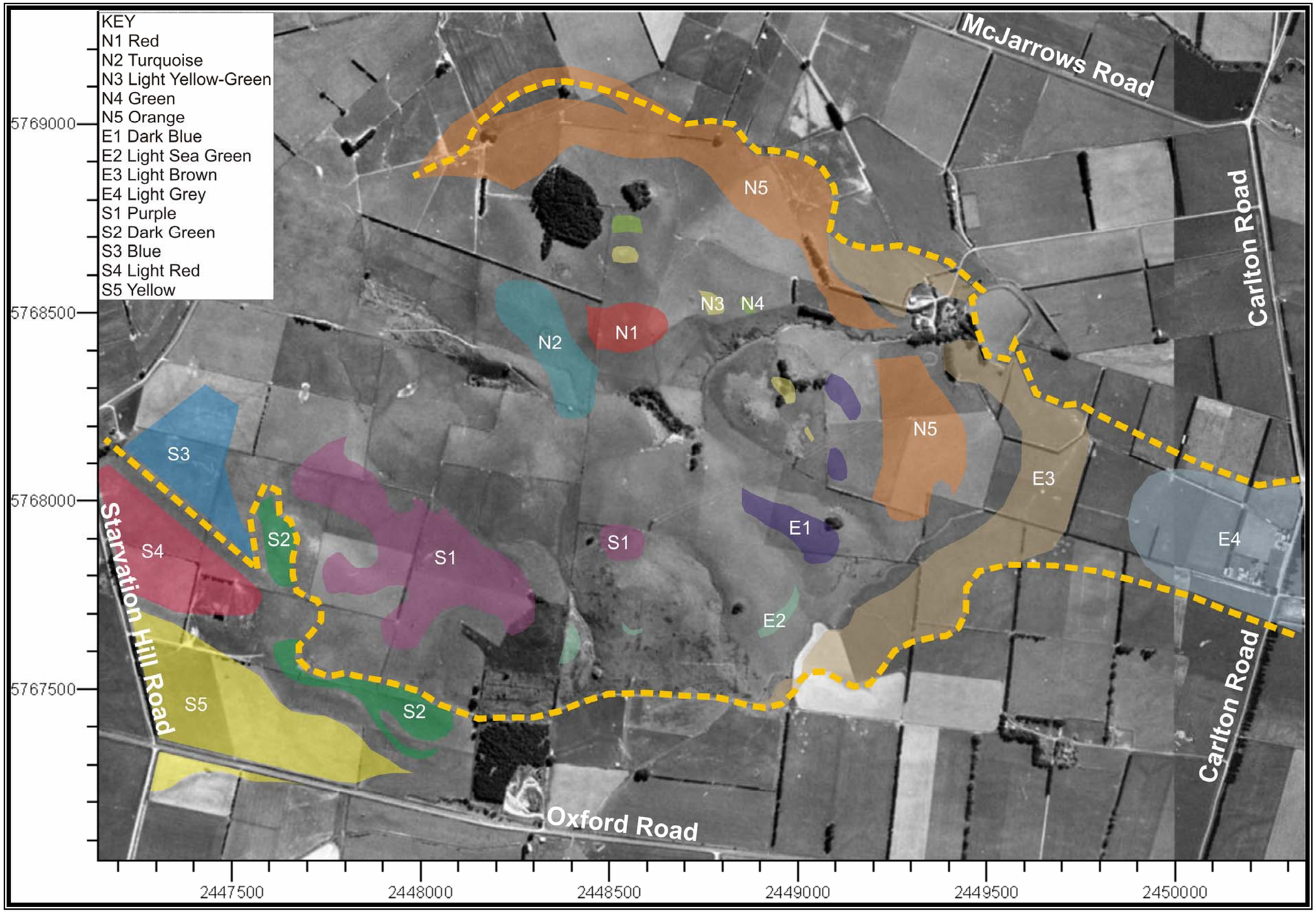

Figure 3.7 – *Aerial view of Starvation Hill showing location of surfaces.*
For descriptions of surfaces, see text. Dashed yellow line represents approximate extent of significant loess cover.

area discussed in section 3.5.3. Stratigraphy profiles located on the surfaces are discussed in section 3.7.

3.5.1.1 Surface N1 (Trig Site): (Red)

This surface appears to roll over slightly towards the south as well as slope west, forming a gentle convexity to the whole surface. The surface is bounded on the south side by a deep gully. To the north and east, the surface was truncated by lower surfaces, and the western edge is truncated by surface N2. Stratigraphy profile 1 was located on this surface, striking presumably a rock at ~1.65 m.

3.5.1.2 Surface N2: (Turquoise)

This surface forms a saddle which separates the two halves of the hill. This seems to have been linked to the three largest gullies leading off from to the west, east and south (see section 3.5.2). The origin of this surface may only reflect headwater erosion that has breached the resistant basalt capping and therefore created the saddle, or it may have been the product of a former antecedent channel that maintained its course across the crest of the structure for a time before being abandoned to form an air gap. Clearly now modified by modern gully erosion, the surface appears to be a rolled over smooth surface truncating the southwest side of surface N1.

Surface N2 potential continues to the southeast, just north of eastern most remnant of surface S1, and forms the spur described as the southern remnant of surface E1, however the distance between these two surfaces is substantial and heavily modified by erosion, such that any correlation is ambiguous.

3.5.1.3 **Surfaces N3 & N4:** (Light Yellow-Green and Green)

These two surfaces, on the northeast flank of the hill, are extensively dissected and approximately mirror each other as paired remnants. Surface N3 is approximately 10 m higher in elevation than surface N4. Surface N3 appears on either side of a significant gully on the east side of the hill. Stratigraphy profile 2 was located on the western edge of surface N3, striking presumably a rock at ~4.3 m.

The correlation of these surfaces is only tentative due to the wide expanses without remnants, and the curved side of the hill slope making correlations difficult, however there does appear to be a general trend of the surfaces rising to the west.

3.5.1.4 **Surface N5:** (Orange)

This extensive surface wraps around the base of the north and east sections of the hill. On the north side, it appears to split in two with marked convexity to the upper surface (shown in figure 3.6), possibly a result of synchronous growth of the Starvation Hill structure. At the western end, the upper surface appears to warp down again quite steeply to intersect the flats around the base of the hill. At the eastern end, the wide combined surface curves around the north-eastern basal flank, climbing with a readily visible gradient to lie above surface E3, but not appearing to separate again, suggesting that the component of warping post-dated the formation of the surface.

Stratigraphy profile 3 was located on the eastern extent of this surface, striking presumably a rock at ~ 6m. Near the northern extent of this surface, on the north side of the hill, two stratigraphy profiles (profiles 4 & 5) were located. Profile 5 was located on the flat area surrounding the north side of the hill, north of surface N5 and located gravels at ~0.5 m. Profile 4 was located on an apparent interfluve, isolated from the majority of surface N5 by an erosional gully. This profile located loess the entire depth of the profile (6.45 m), suggesting that the loess cover on the north side

of the hill is very thick right to the base of the hill and is almost completely eroded on the flat surface extending out from the base of the hill structure.

3.5.1.5 **Surface E1:** (Dark Blue)

These three surface remnants neither appear to align with any other surface nor easily with each other. The northern two are relatively small in extent, possibly small degradation relicts or possibly not of fluvial origin. The southern most remnant appears to cap a spur protruding slightly from other flanks of the southeast side of Starvation Hill.

However these surfaces do appear to follow a general trend of increasing in height to the south, possibly as a result of an eastward directed fold axis. Further detail is given in section 3.10.6.

3.5.1.6 **Surface E2:** (Light Sea Green)

The remnants collectively termed surface E2 are not easily correlated, however the eastern remnant may be a continuation of surface S2, on the basis of elevation. The line of sight was not suitable to correlate them in the field, and they appear too far apart to correlate them on the DEM (see section 3.10). They form a relatively narrow, partially dissected bench on the south to southeast flank of the hill and the eastern remnant is swampy and a trap for slope deposits derived from above. It overlaps the eastward extension of the lowest slopes on the east side of Starvation Hill (surface E3). Because of its relative position, surface E2 must therefore be older than surface E3 if it is formed by a river trimline.

As will be discussed in the context of the distribution of surficial deposits (see section 3.7), problems arise if surface E2 is correlated with surface S2. A possibility that the eastern remnant of surface E2 is a fault scarp has been considered, but does not appear to affect the spur at the eastern end, on strike from the termination of this bench. The alternatives are difficult to test in this setting.

3.5.1.7 **Surface E3:** (Light Brown)

This surface wraps around the eastern flank of the hill and lies below surface N5. It appears to have been truncated at both its northern and southern extents. This surface has been modified by the irrigation scheme, affecting its eastern boundary.

The possibility exists that this surface should be split in two; a surface on the north and east sides, and a separate surface on the southeast side, however field examination suggests the surface is part of a singe feature.

The surface may have been formed by the Ashley River during the period when the Ashley flowed between Starvation Hill and the Cust Anticline. Stratigraphy profile 8 was located on this surface near its southern extent. Depth to gravel was 6.2m. Further south from surface E3, around the base of the hill, three more profiles were located, 9, 10 and 11. These were below the elevation of surface E3 and showed a cover of alluvial gravels around this side of the hill without any loess cover.

3.5.1.8 **Surface E4:** (Grey)

This surface extends from east of the break in slope on the main eastern flank on the hill, below surface E3, to form a low, slightly undulating ridge for at least 1 km to beyond Carleton Road. This surface represents the basal surface on the east side of Starvation Hill, assumed to represent an interfluve area of rivers to the north and south. From the opposite, northwest side of Starvation Hill, in the area of least study, a surface inferred to be representing an interfluve projects northwest, as discussed further in section 3.5.3.

Two stratigraphy profiles (profiles 6 & 7) were located on surface E4, near Carlton Road, with thick loess deposits found in both profiles. In Profile 7, the more easterly of the two profiles, soil appearing to contain sandy units inferred to be an overbank deposit was found, suggesting this surface could be an ancient remnant of downland topography (Tonkin; Campbell, pers. comm.).

3.5.1.9 **Surface S1:** (Purple)

This surface begins below halfway on the western flank of Starvation Hill and rises to the east. This is one of the highest surfaces on the hill, and one of the largest. It possibly projects across a major gully and continues as a flat-floored, slightly channelised remnant north of a knob to the east, where it appears to terminate. This surface has thick loess cover, and gravels were never reached on the four stratigraphy profiles located on this surface (profiles 12, 13, 14, & 15).

On the north side of the surface, an abrupt riser, presumably the channel margin, preserved only near the crest of the hill, marks the surface margin. On the south side, the surface appears to roll over towards the south as well as slope west, forming a gentle convexity to the whole surface. At the western end, it is truncated by erosion around the western end of the hill.

3.5.1.10 **Surface S2:** (Green)

This is a highly dissected surface wrapping around the slopes on the southwest side of the hill. It appears to be significantly warped in an east – west direction, dipping or slumping down in the middle, presumably due to an erosional gully, and rising significantly, as it heads east along the southern flank of Starvation Hill.

Towards the west, as it passes around the base of the hill, it appears to rise slightly again, before being truncated by erosion around the western end, in close proximity to surface S3. It also appears to have a southerly gradient, dipping out from the hillside and almost merges with the rolled over edge of surface S1 in places. This surface has had two stratigraphy profiles located on it (profiles 16 & 17), both reaching gravel by 0.5 m.

The warping of these two surfaces (S1 & S2) is suggestive of influence by two axis of folding. A broad axis trending north, and a narrower axis, trending approximately east are envisaged, more detail is given in section 3.10.6.

3.5.1.11 **Surface S3** (Blue)

This surface is a wide, relatively flat expanse, widening northwest. It is cut-off from continuing southeast and around the southern side of Starvation Hill by the surface below (surface 4). It appears to be a degradation remnant of a meander cutting into the western flank of the hill. Stratigraphy profile 18 was located on this surface, reaching gravels by ~5.6 m.

3.5.1.12 **Surface S4:** (Light Red)

This surface is also a wide, relatively flat expanse, continuing west-northwest. In a similar way to surface S3, it is cut-off around the southern side of Starvation Hill by the next degradation surface below (surface S5). The possibility exists that surface S2 is the uplifted continuation of this surface, as the boundary between these two surfaces is unclear.

Eight stratigraphy profiles were located on this surface (profiles 19 to 26). The profiles show a surface with a thin loess cover typically less than 0.5 m, except for some thickening near the terrace margin to the north, and an interfluve, possibly a dune, where thickness of sediments over the gravel increased to ~5.2 m. Detail of this is shown in figure 3.17.

3.5.1.13 **Surface S5:** (Yellow)

This surface similarly is a wide, relatively flat expanse, continuing much further to the west. Stratigraphy profiles 27 and 28 were located on this surface, both locating gravels virtually to the surface.

Each of these surfaces (surfaces S3, S4, & S5) is bound by distinct terrace margins with much less degradation than the bounding edges of surface S1. In particular the terrace bounding surface S5 to the south, which crosses Oxford Road (see figure 3.7), was the terrace interpreted by Jongens et al. (1999) as possibly formed by a

fault scarp. More detailed mapping makes the morphology more compatible with a simple erosion feature. Eastward, this feature marks the edge of a former meander that cut back around the southeastern side of the hill where surfaces have been consistently truncated, following the line of significant loess thickness. Surfaces S3, S4 & S5 have been surveyed and are discussed further in section 3.7.7.

The area below surface S5 is a wide expanse covering the area to the south of Starvation Hill and extending towards the Eyre River. Four stratigraphy profiles were located on this area (profiles 28 to 31), locating gravels within 0.8 m near the terrace margin, with depth to gravels decreasing to being virtually at the surface within ~70 m distance from the terrace margin, with slight variable thickness expected as a result of drainage related erosion.

3.5.2 Dissection and Gullies:

The erosion channels (shown in figure 3.8) vary greatly over Starvation Hill in terms of width, depth and length of channel. The erosion dissects most of the tilted surfaces, leaving a puzzle for correlation. In some cases deep gullies have developed, usually with streams only visible during or shortly after periods of heavy rainfall or snowmelt.

This would suggest that the erosion has been occurring over a length of years, for the small amount of water flow to have down-cut the structure of Starvation Hill. There are also erosional areas that could have occurred due to landslides or slumps, possibly initiated by undercutting from rivers and streams flowing around the base of the hill.

The general pattern of dissection over Starvation Hill is one of three main erosional valleys, one to the west, one to the northeast, and one to the south-southeast. This pattern may be located and controlled by tectonic folding, discussed in further detail in sections 3.10.2 and 3.11.1.

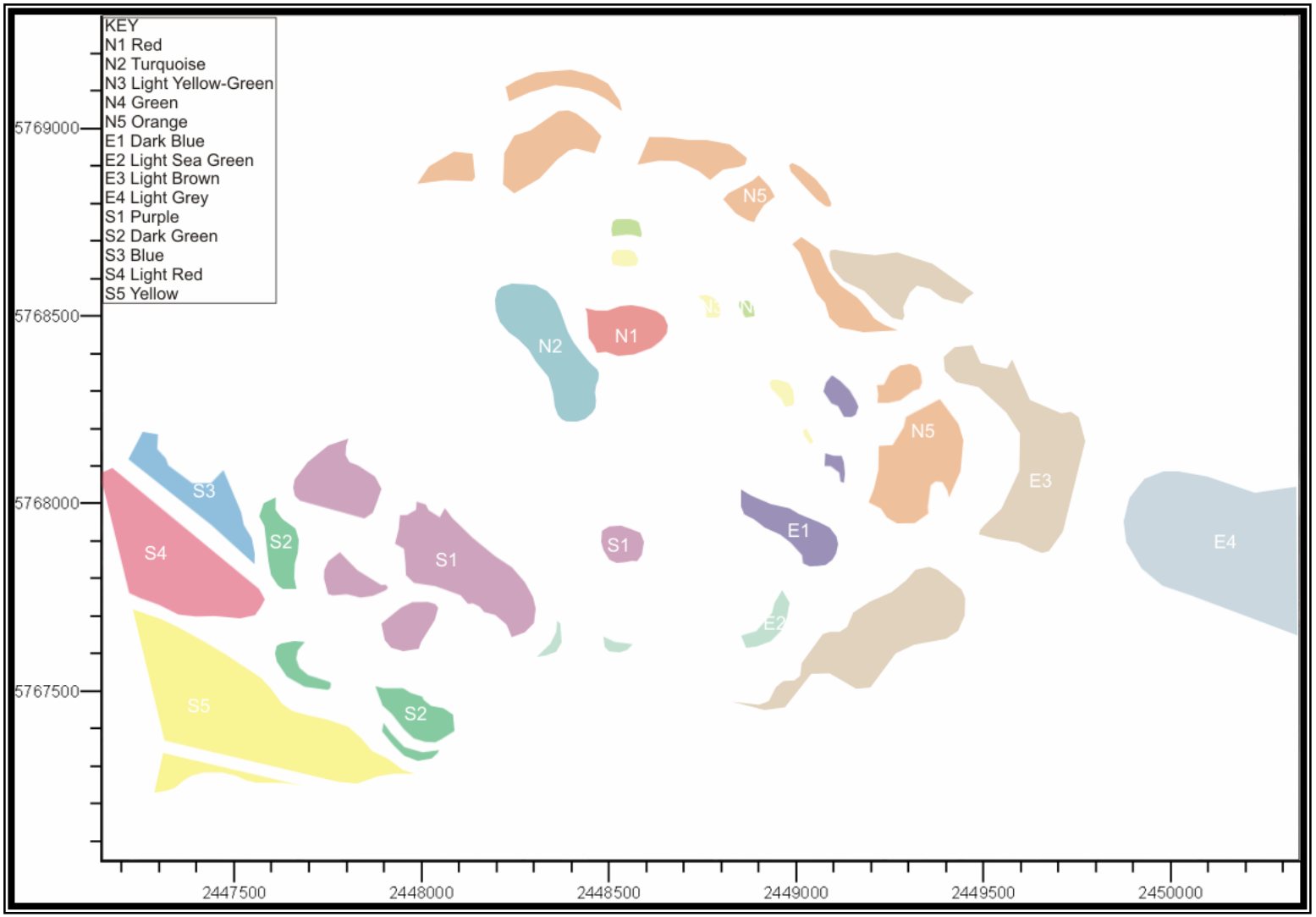
KEY
N1 Red
N2 Turquoise
N3 Light Yellow-Green
N4 Green
N5 Orange
E1 Dark Blue
E2 Light Sea Green
E3 Light Brown
E4 Light Grey
S1 Purple
S2 Dark Green
S3 Blue
S4 Light Red
S5 Yellow
5769000
5768500
5768000
5767500
2447500
2448000
2448500
2449000
2449500
2450000
N5
N2
N1
N5
E3
E4
E1
E2
S3
S2
S4
S1
S1
S5
S2

Figure 3.8 – *Map of terrace margins and erosional channels cutting distinct surfaces on the slopes of Starvation Hill. Terrace margins represented by tic marks.*

3.5.3 Modern Courses and Terrace Systems Relating to the Cust, Ashley, and Eyre Rivers, and Past Drainage Systems Around the West Side of Starvation Hill:

Figure 3.9a shows the current location of the Cust and Ashley Rivers near Starvation Hill. The overlay of terraces and drainage patterns suggests the Ashley River previously flowed south of its current location, across the north flank of Starvation Hill, and south of the Cust Anticline. The Ashley River is currently incised to the north of Starvation Hill and Cust Anticline, inferred by Cowan (1992) as a result of the growth of the Cust Anticline, but may also have been diverted by growth of the Starvation Hill structure.

To the south of the hill is located the Eyre River (figure 3.9b). This river is likely to have caused the degradation terraces along the southwestern and southern flank of the hill, as this system migrated to its present river course. The pattern of terraces suggests the flow of the Eyre was originally oriented southeast, past the southwest corner of the hill. The lower terraces show a change in orientation, suggesting the river flowed eastwards, until the lowest of the terraces in the sequence cuts nearly northeast, eroding into the southeast side of the hill.

Potentially the Waimakariri River could be responsible for the higher surfaces on the southern side of the hill, created during peak glacial maxima, when the Waimakariri River avulsed across the plains at the height of aggradation events.

The orientation of the terrace sequence is suggestive of, in part, the growth of an east-west trending fold axis through the southwest side of Starvation Hill based on slip-off terraces of the Eyre River to the south. The orientation of the fold axis would appear different for the slip-off of the first terrace in the sequence, representing a more northerly orientated fold direction. This is discussed further in section 3.11.1.

To the west and east of Starvation Hill are areas considered to be interfluve deposits. The interfluve to the west of the hill was not studied in detail, with no

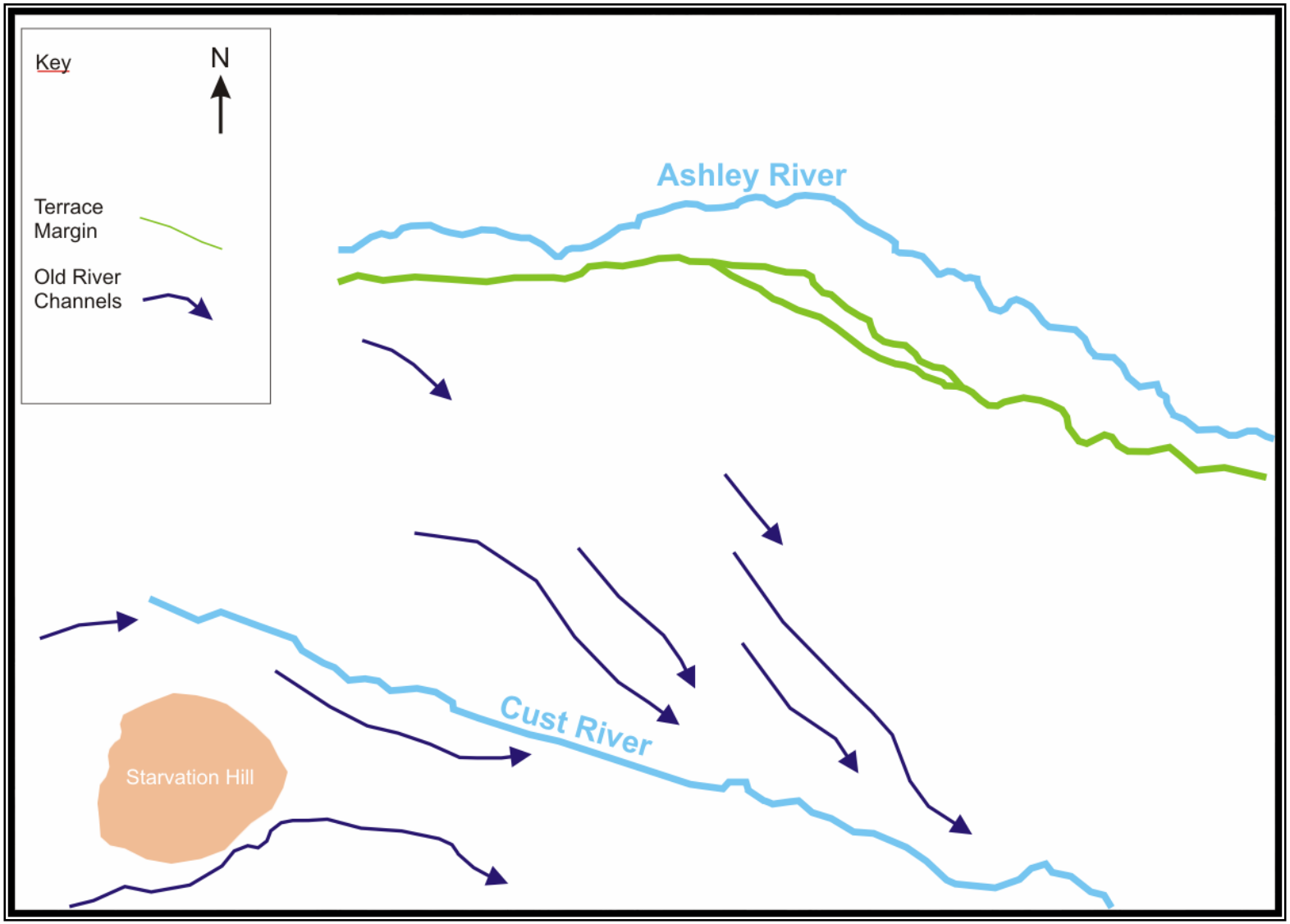
Key
N
Terrace Margin
Old River Channels
Ashley River
Cust River
Starvation Hill

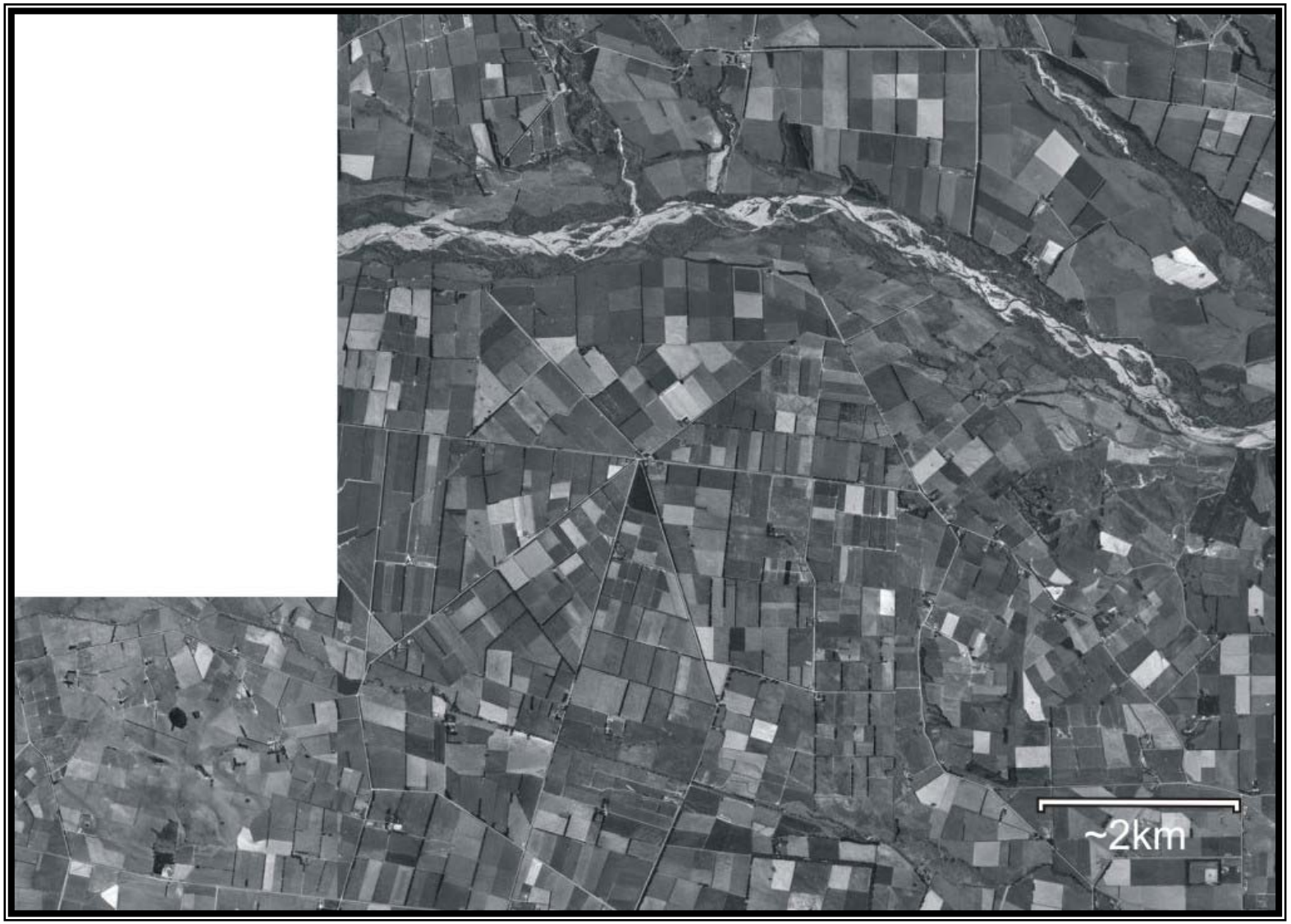

Figure 3.9a - *Aerial photograph of the Starvation Hill area with interpretation overlay of river terraces from the Cust & Ashley Rivers.*

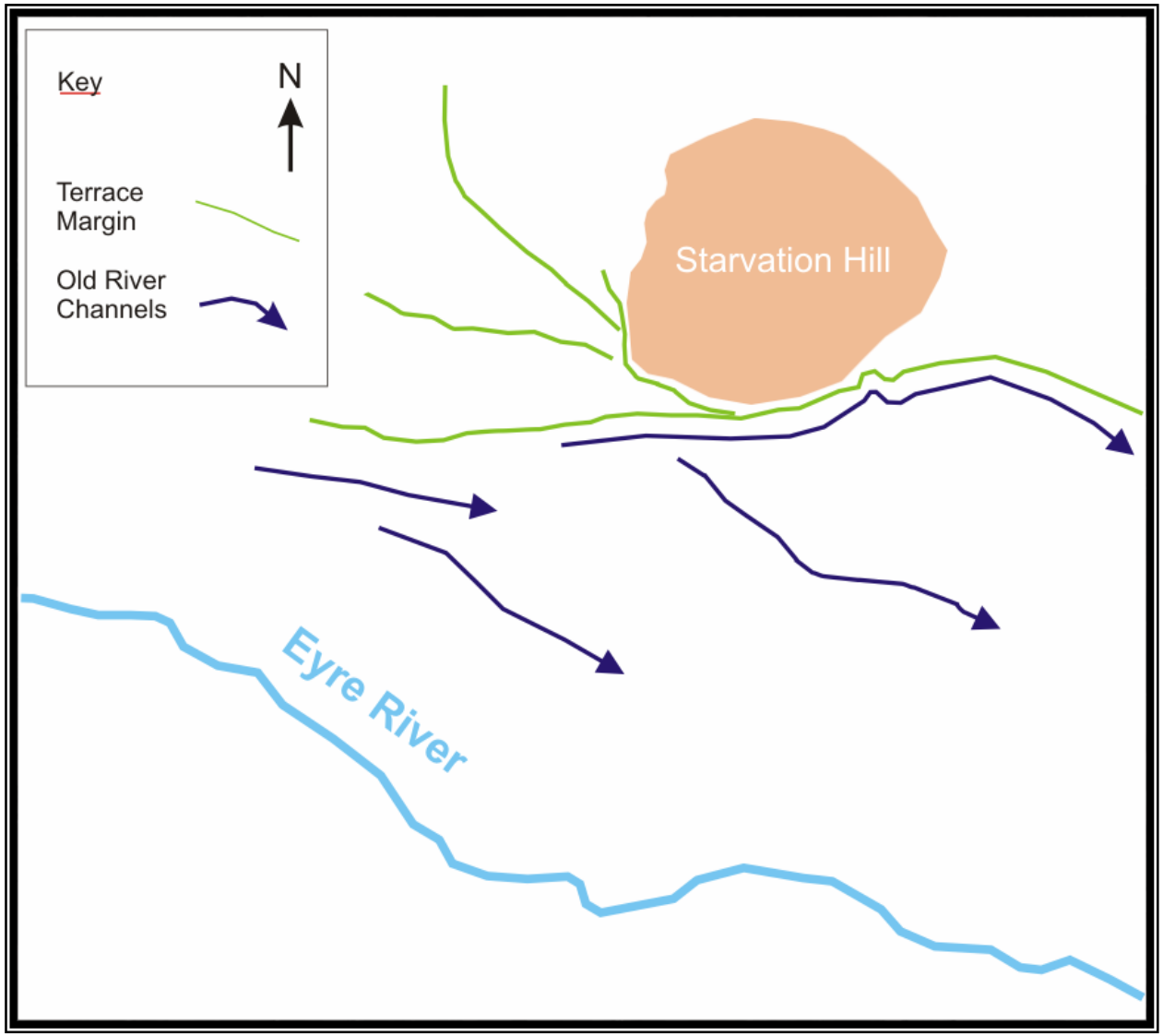
Key
N
Terrace Margin
Old River Channels
Starvation Hill
Eyre River

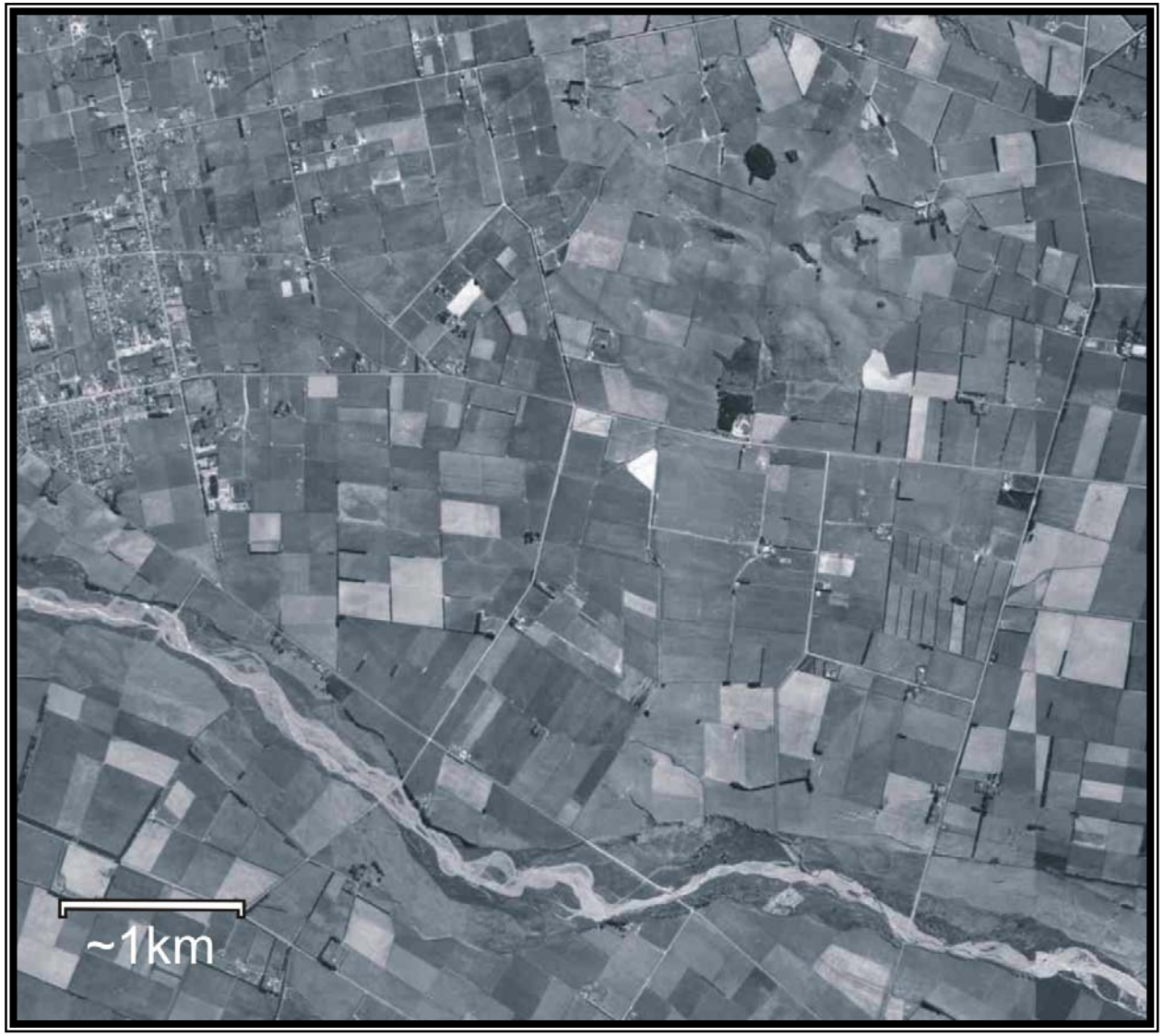

Figure 3.9b - *Aerial photograph of the Starvation Hill area with interpretation overlay of river terraces from the Eyre River.*

stratigraphy profiles surveyed in this area, nor surface remnants found with suitable correlation potential to those focused on around other flanks of the hill. The interfluve to the east of the hill is described in part as surface E4 (section 3.5.1.8).

The interfluves are sections of raised topography left by migration of the rivers away from the hill on both the north and south sides. The eastern interfluve has been preserved potentially as a result of the growth of the eastern hinge of the hill structure, causing rivers to migrate away from this area.

3.5.4 Geomorphology and General Shape of Starvation Hill:

Visual inspection of Starvation Hill has indicated folding and or tilting of the currently warped surfaces. However, the shape of the hill is not a reflection of a simple elongate fold structure, but the shape is crudely triangular in plan view (see figure 3.2). The way in which these reference surfaces are visibly warped is indicative of both a broadly northerly and easterly trending axis. Details of this model of deformation for Starvation Hill are discussed in section 3.11.1

As noted in the introductory section, complex fold structures developed on the intersection of these two trends is characteristic of the North Canterbury structural style as described by Nicol (1991) (see section 1.4.4). The relative timing and evolution of the structure developed on these two trends, together with the underlying system driving the structure, is the subject of both an attempt to arrive at a chronology for the ages of the referenced surfaces by examining the surficial deposits, and more detailed topographic analysis of the deformation of these surfaces.

3.6 Cover Sequence – Present Soil Pattern:

3.6.1 Overview:

As shown in figure 3.10, Starvation Hill and the surrounding area contains a wide variety of soils. The soil map was originally published at a scale of 1:126720, and as such, the boundaries have a low level of precision.

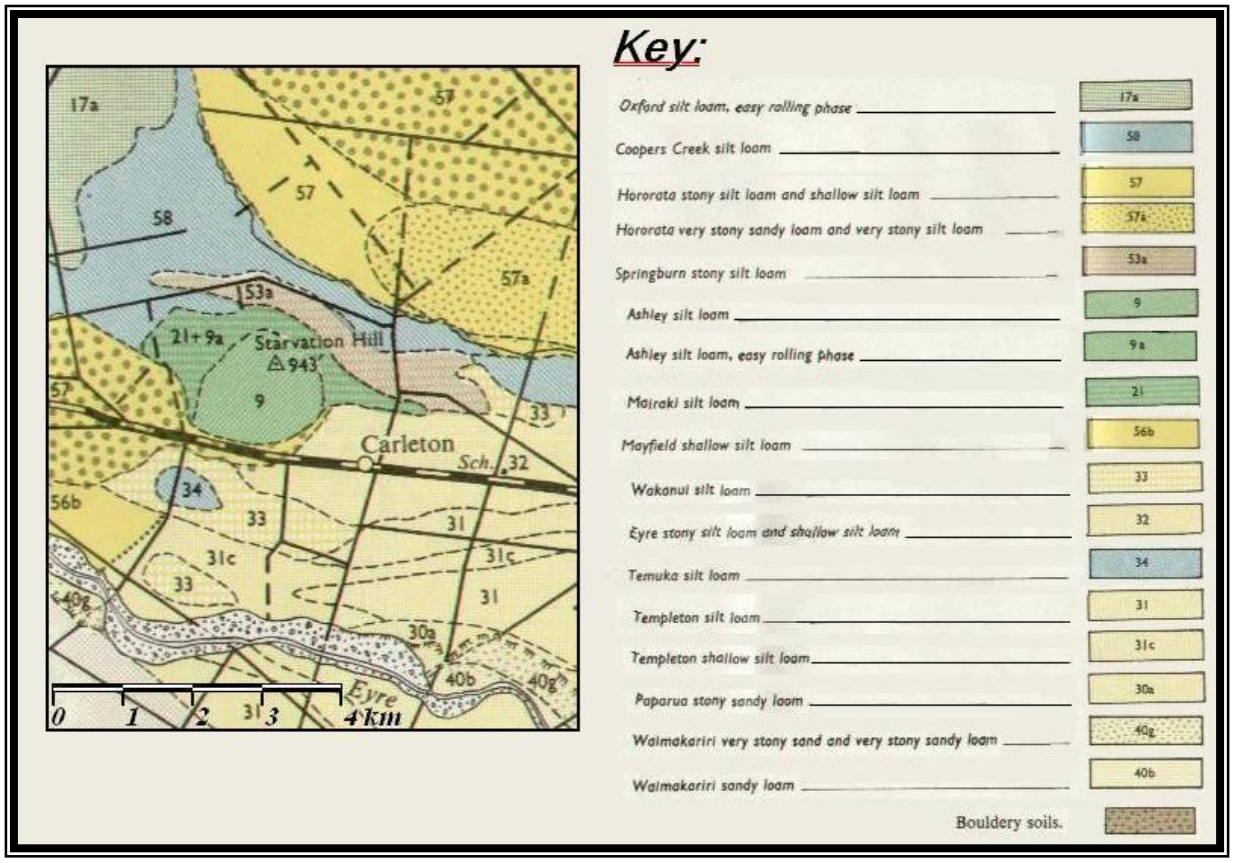

Figure 3.10 – *Soil map detail of Starvation Hill area. Modified from Kear et al. (1967).*

The soils in the Starvation Hill area are predominantly formed in loess. These include the Ashley silt loam (9) covering the majority of the Starvation Hill structure. The Ashley silt loam is described as a soil of the downs, typically formed on loess which overlies older loess units, alluvium or Tertiary sediments. The soils on the higher surfaces of Starvation Hill (N1, N2, N3, N4, E1, E2, & S1) are mapped as Ashley soils.

Surrounding all but the southern side of the hill is a complex of Ashley (9a) and Mairaki (21) soils. The Mairaki soil is considered poorer draining than the Ashley, and as such, would produce features distinctive from the Ashley. Surfaces N5, E3, and S2 appear close to the boundary between this complex and the Ashley soil, however only Ashley soils were noted on these surfaces.

To the northeast of Starvation Hill lies the Springburn stony silt loam (53a), which have a thin veneer of fine textured alluvium or loess overlying gravely greywacke alluvium. This soil may comprise a significant area of surface E4.

The southern side of Starvation Hill is surrounded by a bouldery Hororata stony silt loam and shallow silt loam (57) of fine textured alluvium or loess overlying gravely greywacke alluvium. This soil is considered to include surface S5 of the southwest corner of the field area. It may also include surfaces S4 and S3.

South of the Hororata soil (57) lies the Wakanui (33) and Temuka (34) silt loams formed on fine textured alluvium overlying gravely greywacke alluvium. Further east, to the southeast of Starvation Hill is the Eyre stony silt loam and shallow silt loam (32) typically formed on braided patterns of greywacke alluvium.

3.6.2 Interpretation of the Soil Patterns:

The current channels of the Cust, Ashley and Eyre Rivers, and some indications of their former channels, around Starvation Hill have been shown in section 3.5.3. The pattern of soils around Starvation Hill indicates the location of former river channels. This suggests how periodic migration occurred to both the north and south of the hill, presumably as growth of the structure occurred.

The following interpretations are the result of discussions with P. Tonkin (pers. comm.):

- The Springburn Soil on the northeast side of the hill occurs on either Springston Formation, or more likely Burnham Formation.

- The Hororata soil (57) to the southwest of the hill occurs on a surface which is either of Springston Formation or more probably the Burnham Formation. The younger Wakanui and Eyre soils (33 & 32) to the south of the hill occur on the Springston Formation. This indicates a decreasing age of geomorphic surfaces from the Hororata to the Wakanui and Eyre soils. This has implications for the boundaries of Late Quaternary deposits, discussed in section 3.8.2.

3.7 Cover Sequence – Auger Core Profiles and Stratigraphy:

3.7.1 Introduction:

The landscape of Starvation Hill has been altered by eroding or aggrading rivers and by tectonic tilting, and has changed due to the accumulation or degradation of soil layers. This was largely a consequence of the climatic impact of the Pleistocene.

To determine the timing of tilting on Starvation Hill, an understanding of the build up of cover sequence on the various surfaces of the hill (surfaces described in section 3.5.1) is required. The inferred underlying bedrock or gravely alluvium will have varying amount of loessal soil built up on them, and varying amounts along each individual surface remnant. To determine tilt of surfaces on Starvation Hill, an understanding of the age relationship between the topographic surfaces is needed and to determine the orientation and alignment of the original erosion surfaces that underlie them.

The expectation was that drilling down through the soil cover of the surfaces, to the underlying gravels of the original river terraces, would provide evidence for the interpretation of the surfaces as having a fluvial origin. However, this was rarely the case due to the thick loess cover, as seen in the soil profiles (see figures 3.13a, b and c and section 3.7.3 for discussion of the loess units and Appendix I for stratigraphy profile data).

3.7.2 Methodology:

The auger used is shown in figure 3.11. The 8 cm diameter auger head holds approximately 10 – 25 cm of soil (vertically), depending on soil properties. The auger has six 1 m sections of steel pipe which, together with a handle and the auger head totals 6.45 m in length.

Figure 3.11 – *Hand Auger*
The auger has a maximum length of 6.45 m, as shown.

Ideally, the stratigraphy survey would include two or three profiles on each major section of surface and this would allow identification of variation between the slope of the current topography and the original terrace surface underlying it.

The stratigraphy profiles were drilled first on the highest surfaces, based on the assumption of thickest sediment cover being on these slopes. The higher surfaces had a loess cover of more than 6.45m, however lower parts of the hill were found to have loess cover at least as thick.

A constraint to this aspect of the study was that as it was not possible to drill more than 8 to 10 m per day, and as each deep hole of 4+ m took between 4 and 6 hours, the number of profiles was limited. The comprehensive stratigraphy survey initially envisioned was soon replaced.

Selected higher surfaces were drilled to insure the assumption of thick loess cover was correct, and lower slopes on the northeast and southeast sides were profiled to map the extent of the loess cover.

The locations of the stratigraphy profiles are shown in figure 3.12. The focus of the profiles became the southwest corner, where surfaces S3, S4, and S5 are separated by clearly distinguished terrace boundaries of a flight of terraces dropping down to the south. These surfaces were considered likely to have thin loess cover over gravely alluvium. The profiles in this area are discussed further in section 3.7.7. More detail of the underlying gravels is given in section 3.8.

3.7.3 Auger Core Profiles:

The profiles (figures 3.13a, b, & c) were interpreted from the auger cores. Appendix I contains profile data. Some profiles recorded depth to gravel (if reached) while others record soil stratigraphy.

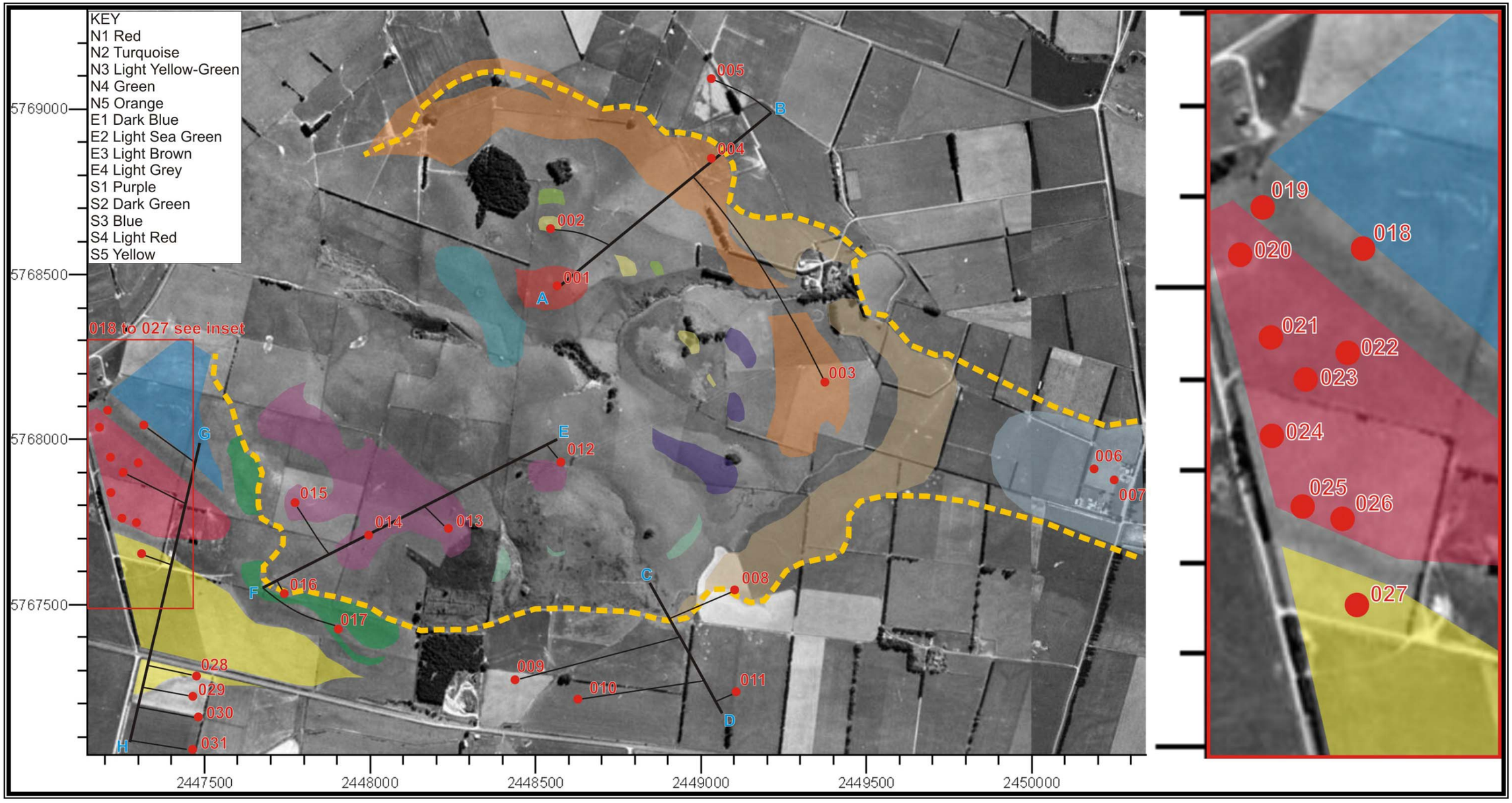

Figure 3.12 – *Location of Soil Profiles.*
Profile sites became focused on the southwest corner of Starvation Hill, see inset, right-hand side. Profile 18 on Surface S3, Profiles 19 to 26 on Surface S4, and Profile 27 and 28 on Surface S5. Lines A-B, C-D, E-F, & G-H represent approximate cross-sections showing the relative heights of profiles projected onto these lines. The cross-sections are shown in figures 3.13a, b & c.

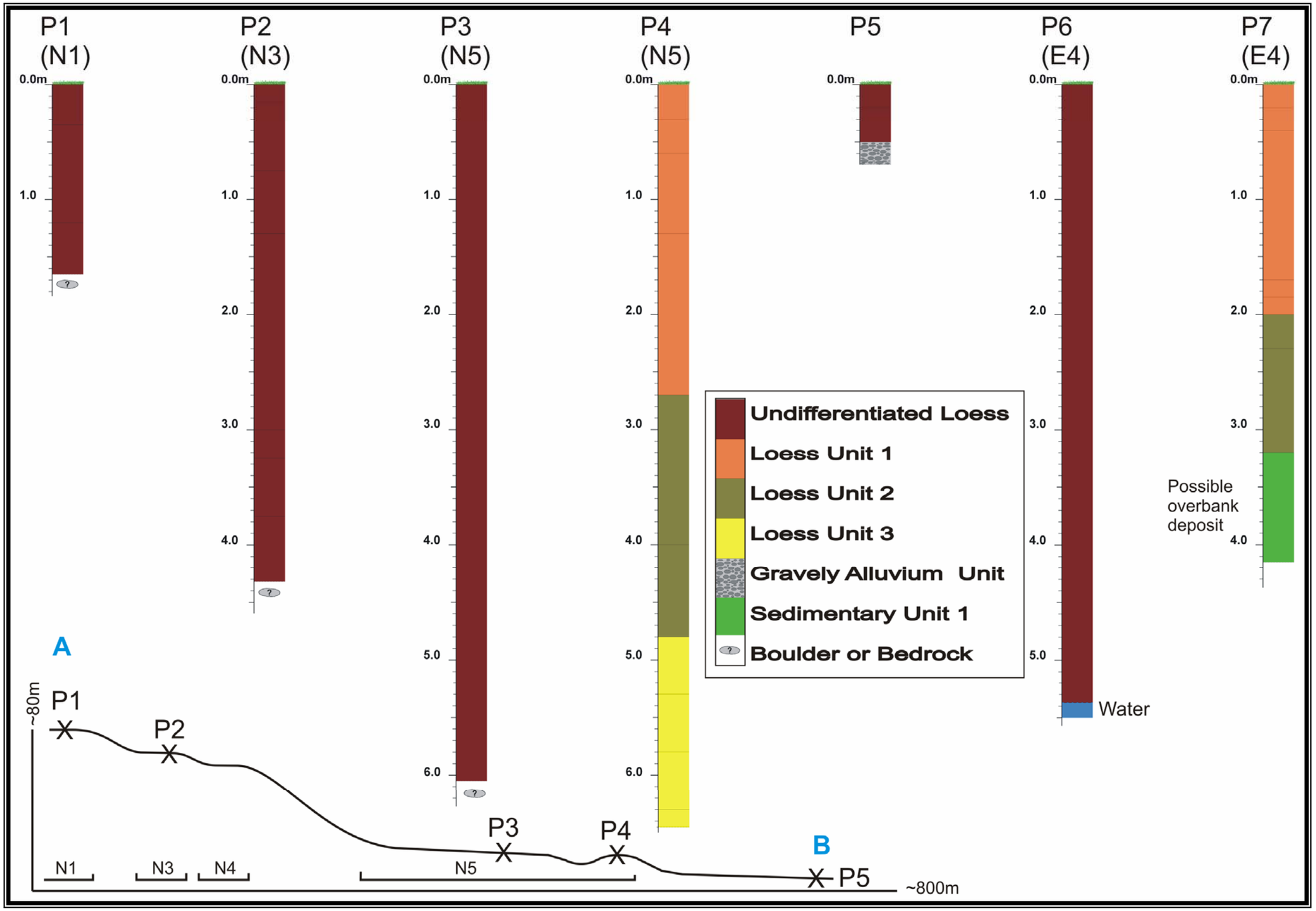

Figure 3.13a – *Auger Core Profiles P1 to P7. See figure 3.12 for profile locations and location of line A-B. See Appendix I for profile details. Surface profiled shown in brackets.*

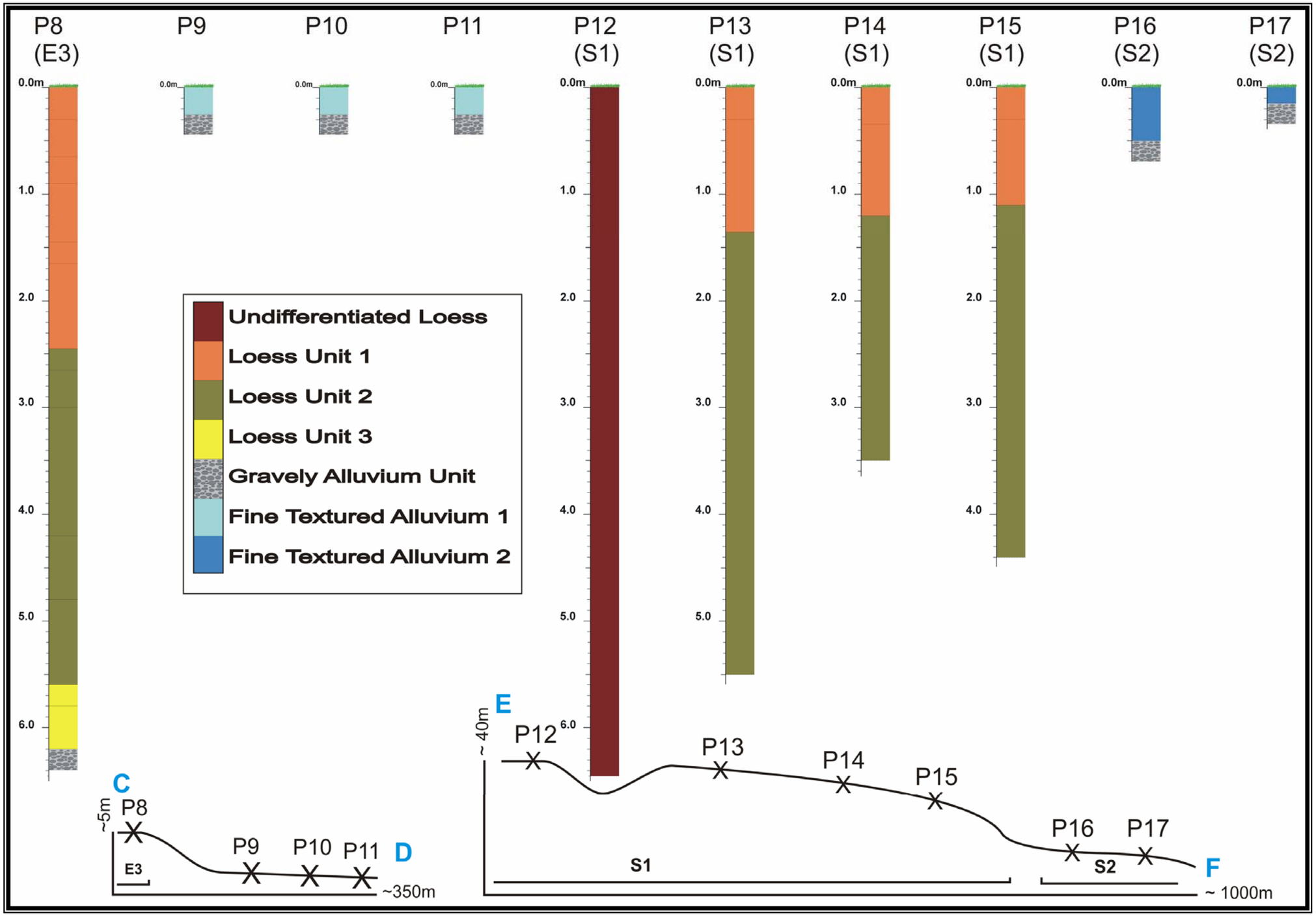

Figure 3.13b – *Auger Core Profiles P8 to P17. See figure 3.12 for profile locations and location of lines C-D & E-F. See Appendix I for profile details. Surface profiled shown in brackets.*

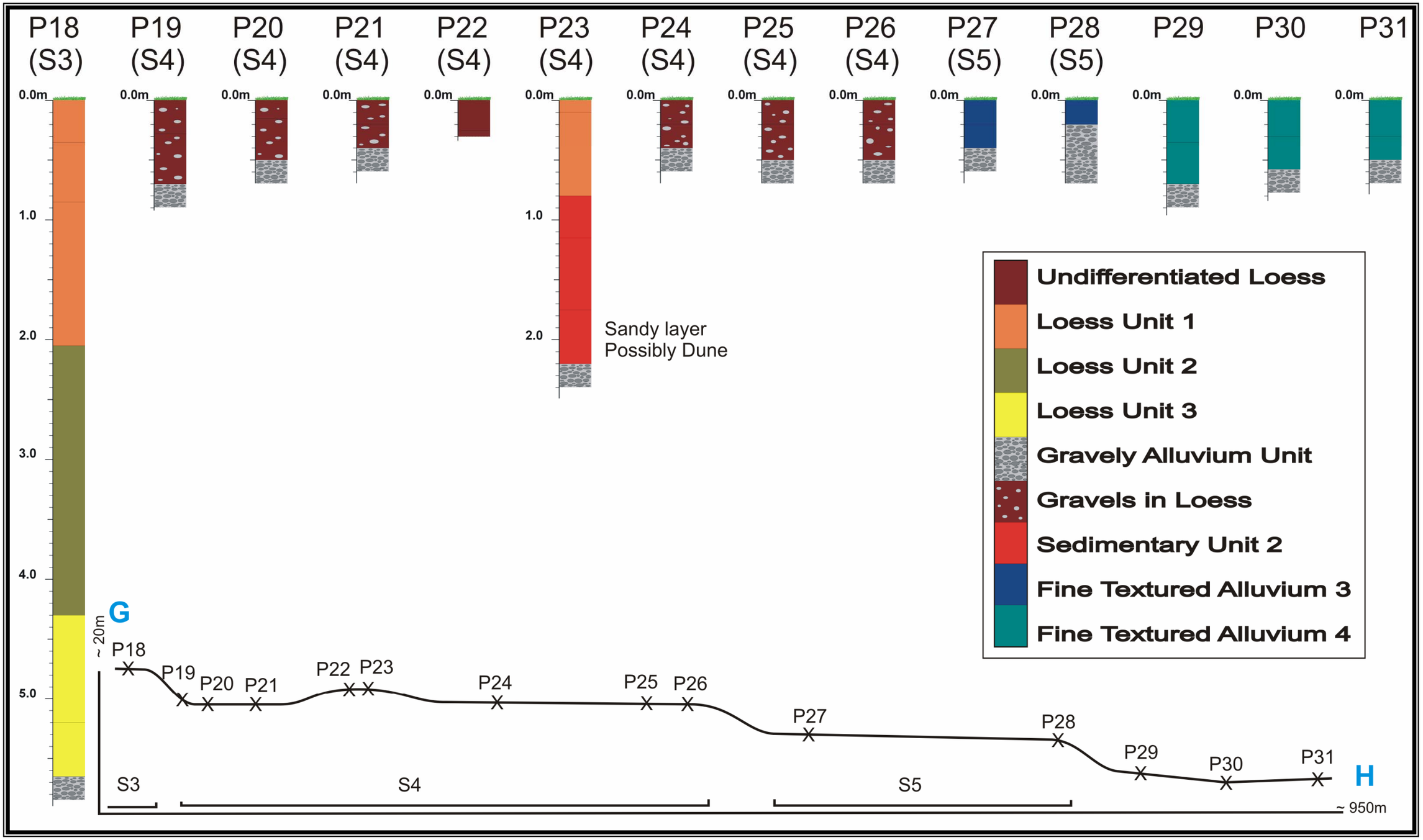

Figure 3.13c – *Auger Core Profiles P18 to P31. See figure 3.12 for profile locations and location of line G-H. See Appendix I for profile details. Surface profiled shown in brackets.*

3.7.4 Starvation Hill Loess Cover Stratigraphy:

Figures 3.13a, b & c show the variation in loess cover over Starvation Hill and surrounding areas. The majority of the hill is covered in a thick blanket containing up to three loess units, more than 6.45 m thick.

The drilling of some cores was stopped by rock, which was unable to be differentiated between an in situ rock and a rock deposited amongst the loess. These rocks are inferred to be basalt boulders, which were seen deposited within the loess in the side of a pit. The pit was located on the southwest side of the hill between surfaces S1 and S2

The stratigraphy in some cores was not recorded. Up to three loess units, differentiated on soil morphological criteria, could be identified in various profiles, separated by a recognisable colour change marking a hiatus in loess deposition. Figure 3.14 shows a generalised morphology of the three stratigraphic units within the loess, described in section 3.7.5.

Soil augers have limitations in that they only survey the diameter of the core (8 cm for this auger) and in the process of extraction, remould the sample, inevitably obscuring some morphological properties.

Many boundaries between horizons are gradational and often difficult to judge until a contrasting horizon has been drilled into.

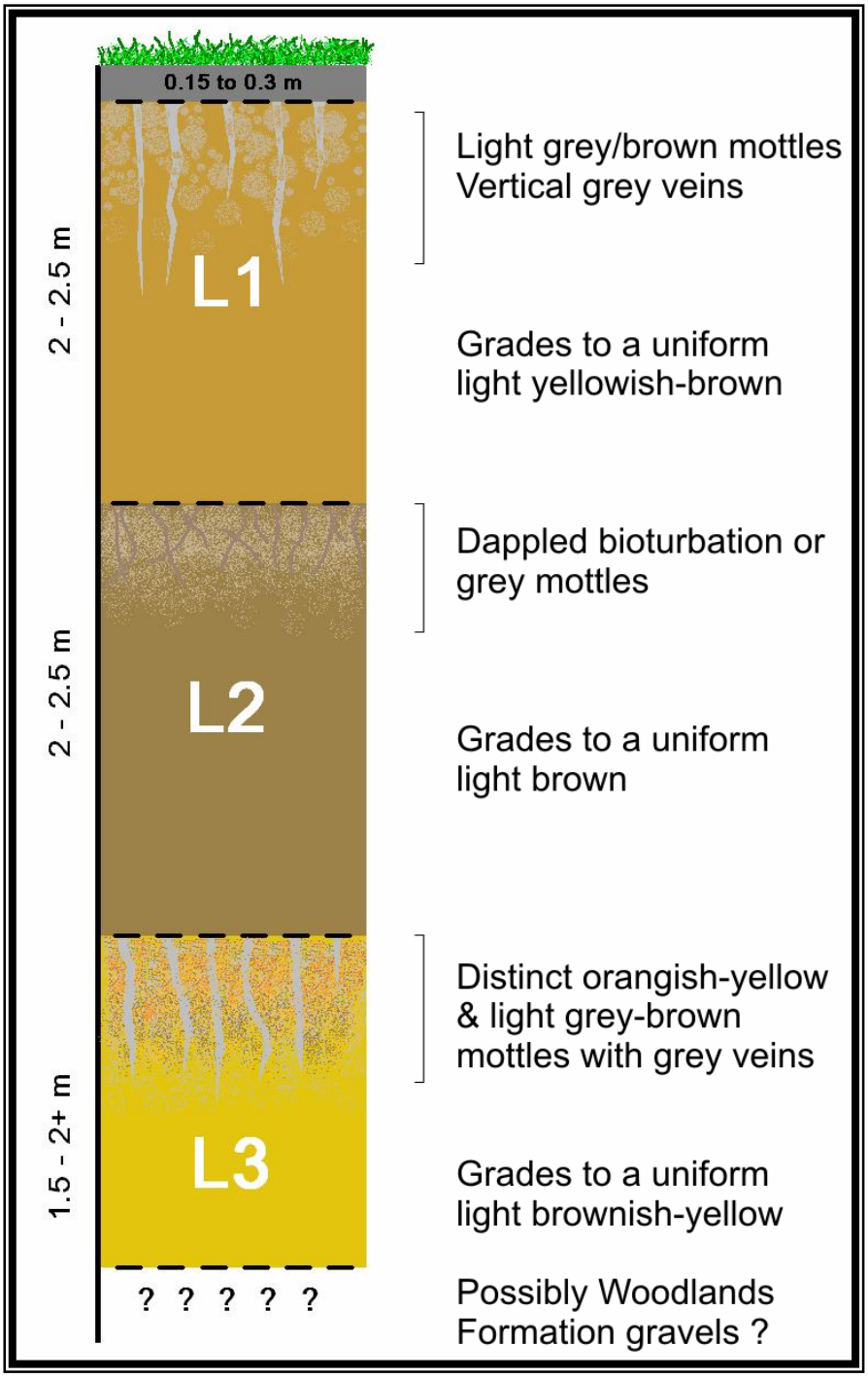

Figure 3.14 – *General morphology of the three loess units found on Starvation Hill*
This general morphology is found on the majority of the hill structure, with variation as discussed above. See section 3.7.5 below for descriptions of loess units.

3.7.5 Descriptions of the Loess Units of Starvation Hill:

Loess Unit 1 (2 – 2.5 m):

Consists of a topsoil of 0.15 to 0.3 m, underlain by a zone of light grey/brown mottles extending to a maximum depth of 1 m, about halfway through the unit. Vertical to sub-vertical grey veins are also typical in this zone, becoming less common and less distinct with depth. The lower half of this unit grades to a uniform light yellowish-brown colour.

Loess Unit 2 (2 – 2.5 m):

Consists either of a zone of dappled bioturbation, or grey mottles extending to a maximum depth of 0.5 m, about quarter of the depth of the unit. The lower section grades to a uniform light brown colour, darker brown than Loess 1.

Loess Unit 3 (1.5 – 2+ m):

Consists of distinct orangish-yellow and light grey-brown mottles in the top 0.5 m, with grey veins also present, and extending down through the top 0.8 m. This unit grades to a uniform light brownish-yellow colour. On some of the lower surfaces of Starvation Hill, gravels inferred to be of Woodlands Formation are underlying this loess (see Soil Profiles), however on the slopes of the hill, the base of this loess was too deep for the auger, leaving the unit underlying the loess as unknown, presumably Woodlands Formation gravels or bedrock.

3.7.6 Correlation with Loess of the Cust Area:

The loess stratigraphy of Starvation Hill appears to correlate with that of the Cust area (Tonkin, pers. comm.). The loess of the Cust area has been studied to provide age correlations with other sites in the South Island (Tangmar, 1987; Berger et al. 2001). The site of study is an exposed section of loess in a quarry ~7.5 km south of the eastern end of the Cust Anticline and ~15 km east-southeast from Starvation Hill.

At the site, the vertical 6.5 m of loess comprises three or four loess-paleosol units resting on outwash gravel (Trangmar, 1987). The outwash gravels are mapped by Gregg (1964) as the Woodlands Formation (see section 1.6.3.2.), with an age of c. 150,000 years (Wilson 1989).

Trangmar (1987) originally recognised four loess units as shown in figure 3.15, and discussed the possibility of loesses 2 and 3 representing one major accumulation episode.

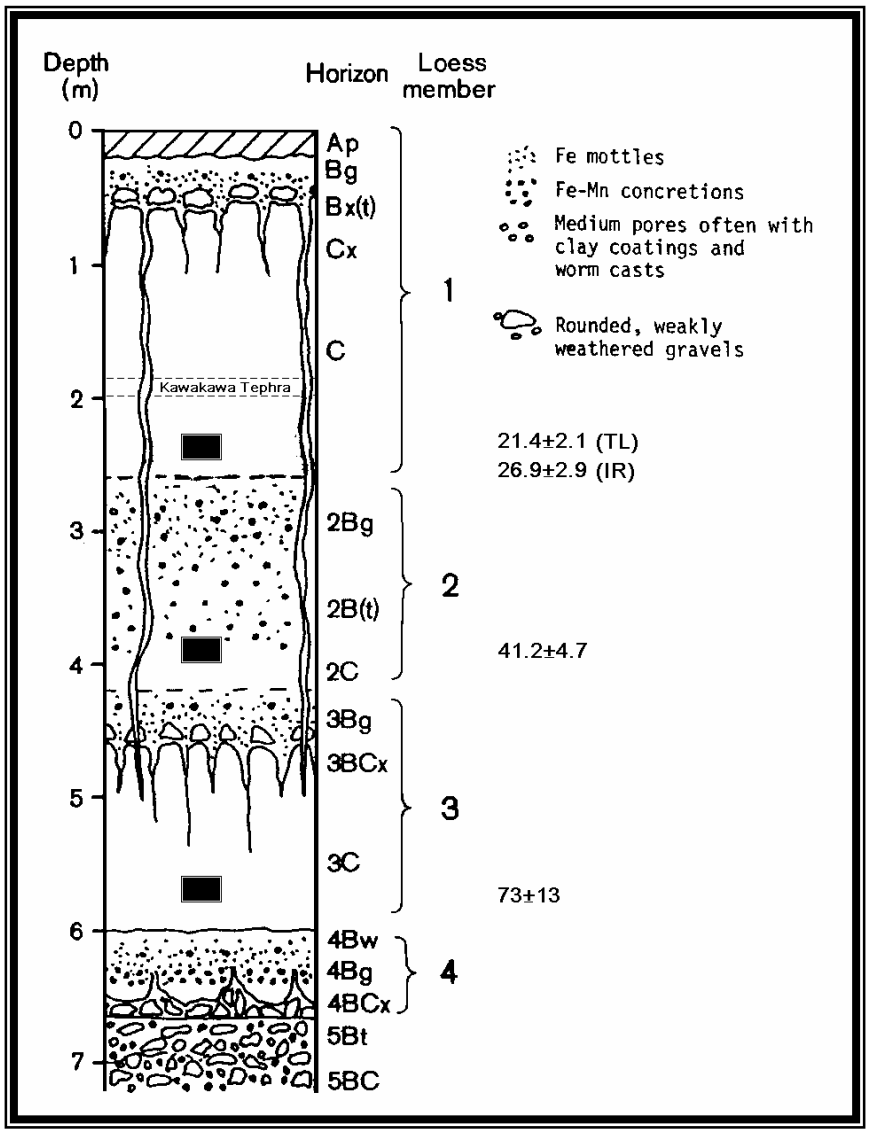

Figure 3.15 – *Soil-Stratigraphic Section for the Cust Site.*
Modified from Trangmar (1987).
Luminescence age estimates from Berger et al. (2001) are shown.

Berger et al. (2001) conducted luminescence age dating on four samples of the same site, as shown in figure 3.15 and discussed the site as potentially representing only two or three loess units, with Trangmar's (1987) L4 unit being an overbank deposit in which a soil formed. Of the younger three units, L2 was considered as a local derivation from erosion of a nearby gravel formation and its boundary with L3 was not discussed. Berger et al (2001) also gave an inferred maximum age of the entire loess stratigraphy of the site as c. 120-125 ka, or possibly younger than c. 80 ka, based on correlations of interglaciation periods with marine (oxygen) isotope stages.

The loesses of Starvation Hill are inferred to correlate with the top three loesses of the Cust area profile, giving a maximum age for loess deposition of ~73 ka.

3.7.7 Southwest Terraces Survey:

A total station (integrated theodolite and electronic distance measurement instrument) was used to survey changes in topography across surfaces S3, S4 and S5 as shown in Figure 3.16. The surfaces are separated by clearly distinguished terrace boundaries of a flight of terraces dropping down to the south. The terrace boundaries extend westward, away from Starvation Hill. The possibly of varying ages of gravels underlying the surfaces of each terrace was hoped to provide information as to the history of aggradational periods on this side of the hill (see section 3.8.2).

These three surfaces were of particular interest due to two boundaries of the Late Quaternary map (see figure 3.18) and conflicting boundaries of the soils map (see figure 3.10) crossing this area. The layout of the survey was chosen to provide line of sight through hedges and other obstacles.

Combining the topographical data with the stratigraphy profiles, figure 3.17 shows a general cross-section of a segment of the surfaces S3 and S4. The figure shows in

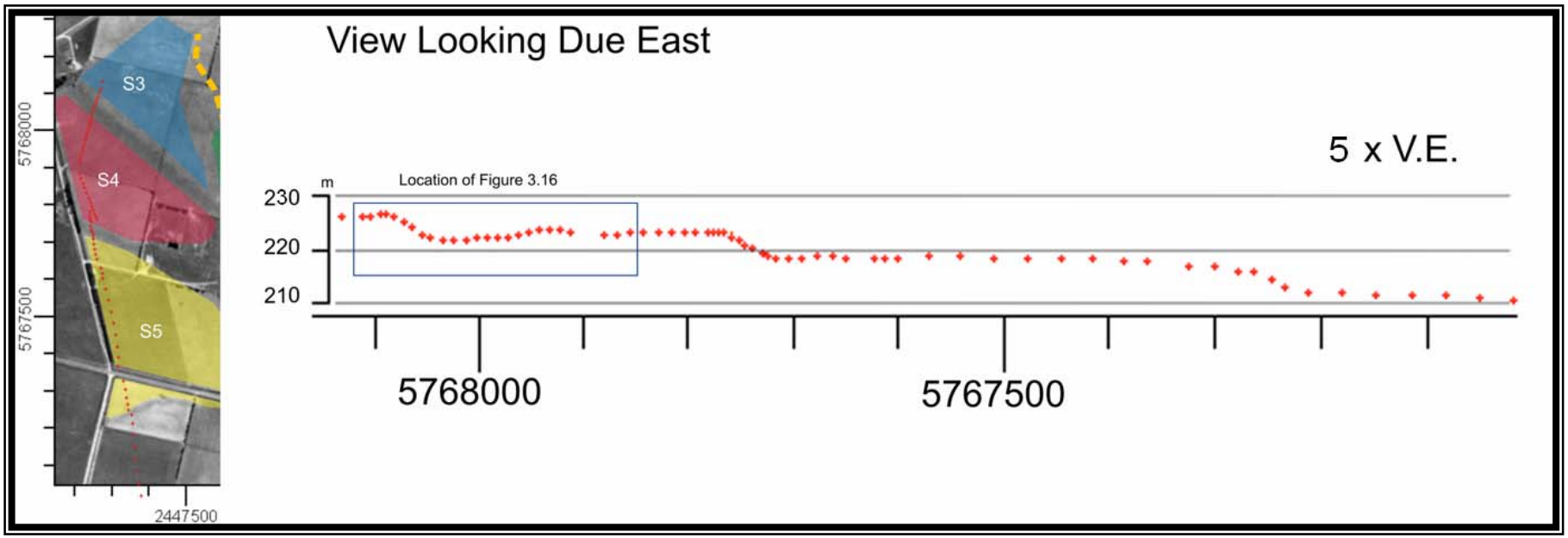

Figure 3.16 – *Survey location over the SW corner of Starvation Hill.*

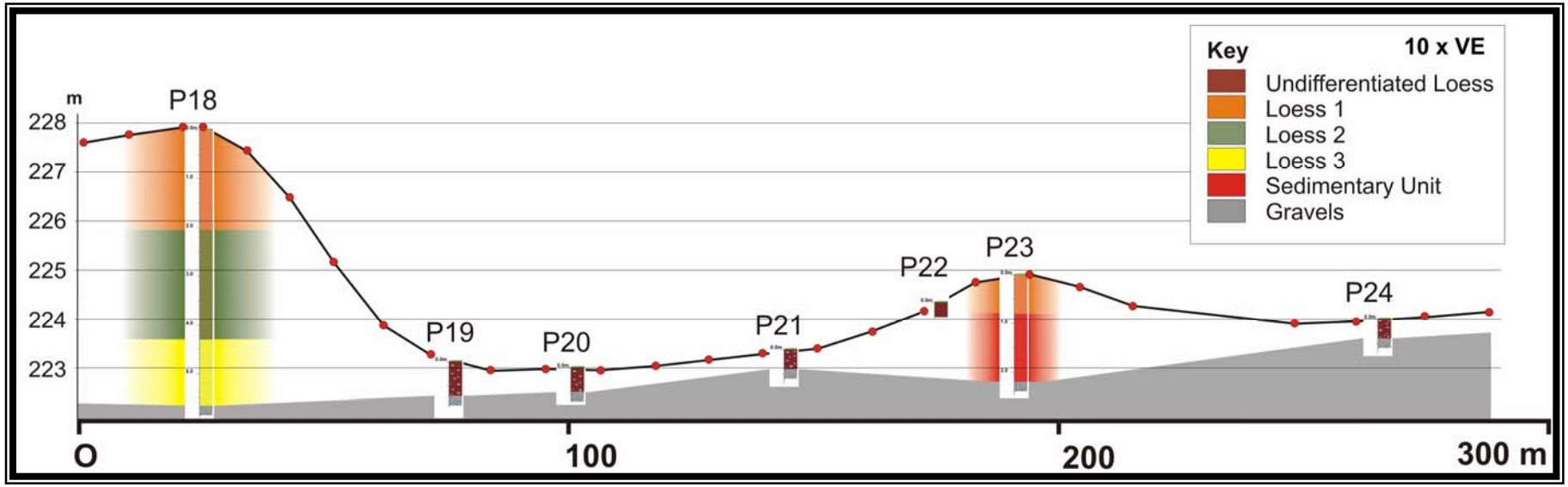

Figure 3.17 – *Detail of survey.*
For location, see figure 3.15. Gravels are thought to be of Woodlands Formation, see section 3.7.
Projection of loess layers inferred only.

detail the 5.8 m cover of loess on the highest surface, S3, an interfluve or dune formation on part of surface S4, and little loess cover on the remainder of S4.

3.7.8 Interpretation of Profiles :

The loess cover of Starvation Hill is correlated with that of the Cust site which has an age of ~73,000 years old. Based on the three loess units of Starvation Hill (L1, L2, & L3) correlating in age with loess units of the Cust site (see section 3.7.6), the formation of L3 at Starvation Hill began ~73,000 years ago which is correlated with the assigned basal age of the Windwhistle Formation (see section 1.6.3.3), of c. 70,000 years ago (Wilson, 1989).

The formation of L1 at Starvation Hill began either ~26,900, or ~21,400 years ago, correlated with the Burnham Formation (see section 1.6.3.4), which has a basal age of c. 27,000 years ago and culminated at c. 15,000 years ago (Wilson, 1989). The formation of L2 of Starvation Hill began ~41.200 years ago, which does not correlate with the basal age of any currently recognised gravel formation.

Summary of correlations of loess units at Starvation Hill:

- L1 – Burnham Formation
- L2 – Unrecognised Formation
- L3 – Windwhistle Formation

Underlying L3 is inferred to be gravels of the Woodlands Formation.

The implications of the three loess units of Starvation Hill (see section 3.7.4) is that most of the topography of Starvation Hill on which loess has accreted, has to be older than ~73,000 years ago, around the time of the last glaciation (Otiran).

The following inferences are based on the stratigraphy overlying the gravely alluvium, or inferred gravely alluvium or bedrock where the alluvium was not found. The stratigraphy is determined from auger core profiles:

- On the northern side of Starvation Hill, the thick loess cover of three loess units on the higher slopes of the hill, is found extending to the base of the hill (see profile 4, figure 3.13a).

- Projecting from the eastern side of Starvation Hill is a low ridge interpreted as an interfluve which formed a divide between ancient channels, discussed in section 3.5.3. Surface E4 makes up the majority of this interfluve.

    - The stratigraphy of profile 7 on surface E4 (see figure 3.13a) shows only two loess units (L1 and L2) grading into underlying sandy sediments of either alluvial or bedrock origin. These sediments are interpreted as either depositional or erosional, on which loess units L2 then L1 are deposited. The underlying stratigraphy of surface E4 is inferred to have been eroded and modified later than that of surface E3 comprising three loess units (see profile 8, figure 3.13b). The sandy sediments of profile 7 are inferred as contemporaneous in age with that of the third loess unit (L3).

- On the southeast side of the hill, on the southern extent of surface E3, 6.2 m of loess cover was drilled through, in which were recognised L1, L2, & a thinned expression of L3. The surrounding plains show no loess cover, with gravels virtually to the surface (see profile 8 compared to profiles 9, 10, and 11, figure 3.13b).

- On the southwest corner of Starvation Hill and extending southwest, a descending sequence of surfaces from S1 to S5 is recognised. Surface S1 has thick loess deposits (see profiles 12, 13, 14, and 15, figure 3.13b). The stratigraphy underlying the third loess unit (L3) on surface S1 was never reached.

- Surface S2 has a thin 15 – 20 cm veneer of fine textured alluvium overlying gravely alluvium (see profiles 16 and 17, figure 3.13b). The relationship

between this surface and those to the west (S3, S4 & S5) is unclear. The southern part of this surface may be the uplifted continuation of a lower surface such as surface S4, however this was not evident in the field. Surface S2 may also be the result of incision into a gravel formation. If surface S2 is uplifted, it is possibly the result of a second fold developing across the hill structure, discussed further in section 3.11.1.

- Surfaces S3, S4, and S5 are separated by clearly distinguished terrace boundaries of a flight of terraces dropping down to the south. This flight of terraces was surveyed, shown in figure 3.16, with detail of surfaces S3 and S4 shown in figure 3.17.

    - Surface S3 has a 5.8 m loess cover in which were recognised L1, L2, & a thinned expression of L3 (see profile 18, figure 3.13c). The gravely alluvium underlying the loess is inferred to be of the Woodlands Formation based on the thickness of the loess cover.

    - Surface S4 has a dune formation (see profile 23, figures 3.13c and 3.17) of sandy sediments overlain by L1, and a ~40 cm cover of gravely loess on the remainder of the surface overlying gravely alluvium.

    - Surface S5 has a 20 to 40 cm cover of fine textured alluvium over gravely alluvium. The plains to the south of this surface have a 50 to 70 cm cover of fine textured alluvium over gravely alluvium, see figure 3.13c.

3.8 Cover Sequence – Late Quaternary:

3.8.1 Overview:

Figure 3.18 shows a section of the Wilson (1989) map showing the division and labelling of Late Quaternary surfaces. See section 1.6.3 for descriptions of the units discussed. The figure shows Starvation Hill with Woodlands Formation on the west and east sides which are interpreted as interfluve surfaces as discussed in section 3.5.3.

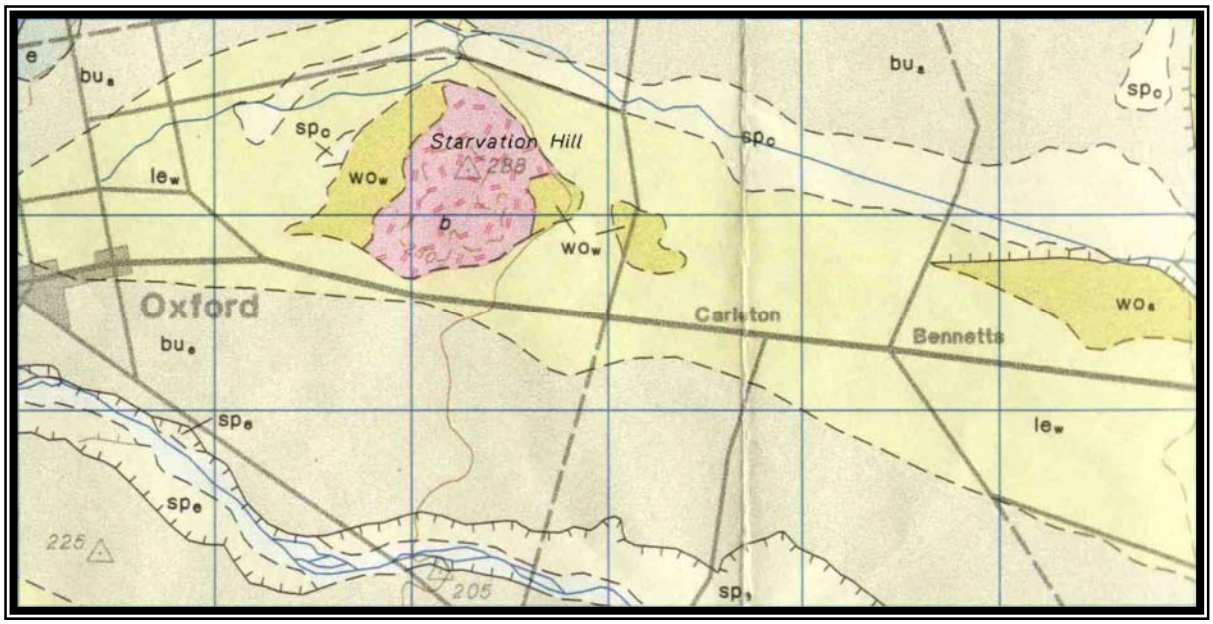

Figure 3.18 – *Detail of geological map from Wilson (1989). Woodlands Formation* (wo)*, Whindwhistle Formation* (le)*, Burnham Formation* (bu)*, and Springston Formation* (sp)*, subscript letter represents suggested river catchment (Ashley* ($_a$)*, Cust* ($_c$)*, Eyre* ($_e$)*, and Waimakariri* ($_w$) *Rivers). Blue grid equals 1 km^2 divisions.*

Wilson (1989) bases the boundary of the Woodland Formation on a typical loess thickness of ~6m+, and gravels typically oxidised to a depth of 2 or 3 mm.

The Windwhistle Formation is considered the highest aggradation surface below the Woodlands Formation, and typically has a loess cover of 0 – 4 m (averaging about 1m). There is a marked difference between the Windwhistle and Woodlands

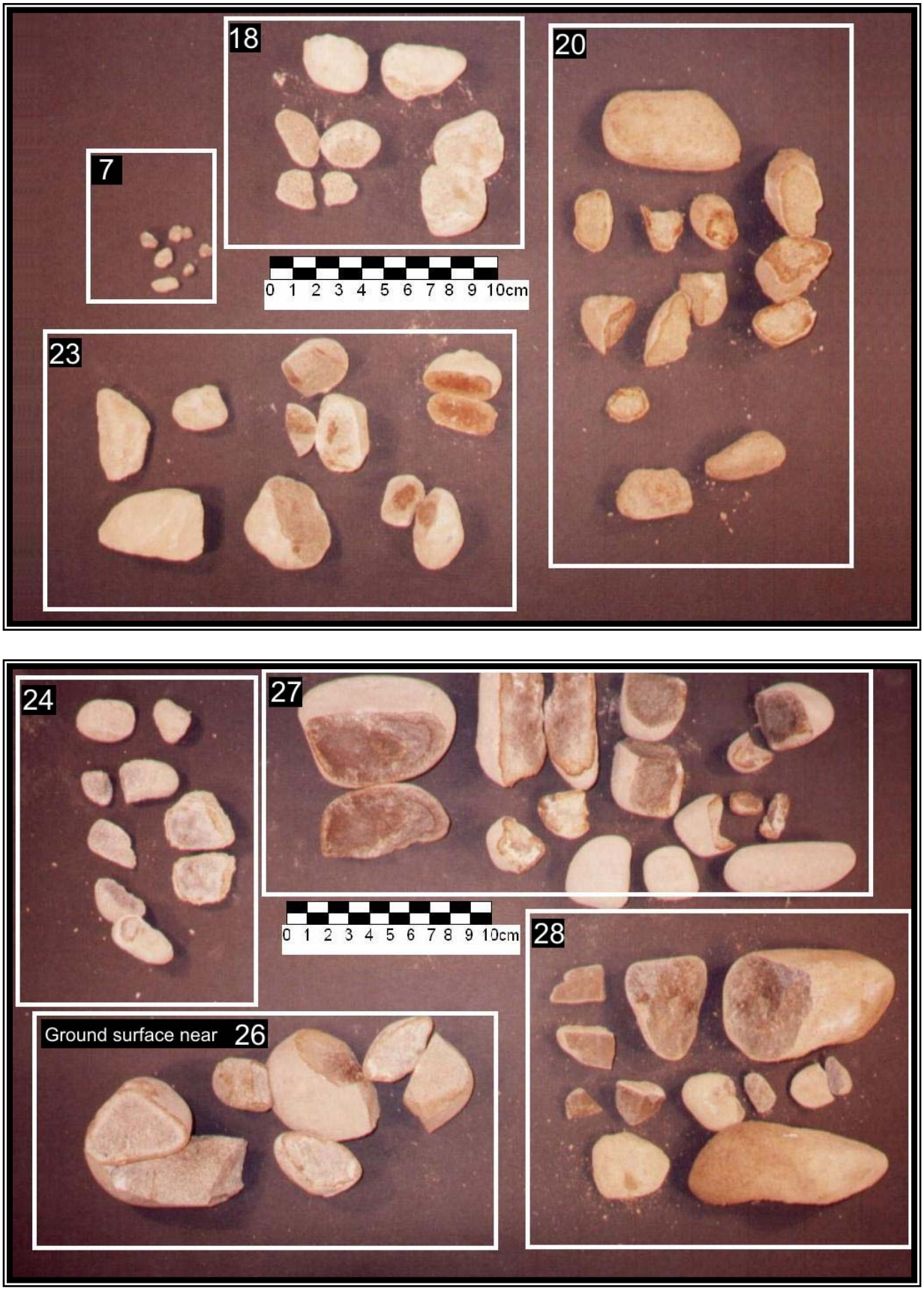

Figure 3.19a & b – *Weathered Gravels – Sample numbers represent soil profile locations*

Formations as the former is lighter in colour, especially in the matrix material, and individual clasts are fresher, without the marked weathering rinds of the Woodlands Formation.

The Burnham Formation is discussed as extremely difficult to positively identify, due to the significantly smaller timeframe of formation, resulting is substantially less material being spread over a similar area to the Windwhistle and Woodlands Formations. The Burnham Formation unpredictably has 0 – 3m of loess cover.

Figures 3.19a &b show samples of gravels collected from the base of soil profiles on surfaces S3, S4 and S5 and pebbles from a depth of 2.9m in profile 7 on surface E4. The thick weathering rind of all but sample 7 implies Woodlands Formation (Tonkin, pers. Comm.).

There were insufficient gravels sampled to provide detail of the weathering profile of the gravels underlying the surfaces on the southwest side of Starvation Hill. Weathered gravels of older formations such as the Woodlands Formation may have been incorporated into earlier aggradation episodes.

3.8.2 Late Quaternary Interpretation:

Gravels under the third loess unit, L3, around the base of Starvation Hill being of the Woodlands Formation would be compatible with a penultimate glaciation aggradation, onlapping the rising flanks of a growing anticline and grading to the high surfaces. The gravels under L3 were only found in two stratigraphy profiles (profiles 8 and 18).

The following interpretation of Late Quaternary features of the Starvation Hill area are shown in figure 3.20. These interpretations are based on assumptions that could be improved with further studies of the cover sequence:

- The base of L3 was not reached on the north side of Starvation Hill which has a cover of all three loess units extending to edge of the surrounding plains. The plains on the north side of the hill are mapped as Windwhistle Formation by Wilson (1989), however the soils of this area form on Springston, or more likely Burnham Formation.

- The low ridge forming an interfluve to the east of Starvation Hill (surface E4) is underlain L1 and L2, which overlie a Windwhistle equivalent deposit of sandy sediments. This area appears to be marked as Woodlands Formation by Wilson (1989). This eastern ridge is indicative of the eastward propagation and emergence of the Starvation Hill structure.

- The ~25 cm fine textured alluvium overlying gravely alluvium of the plains to the south of the hill, along with inferences from the soil map, is suggestive of either Burnham or Springston Formations. Wilson (1989) marks this area as Windwhistle Formation.

- On the southwest slope of the hill structure, the abrupt change from over 5 m of loess cover of surface S1 to a 15 to 50 cm cover of fine textured alluvium overlying gravely alluvium at on surface S2 is indicative of incision into an older formation, probably Woodlands.

- The southern boundary of surface S3 is inferred to be the boundary of the Woodlands Formation. This is based on the criteria of the Woodlands Formation by Wilson (1989) being oxidised gravels typically overlain by ~6 m of loess. For surface S3, there was 5.8 m of loess overlying weathered gravels.

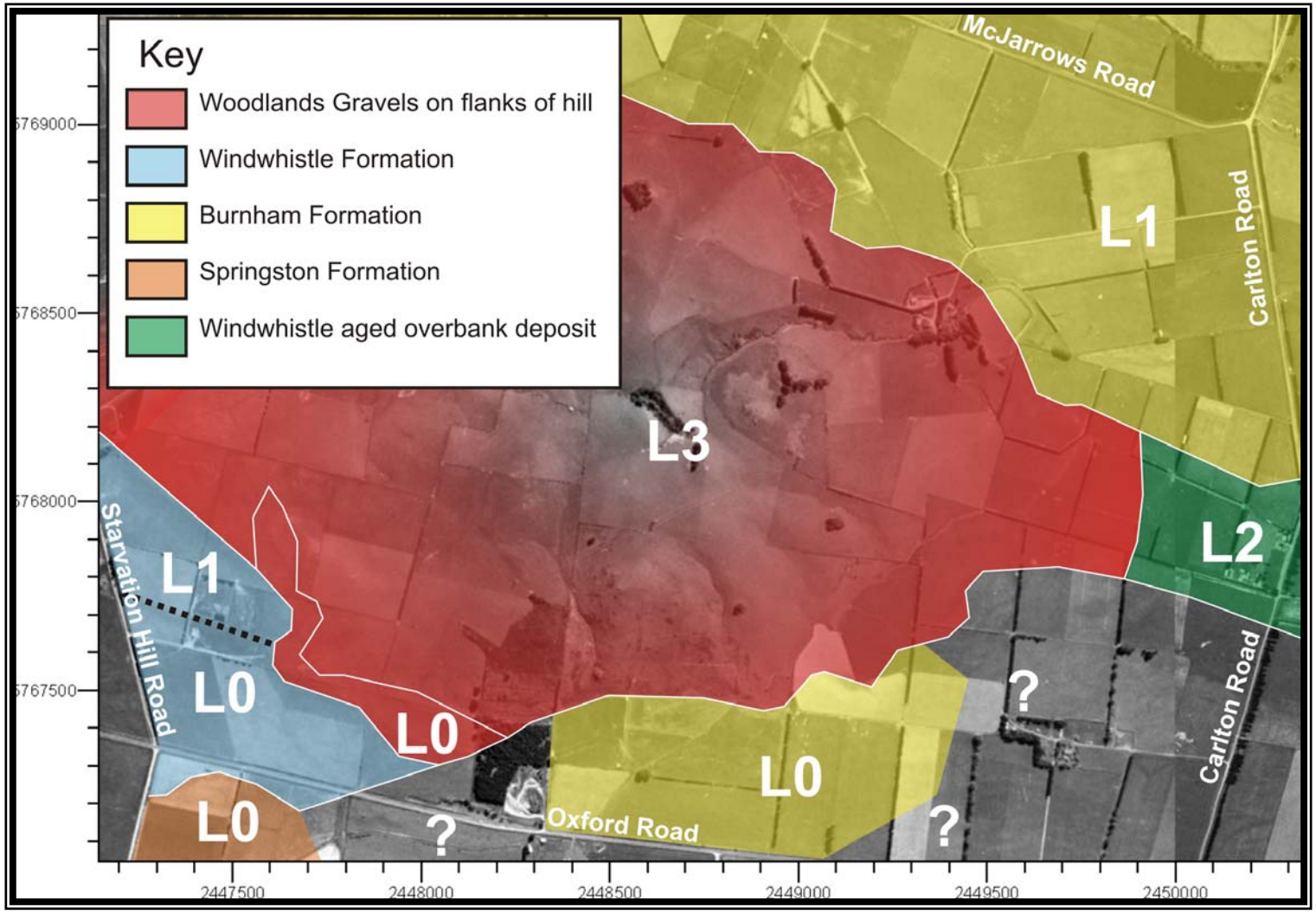

Figure 3.20 – *Map of Late Quaternary Features.*
Many uncertainties remain. Number of loess units (L0 to L3) covering Quaternary features indicated for each area.

3.9 Cover Sequence – Discussion and Summary:

The soil map shows the soil pattern around the Starvation Hill area. This provides many inferences about the history of the Starvation Hill area. Selected soils that are indicative of Late Quaternary formations are summarised below. This has lead to questioning of some Late Quaternary formations in the Starvation Hill area.

- Springburn Soil to the north - Springston Formation
- Hororata Soil to the southwest - Burnham to Springston Formation
- Wakanui & Eyre Soils to the south - Springston Formation

The age difference between the Late Quaternary aggradation formations suggests the soils formed on these surfaces should be significantly different. However, soils may be completely eroded before younger soils form, resulting in the age of the overlying soil being significantly younger than the underlying formation.

The apparent correlation with the loess at Cust suggests this loess cover is at most ~73,000 years old for the oldest loess.

Summary of correlations of loess units at Starvation Hill:

- Loess 1 – Burnham Formation
- Loess 2 – Unrecognised Formation
- Loess 3 – Windwhistle Formation

Underlying Loess 3 is inferred to be gravels of the Woodlands Formation.

The underlying sediment below the third loess unit (L3) was not reached on the Starvation Hill structure except for two profiles on its lowest margins, leaving the question of the extent of the inferred Woodlands Formation on the Starvation Hill structure largely unanswered.

Combining the interpretation of the sections of cover sequence discussed in sections 3.6 to 3.8, the following inferences have been made. These are based on aspects that could be improved with further studies of the cover sequence:

- Thick loess cover, comprising three loess units, extends to the base of the north side of Starvation Hill. This loess buried the landscape and subsequent erosion of the loess by river activity is unapparent. This is inferred to be the result of uplift of the hill structure causing the northward migration of rivers on the north side of the hill. The surrounding plains to the north have a loess cover of ~0.5m overlying gravels. The soil pattern of this area suggests it is Springston, or more likely Burnham Formation. This area is mapped by Wilson (1989) as Windwhistle Formation.

- The eastern side of Starvation Hill suggests an interfluve area, containing buried overbank sediments. These sediments are inferred to be equivalent in age to the Windwhistle Formation as both have two loess units (L1 and L2) on them. This area is mapped by Wilson (1989) as Woodlands Formation.

- The south side of the hill has a thick loess cover of three loess units, extending to the base of the hill. The surrounding plains have a thin veneer of fine textured alluvium overlying gravels. The soil pattern suggests this area is Springston, or more likely Burnham Formation. This area is mapped by Wilson (1989) as Windwhistle Formation.

- The southwest corner of the hill structure suggests either an uplift episode of the structure, and/or incision of surface S2 into older gravels. The relationship of surface S2 with surrounding surfaces is unclear. This area is marked by Wilson (1989) as Woodlands Formation.

- The flight of terraces to the southwest of the hill show a progression of thinner covered gravely alluvium. The terrace sequence dropping to the south indicates southward migration of the Eyre River.

3.10 Creation of DEM using GPS Data:

3.10.1 Methods:

In order to determine the affects of tectonic activity on Starvation Hill, a topographic computer model was required to objectively demonstrate tilting of the hill surfaces (the surfaces described in section 3.5.1) and hopefully rebuild the surfaces back to their original shape, extent and orientation, prior to deformation.

A Digital Elevation Model (DEM or Digital Terrain/Topography Model DTM) existed, entitled *New Zealand Digital Elevation Model*, and was based on contours and spot heights of a 20m grid. This did not produce the necessarily high resolution required for this study (see figure 3.21). To remedy this situation, an intensive GPS survey of Starvation Hill and various sections of the surrounding area was undertaken.

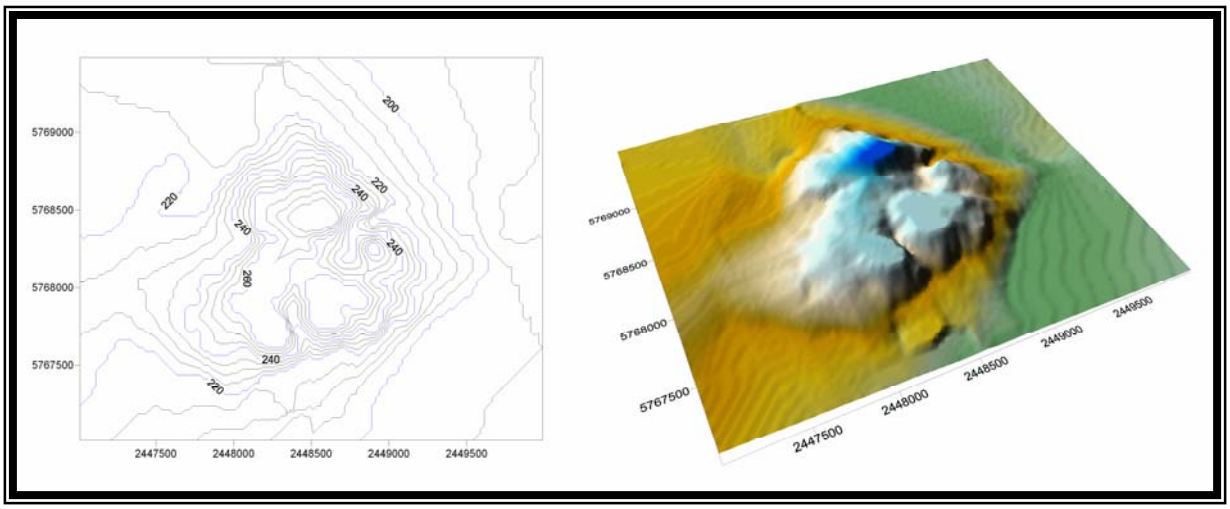

Figure 3.21 – *Views of the original DEM from New Zealand Digital Elevation Model. Note the flat tops of the southern section of Starvation Hill, dissimilar to the current topography.*

Originally the survey was to focus on the surface remnants and lightly cover the remaining areas. However it was decided that combining new and old topographic data for the same area would be more difficult than joining two areas together. Subsequently the entire hill was surveyed, using the original DEM to provide data on the surrounding plains only.

A base station is required for relational correction of the GPS data collected in the field. There is a trig station on Starvation Hill (Geodetic Code B2PH), which was used as the base station site for the GPS surveying. The base station at the trig location, the highest point of the hill, required setting up on foot and battery servicing, sometimes twice on longer days

The process of acquiring GPS data involved traversing the hill structure with the GPS unit. This was carried out in a paddock-by-paddock survey, spiralling inwards on each paddock.

Due to the nature of the GPS system, the repeatability of the data is significantly more accurate for horizontal position than vertical. The Trimble® help file suggests this horizontal accuracy to be ~1m or more for code-phase differential correction, increasing in accuracy to ~0.1 m for carrier-phase. Vertical accuracy is thought to be up to ~3 times less accurate than horizontal accuracy. Appendix II gives a brief description of the workings of GPS.

3.10.2 Creation of DEM:

Figure 3.22 shows views of the new DEM of Starvation Hill combined with the DEM of the surrounding area.

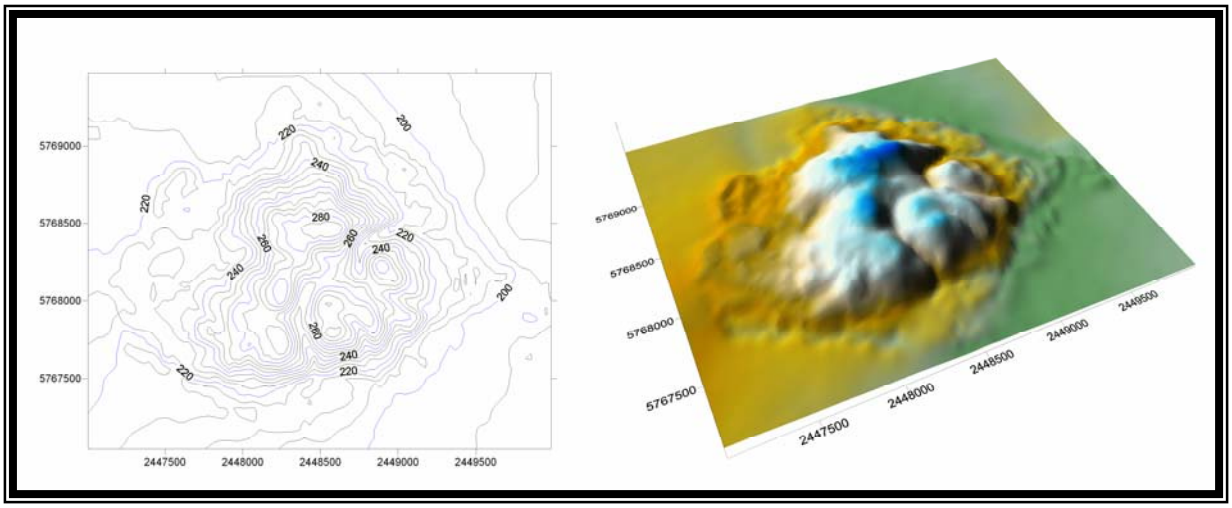

Figure 3.22 – *Views of the new DEM*

Once the entire survey data was collected, and corrected against the base station data, it was exported to MS Excel™ files (via MS Access™) and used in the 3D mapping program Surfer™. Surfer™ (version 8.04) is a surface mapping system. It allows importing of 3D terrain co-ordinates, including in the form of an MS Excel™ spreadsheet of three columns (X, Y, and Z values). The program initially processes the data into a regularly spread grid, with various options for how the grid is calculated. The grid can then be expressed as, amongst other options, a 3D surface (see figure 3.22) or contour map (see figure 3.23).

The contour map (figure 3.23) shows 5m contours as apposed to the 20m contours of a traditional topographical map. The software (Surfer™ version 8.04) allows the contour level to be specified to 1m contours, however this level of detail was unnecessary for produced maps.

The contour map has an overlay of the surfaces defined in section 3.4, allowing comparisons of height and slope to be made, used in detail in section 3.8.6. There are some anomalies around the base of the hill structure, which are explained in section 3.10.3.

The contour map shows three main gullies, one to the northeast, one to the south, and one to the west. These may be tectonically influenced, forming along axis of synclines as first discussed in section 3.5.2, and further discussed in section 3.11.

The 3D surface (figure 3.22) allows viewing from any angle, and overlaying of aerial photographs onto this surface. This allowed viewing of the surfaces in detail as shown in figure 3.24.

Changing the orientation of viewing direction of the 3D surface, approximate correlations of the surface remnants making up the various surfaces on the hill could be made, however extensions of these surfaces were not possible in the detail required for this study using the Surfer™ software. This situation was rectified with use of further computer software as discussed in section 3.10.4.

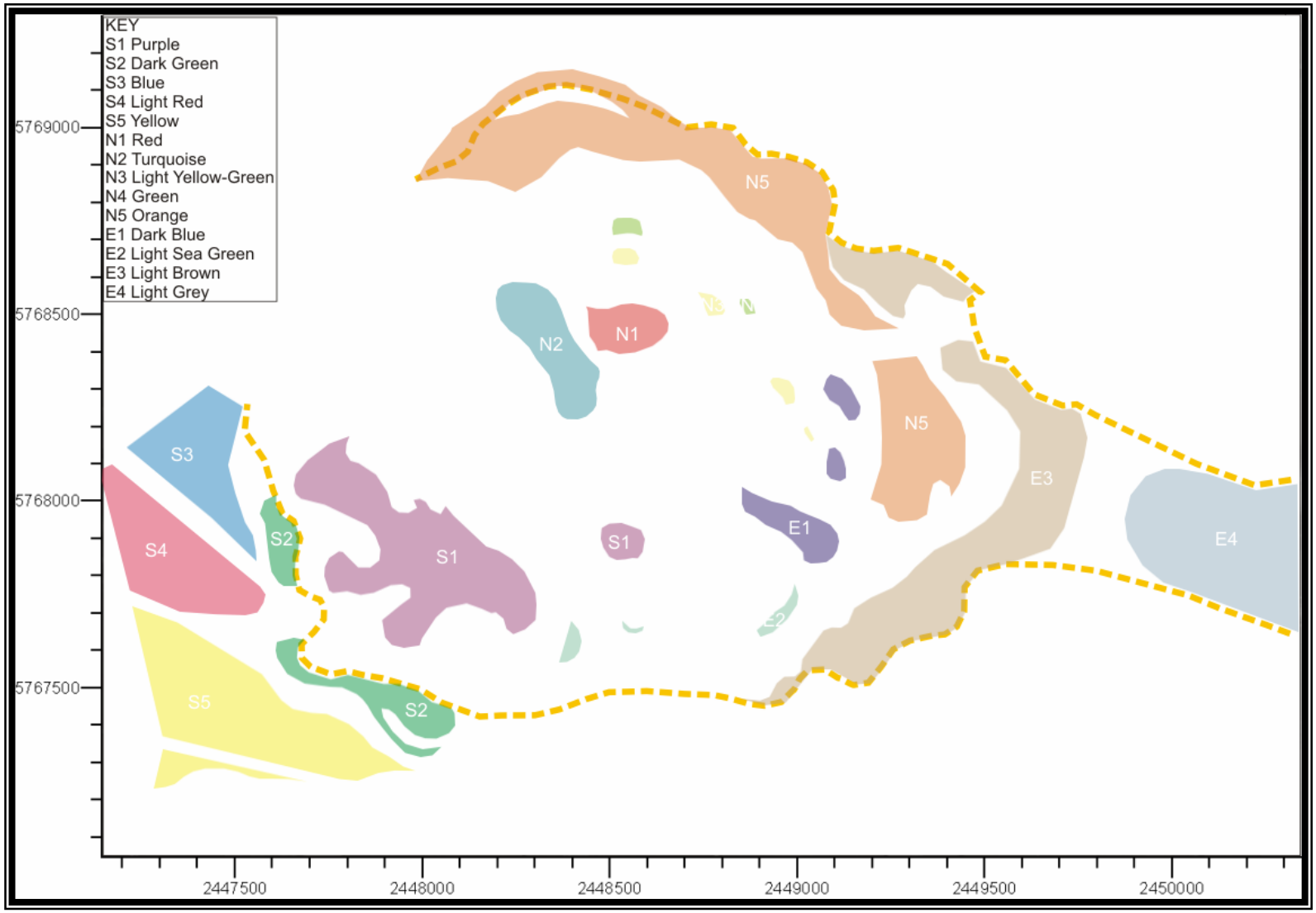
KEY
S1 Purple
S2 Dark Green
S3 Blue
S4 Light Red
S5 Yellow
N1 Red
N2 Turquoise
N3 Light Yellow-Green
N4 Green
N5 Orange
E1 Dark Blue
E2 Light Sea Green
E3 Light Brown
E4 Light Grey
5769000
5768500
5768000
5767500
2447500
2448000
2448500
2449000
2449500
2450000
N5
N2
N1
N5
S3
S4
S2
S1
S1
E1
E3
E4
S5
S2

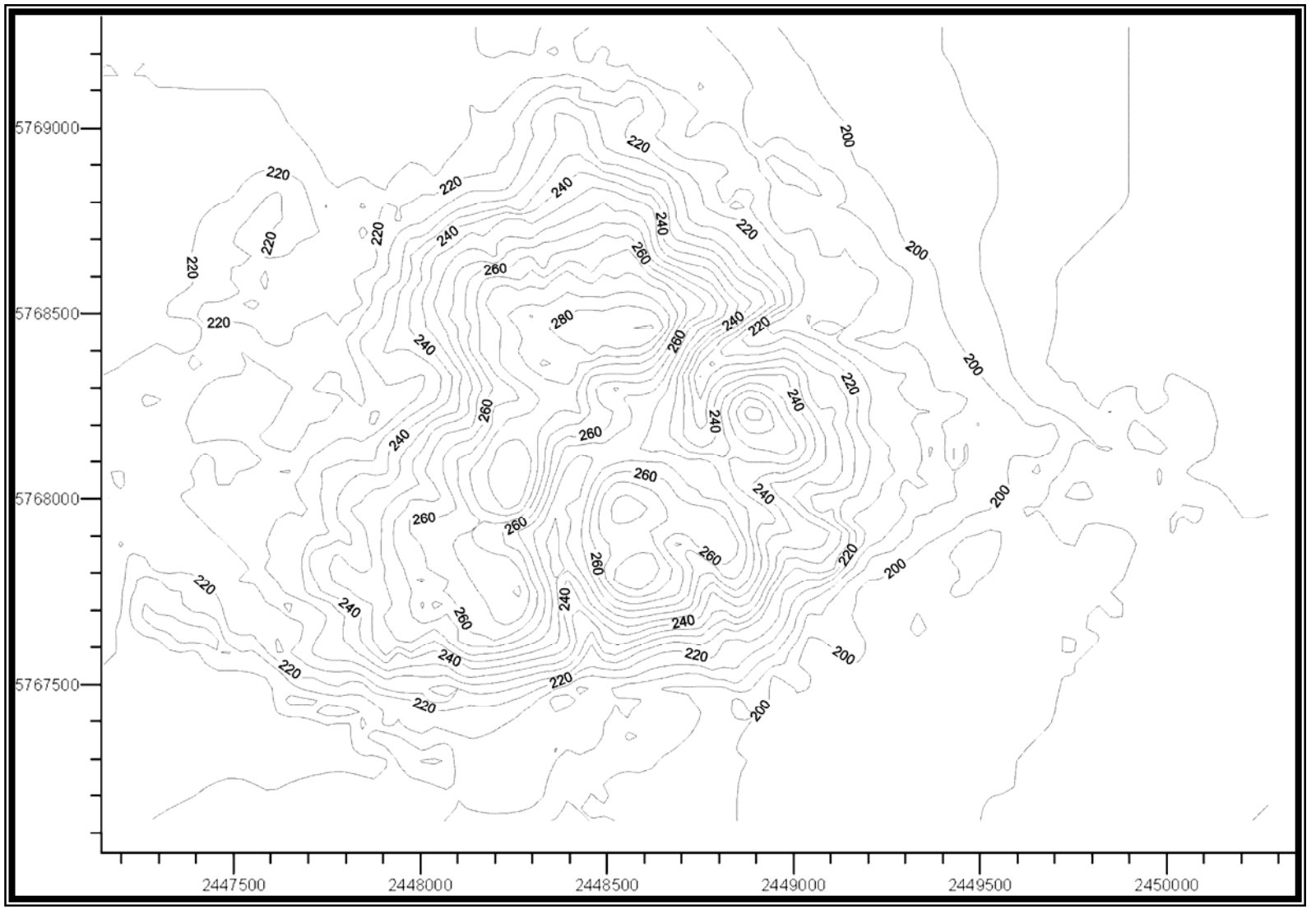

Figure 3.23 – *5m Contour Map of Starvation Hill with surfaces overlay.*

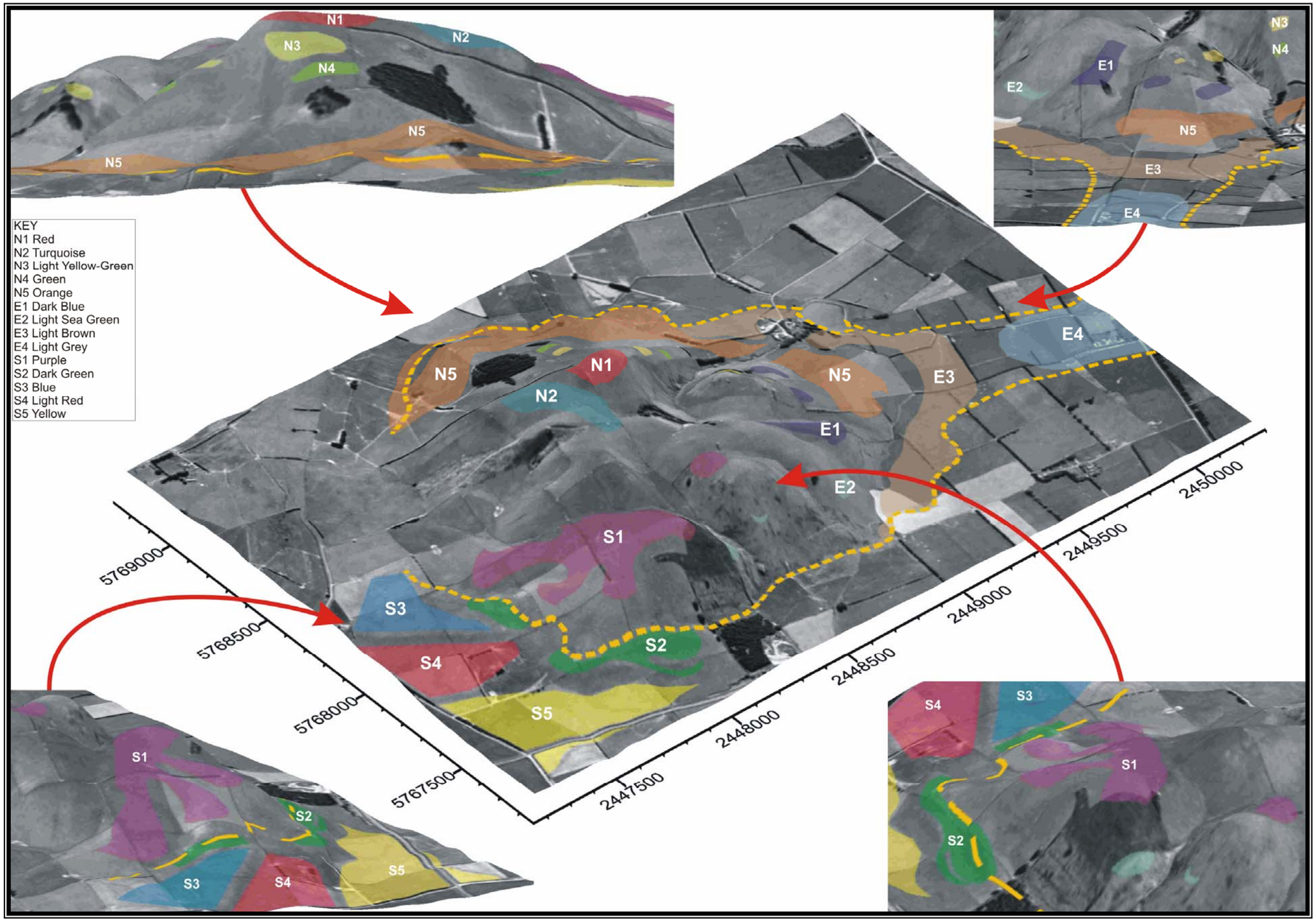

Figure 3.24 – Oblique view of *Aerial Photograph Overlay on DEM, showing surfaces and outline of approximate extent of significant loess cover (yellow dashed line),(~4x V.E.).*

Other data could also be incorporated and shown on the 3D surface, such as the GPS trace paths (see figure 3.25) showing the coverage of the Starvation Hill site.

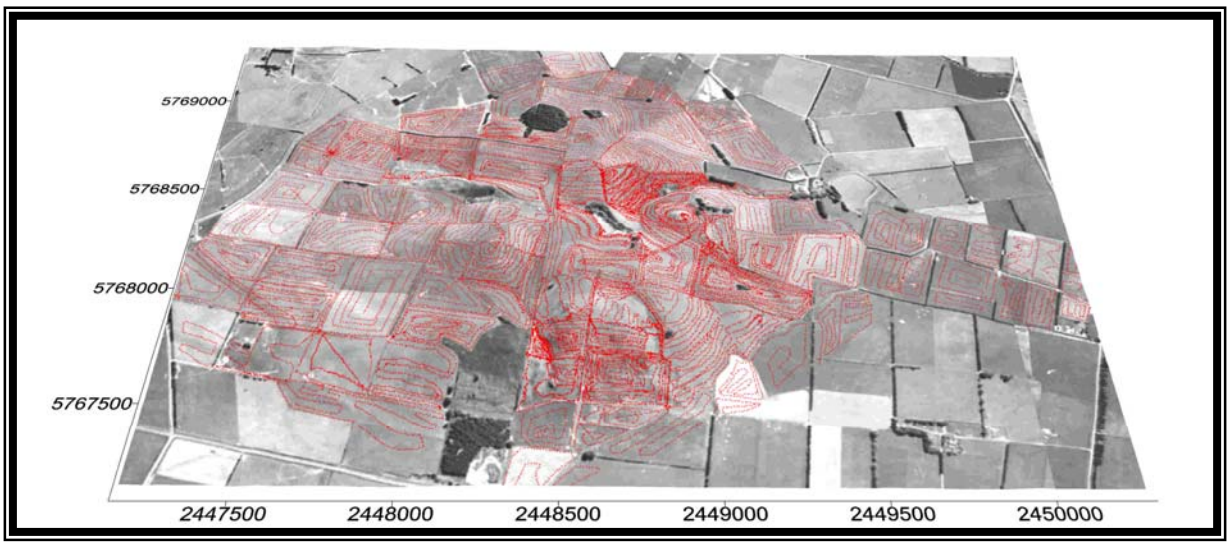

Figure 3.25 – *GPS trace paths.*
Topographic data for the surrounding area was incorporated from an existing DEM

3.10.3 Integration and Comparison:

The limits of the new DEM were defined and data of the original DEM was incorporated, extending the new DEM to include the plains surrounding Starvation Hill. As shown in figure 3.26, the resulting 3D image of the hill shows significantly higher detail than the original. The higher resolution of data points has produced a more accurate model, rectifying such features as the very flat tops of some of the peaks in the original model, which do not resemble the actual current topography of the hill.

The process of incorporating the new DEM with surrounding topographic data involved a 'best fit' process where by the extents of the new DEM were matched as closely as possible with the older, less accurate data. Not all edges matched exactly, and the 'best fit' has left most of the boundary between old and new DEMs fairly smooth, with little noticeable anomalies. The southwest edge in particular seems to have the worst fit, resulting in an apparent gully along the northern edge of surface S5, south of rise up to surface S4.

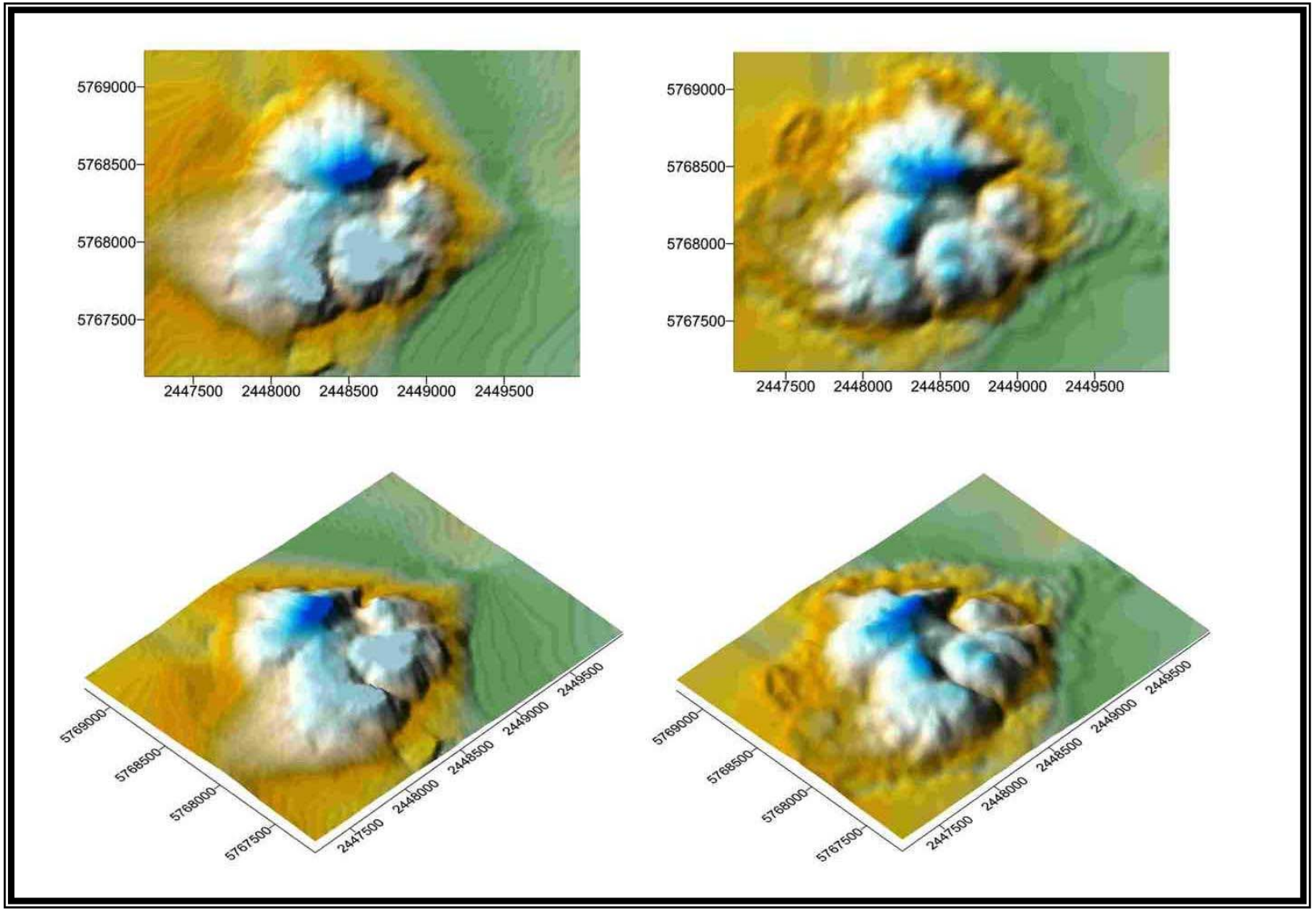

Figure 3.26 – *Comparison of original DEM (left side) and new DEM (right side).*

The accuracy of GPS data comprising the DEM has been found to be most accurate from surveys conducted during extensive and consistent GPS satellite coverage. During episodes of low or dramatically changing coverage, especially due to traversing through areas surrounded by steep topography, the vertical accuracy was found to be slightly more than 1 m, even using carrier-phase differential correction where possible.

These errors have produced a variety of anomalies or artefacts on the DEM compared to the actual topography of the hill. Of note include the rubbly appearance of the area comprising the eastern extent of surface E3 and towards surface E4, which has apparent dimples of up to ~1.5 m. The landscape itself is reasonably smooth, suggesting the data varied over ~1.1 m from actual elevation. This is due in part by satellite receiving being 'interfered with' by the high hedges surrounding many of the paddocks on this surface.

Another anomaly is the lack of resolution where traverses were spaced too far apart resulting in such features as the slight scarp between surfaces N1 and N2 not showing up, as shown in figure 3.27. However, the scarp height of ~0.5 m may have fallen within the accuracy of the surveying, especially as the two surfaces, separated by a fence line, were surveyed on different days.

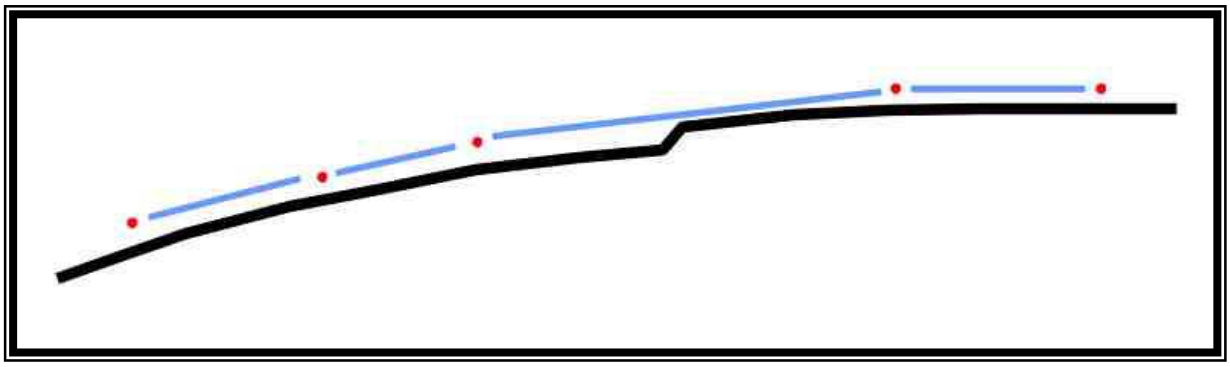

Figure 3.27 – *Loss of resolution due to spacing of traverse lines.*
The scarp on the actual surface (black line) is not distinguished due to the lack of apparent elevation difference, resulting in a surface expression as suggested by the dashed blue lines between GPS points of the surface traverses (red dots).

3.10.4 Topographical Analysis and Reconstruction:

Surfer™ has some limits as to defining and manipulating the surface remnants, so a digital version of the contour map of the new DEM, and incorporated surrounding data, was produced from Surfer. This contour map was subsequently imported into AutoCAD™ 2002. AutoCAD™ allows the interpolation of the surface remnants, enabling them to be joined together to view the terrace surface as a whole as it may once have been, not necessarily following the current topography. As well as joining the remnants together, AutoCad™ allows the projection of the terraces into 3D space, to see the relationship of the terraces and compare angles of tilt. Results of the topographical analysis and reconstruction are discussed in section3.10.6.

3.10.5 Discussion of Methodology and Objectives:

Although the GPS survey was extensive and time consuming with terrain and grumpy livestock conditions being occasionally problematic, the outcome of the survey certainly met the objective of creating a high resolution, useable and accurate DEM.

The new DEM was critical to meeting the objectives relating to Starvation Hill as the surfaces simply did not show up at all on current topographical maps of 1:50,000 scale or the New Zealand Digital Elevation Model.

The new DEM allowed partial reconstruction of the surface remnants into surface structures as described in section 3.5.1. From these surfaces, projection of their boundaries allowed detailed examination of the comparative properties of the surfaces, such as tilting and warping. The results of these comparisons are discussed in section 3.10.6 below.

3.10.6 Results:

Figure 3.28 shows the 3D surfaces from the AutoCAD™ model of Starvation Hill. The model allowed detailed examination of the surfaces, difficult to fully represent in detail with 2D images. All images of the DEM in section 3.10.6 have a 5 x vertical exaggeration.

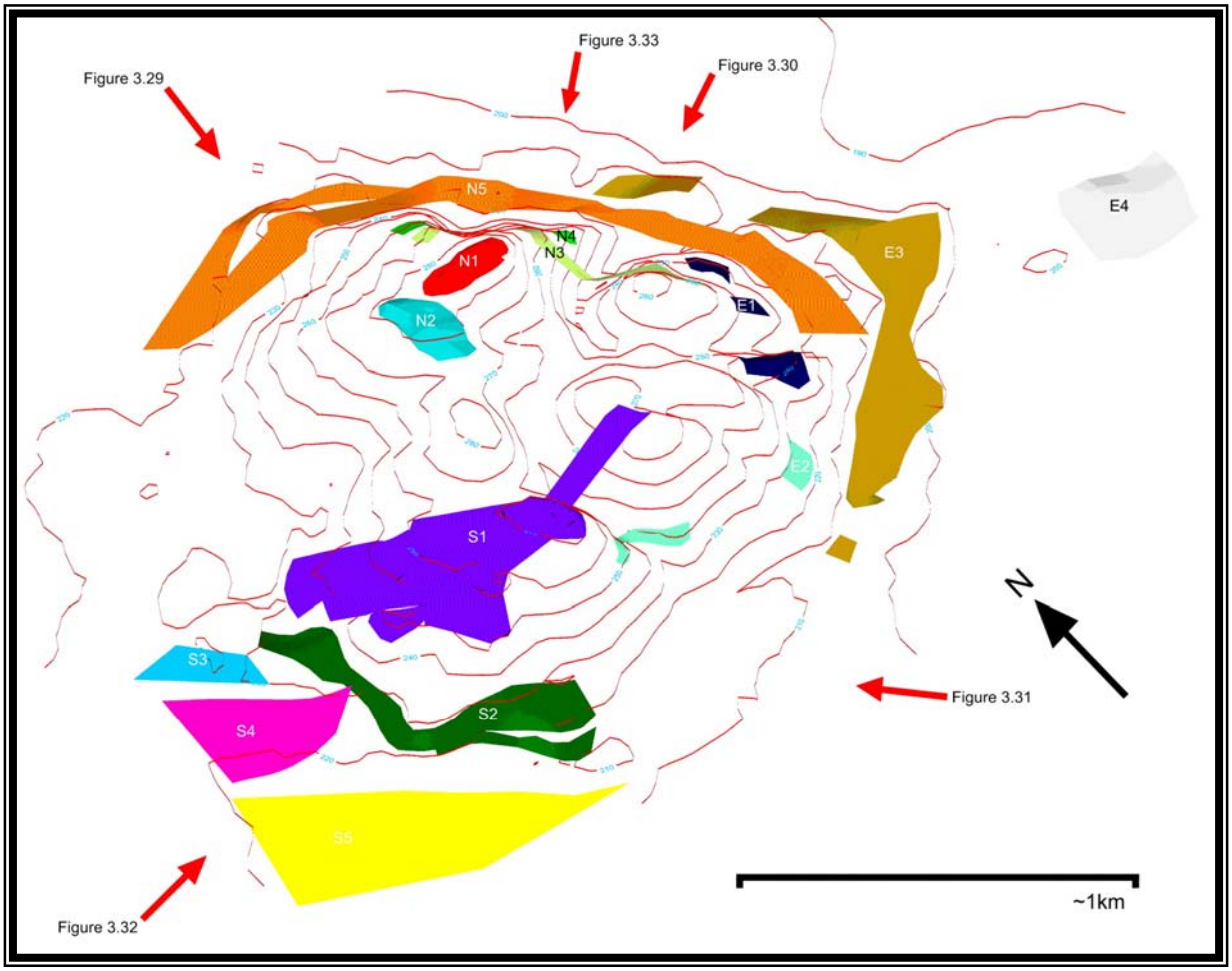

Figure 3.28 – Overview of *final DEM showing warped surfaces. View looking obliquely to the northeast. Views of following figures 3.29 to 3.33 indicated by red arrows. 10 m contours are shown.*

The surfaces across the face of the northern side of the hill appear to have been warped upwards in the middle as shown in figure 3.29, suggesting a fold axis through the north side, producing the slip-off feature of surface N5.

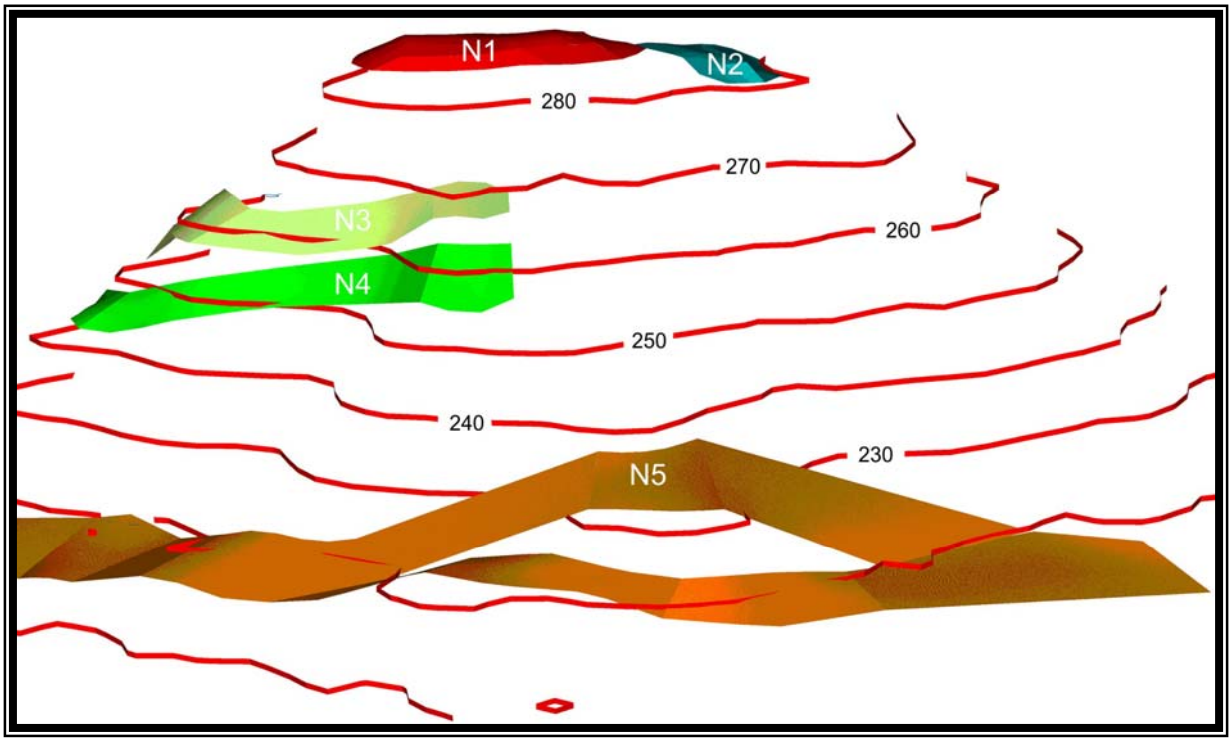

Figure 3.29 – *North face of Starvation Hill showing warped surfaces. The slip-off of surface N5 and the apparent upwarping of surfaces N3 and N4 to the west suggests a fold axis through this area of uplift. 5 x VE.*

The north-western extent of surface N5 shows evidence of downcutting coeval with ongoing folding, shown by the slip-off feature, which is apparent from both 3D modelling and field examination. Figure 3.29 also shows apparent cross-folding of surfaces N3 and N4 as they appear to be warped to the east (left of figure).

On the north side of Starvation Hill, the surfaces E3 (see figure 3.30) and N5 appear to dive into or be onlapped and partially eroded by the Ashley-Cust related surfaces, but there are no raised terraces or any sign of those surfaces being warped.

The surfaces on the east side of the hill (left side of figure 3.30) appear to warp upwards to the south, indicating a fold axis through the east-to-southeast side of the hill. The surfaces appear at their lowest approximately aligning with the major gully

system bearing northeast from the centre of the hill (mid section of figure 3.30), suggestive of a synclinal feature through this side of Starvation Hill.

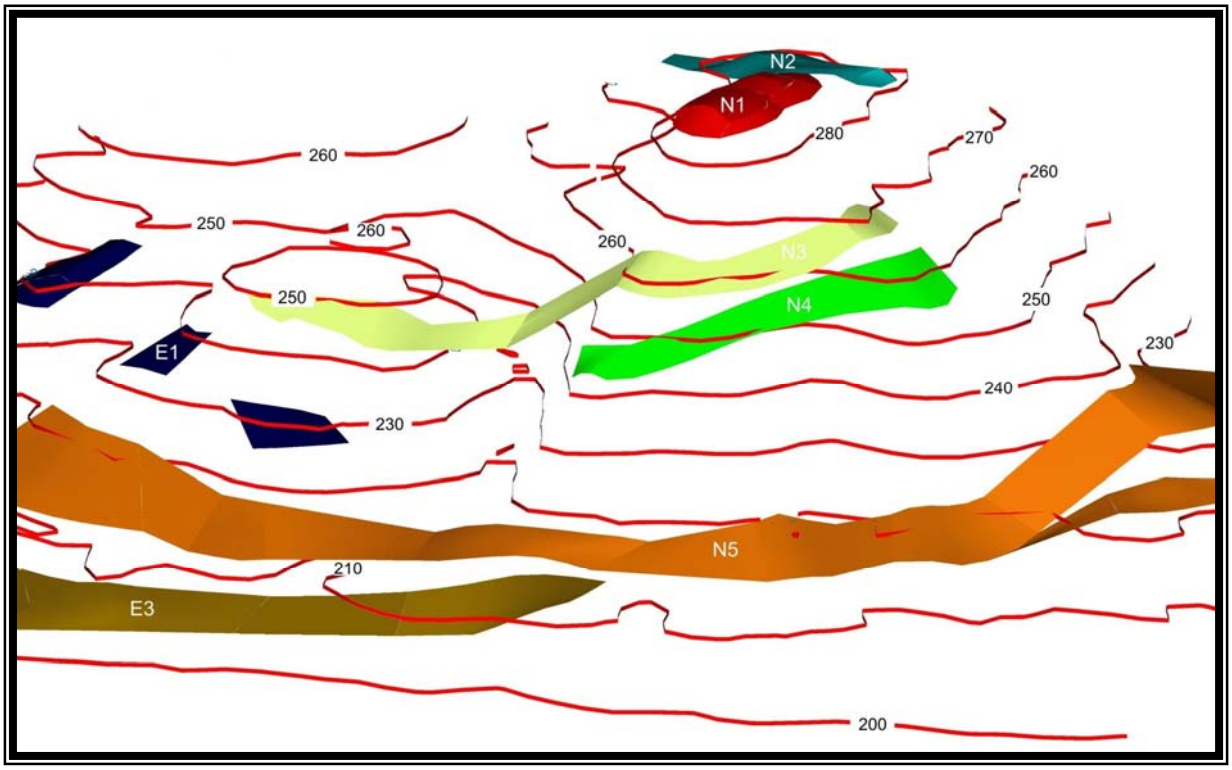

Figure 3.30 – *East face of Starvation Hill showing warped surfaces. The surfaces appear to warp down in line with a significant gully system to the northwest, and warp upwards again to southeast and north sides of the hill. At this vertical exaggeration (5 x VE) the correlation the southern extent of surface N3 (to the left of figure 3.30) appear to align better with surface N4 however this was not the case in the field.*

The figure also appears to show the correlation of eastern remnants of surface N3 (the left section of N3 in figure 3.30) appear to align better with surface N4, however this is mostly a feature of the angle of view and the vertical exaggeration. If the remnants were correlated with surface N4, the pattern of warping would produce similar points of infliction, however the amount of warping would decrease. Either situation would produce a similar interpretation for this side of the hill.

Surface E2, on the south side of the hill, appears to warp upwards to the west shown in figure 3.31, however as discussed in section 3.5.1.6, the correlation of the remnants making up this surface is not clear. A potential surface recognised from field examination in the approximate location of the plantation (not shown in figure)

could align between surface S2 and the eastern extent of surface E2 (right side of figure 3.31) suggesting these two surfaces represent an originally continuous surface. However the distance between these surfaces is considered to large for correlation. The figure suggests a syncline axis through, slightly westward of, the middle of the south side of the hill, aligning with the erosional gully. The warping broadens out for the higher surface S1.

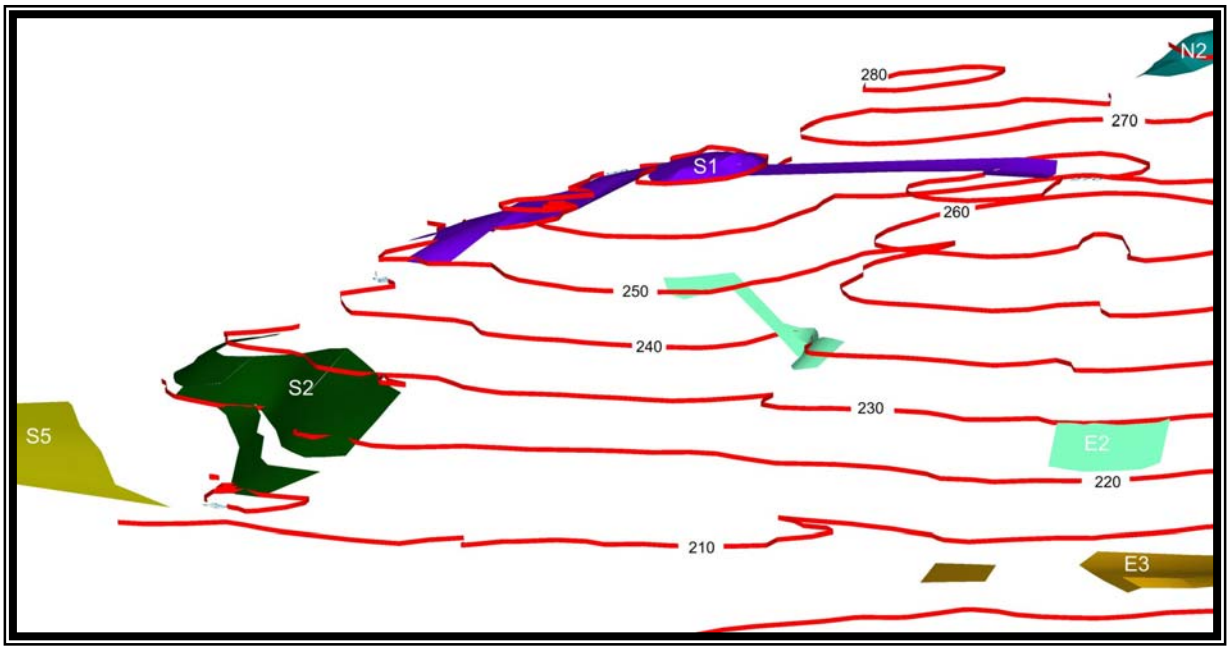

Figure 3.31 – *South side of Starvation Hill showing warped surfaces. The view is looking north-northwest. 5 x VE.*

The extension of surface S1 to the east, across the erosional gully, is shown as a flat, plannar extension, however, the extension may well warp downwards, correlating with the inferred syncline through this area.

The eastern extent of surface S2 shows evidence of downcutting coeval with ongoing folding. This is shown by the slip-off feature, which is apparent from both 3D modelling and field examination. The upwarping of surface S2 is indicative of a fold axis through this western half of the southern side of the hill, likely trending northwards.

The southwest corner shows a complex warping pattern for the surfaces on the slopes of the hill. Surface S1 appears to curve in two directions comparing figures 3.31 and 3.32.

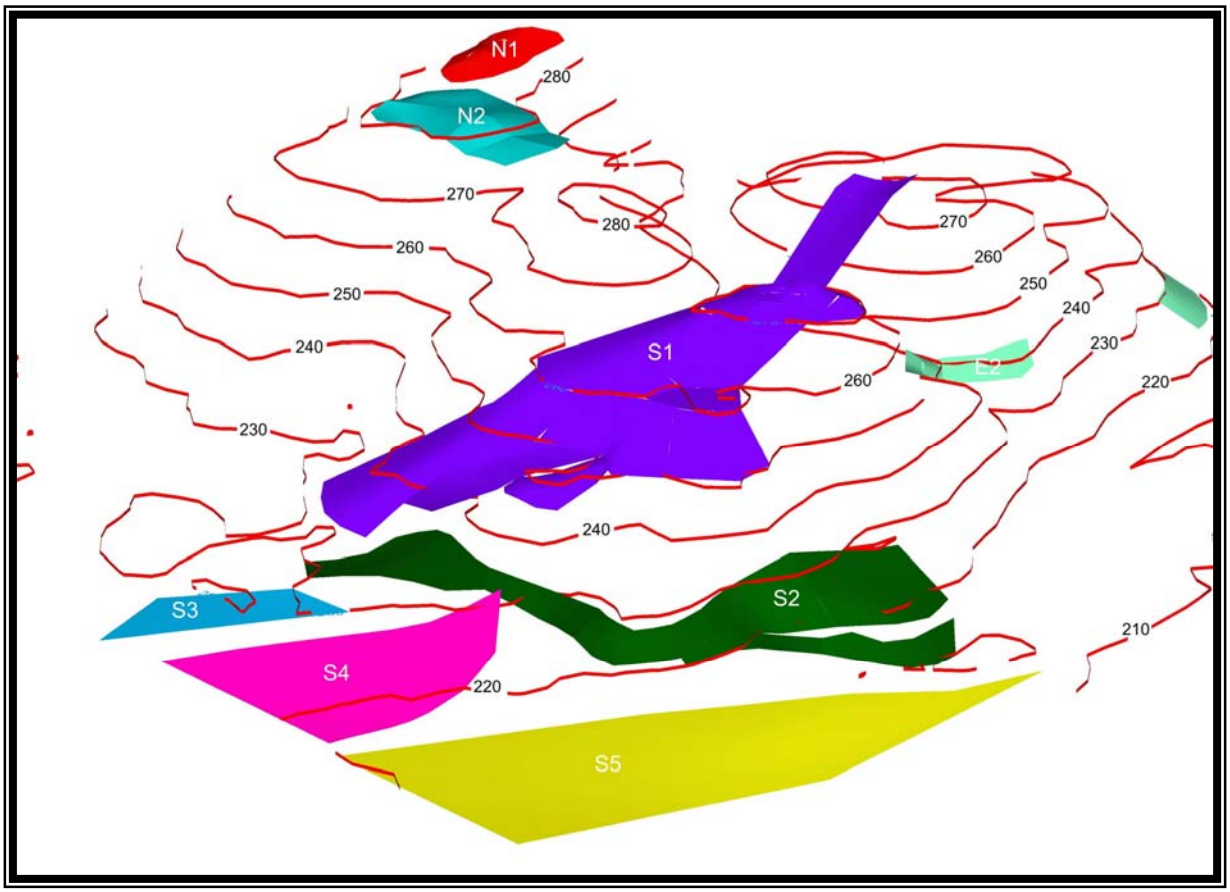

Figure 3.32 – *Southwest corner of Starvation Hill showing a complex pattern of warping. View looking northeast. 5 x VE.*

Surface S2, wrapped around the truncated slopes of the hill, appears to be significantly warped, upwarped in the southwest corner and dipping down to the east. The complex warping of this southwest side of the hill is inferred to be representative of two directions of warping., one trending approximately north-south, the other approximately east-west. The intersection of these two trends is inferred to be located north of surface S1, high up on this southwest corner of Starvation Hill.

The projection of surfaces N1 and N2 towards surface S1 indicates they may be warped in opposite directions shown in figure 3.33. This indicates synclinal warping may be located between these two surfaces, possibly coinciding with the major

erosion gully system to the west side of Starvation Hill, between the projection of these two surfaces.

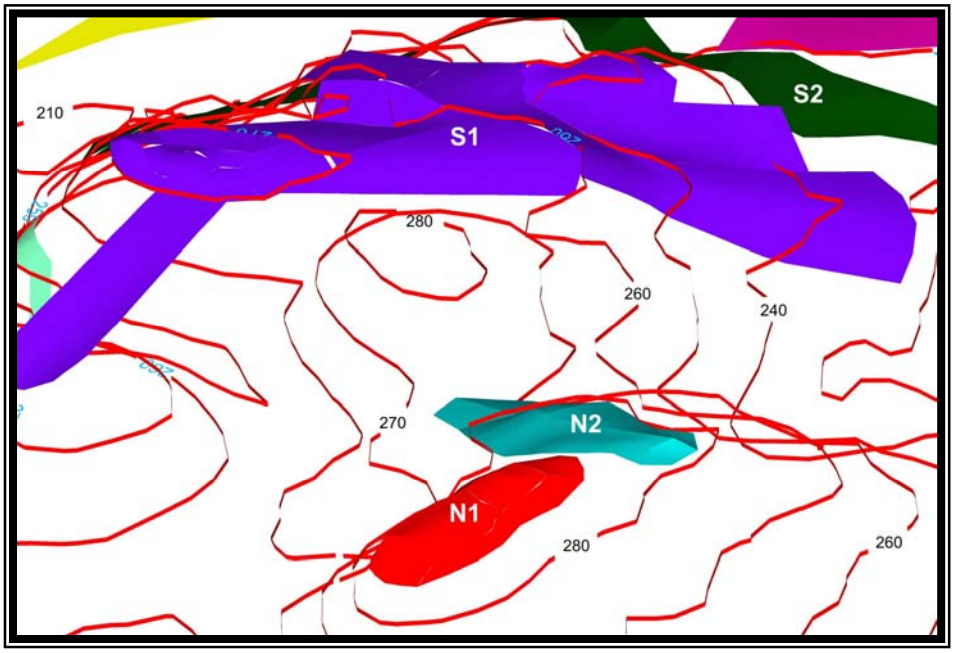

Figure 3.33 – *The superposition of surfaces N1 and S1. This is indicating a synclinal feature may be present between them. The relative east-west angle of curvature of these two surfaces suggests they would not correlate, and the apparent alignment of the suggested syncline would tentatively align with a significant drainage gully system to the west. 5 x VE.*

This synclinal warping trending to the west-northwest would align between the two inferred anticlinal fold trends, and approximately follow the trace of the main erosional gully on that side of the hill.

3.11 Discussion:

3.11.1 Implications of Geometry and Growth of Starvation Hill Fold Complex:

Studies by such authors as Nicol (1991) and Savage and Cooke (2004) suggest that structures of complex shapes such as Starvation Hill are likely to be the result of the influence of more than one fault. The resulting fault related folds, forming either synchronously or sequentially, produce irregular shapes as the areas of multiple fold influence overlap.

Mapping of erosional gullies at Starvation Hill indicated three main gully systems (see section 3.5.2). These main gully systems trend northeast, south-southeast, and west. If the locations of these three main gullies are tectonically controlled, they may approximately indicate coaptation synclinal hinges of the hill structure.

Degradation and river incision has been significant on the north and south sides of the hill. The orientation of the terrace margins near the southwest corner of Starvation Hill suggests the Eyre River changed orientation from flowing southeast, to more easterly direction as discussed in section 3.5.3, as it incised into the underlying gravels. This is inferred to be the result of a growing structure to the northeast of the former channels. The subsequent terrace sequence shows slip-off of the Eyre River to the south, suggesting an east-west trending fold structure, and the lowest terrace margin appears to trend east-northeast, incising into the southeast flank of the hill.

The general shape of the hill structure suggests the hill is not a typical antiform, instead it is suggestive of two directions of folding (see section 3.5.4).

The cover sequence of the Starvation Hill area (sections 3.6 to 3.9) suggests the northern section of the hill has undergone no significant modification for some time. The eastern extent of the hill appears to form an interfluve, suggesting uplift and preservation of this area after initial uplift of the northern section of the hill. The southeast side of the hill appears to show sign of the most recent river incision. The southwest corner of the hill has a complicated cover sequence history, possibly explained by two differing trends of episodic uplift.

The 3D modeling of the surfaces on the hill suggests significant tilting and warping, representative of at least two directions of folding as discussed in sections 3.10.2 and 3.10.6.

Combining these factors, a model of folding of the Starvation Hill structure is shown in figure 3.34. One fold axis trends to the north, and the other to the east. The

influence of two folds on Starvation Hill is inferred to account for the complex shape of the hill structure.

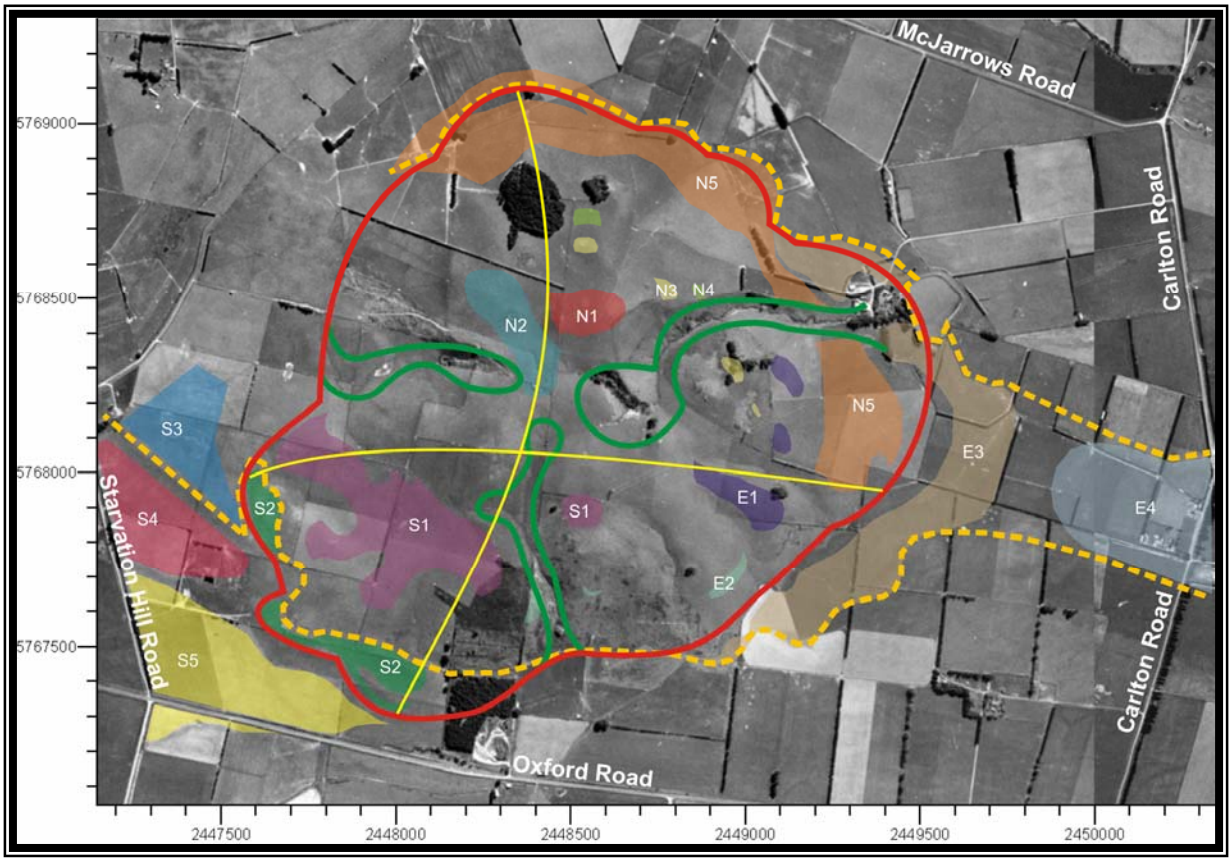

Figure 3.34 – *Model of fold trends affecting Starvation Hill.*
This shows the suggested fold trends (yellow solid lines) and the three main gully systems (green lines) which may correlate with synclines as a result of the interaction of the two anticlines. The base of the hill is shown (red line). This is overlain on the surfaces map of Starvation Hill.

The complex evolution of the Starvation Hill structure is inferred to represent an equally complex tectonic setting in the surrounding area. Figure 3.35 shows a model of the inferred history of this tectonic setting between the Ashley-Loburn Fault System to the east, and a projection towards the View Hill Fault in the west.

The model shown in figure 3.35 is based on two thrust faults, neither of which propagate to the surface, which have produced the complex shape of Starvation Hill. The shape is the result of overlap of areas of fold influence on differing trends.

The north trending anticline is inferred to have formed as a result of a southwest to south trending, southeast dipping thrust fault, at the westward projection of the Ashley-Loburn Fault System, similar to those terminating the Cust Anticline and uplifting Burnt Hill and basement near the Waimakari Gorge Road bridge. This fold emergence is suggested to be pre-Otiran, and is based on:

- Splitting of near coeval surfaces across the north trending fold axis.
- Differential uplift and southward tilting of surfaces on the south face.
- Initial southwest directed slip-off of the Eyre drainage system.
- Lack of young activity on the northern side of the hill.
- The thick loess cover over all these surfaces post erosion and coeval tilting.

A second anticline trending east is inferred to have formed as a result of an east trending, south dipping thrust fault. This is possibly the eastward projection of the transfer fault bounding the northern end of the View Hill Thrust Fault. This fold emergence is based on:

- The later folding of those coeval surfaces, split on the north trending fold axis, but tilted as single surfaces up the flank of the east trending cross-fold.
- Differential uplift and southward tilting of surfaces on the south face.
- The highest of these surfaces without a loess cover (S2) is tilted above the elevation of topography with a thick loess cover to both the east (E3) and west (S3) of Starvation Hill.
- The southern migration of Eyre drainage patterns and slip-off terraces.
- The apparent uplift of the eastern interfluve, preserving Windwhistle aged deposits above the level of subsequent degradation.

The anticlines have been modified by significant degradation and eroded by river incision, especially across their southwestern and northern extents.

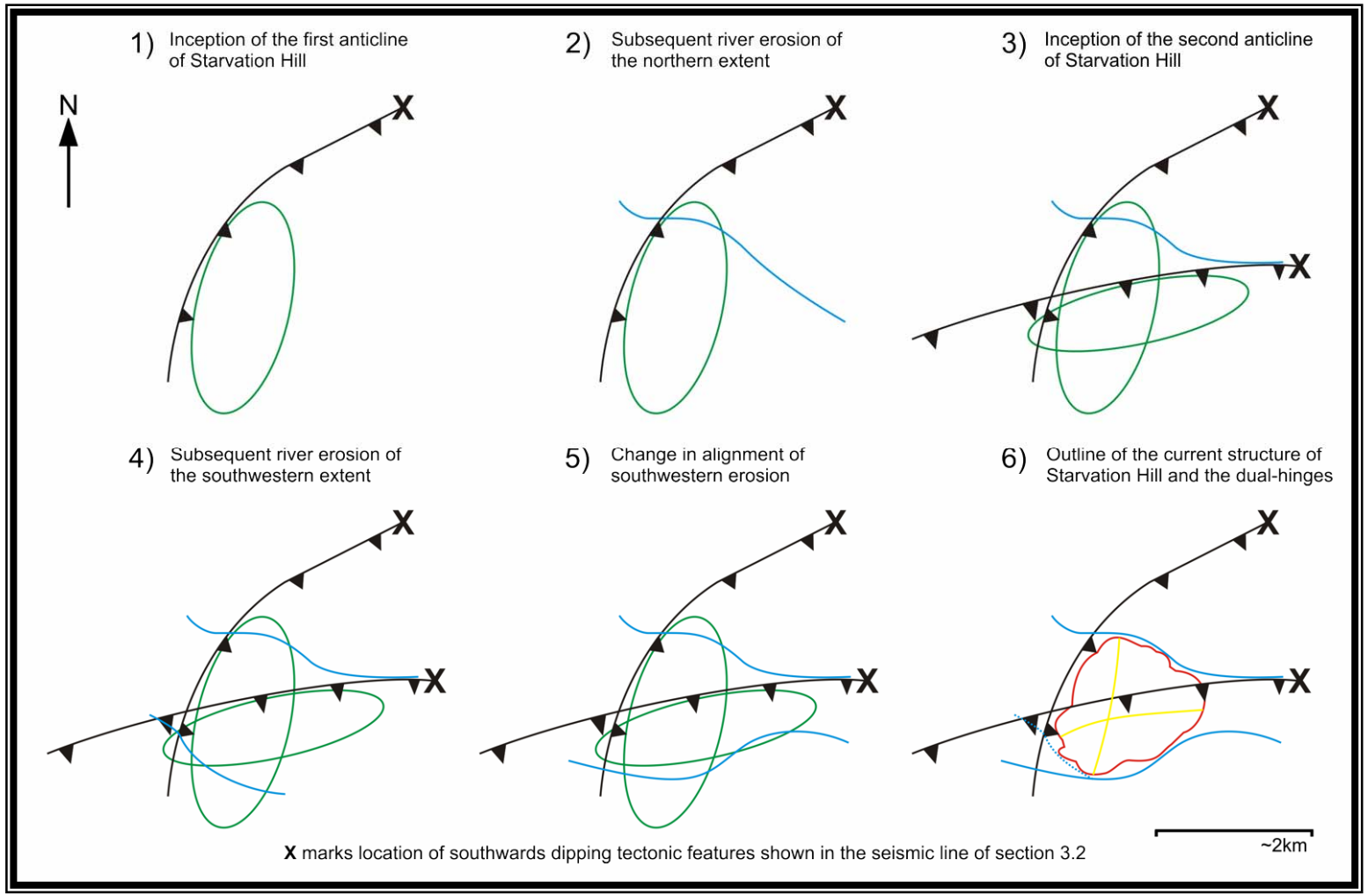

Figure 3.35 – *Model of the history of the tectonic setting of the Starvation Hill area.*
*Location of approximately south dipping tectonic features based on seismic line interpretation (**X**) (see section 3.2). Inferred thrust faults shown (black lines). Extent of growth of resulting anticline (green rings) and subsequent river trim lines (blue) are shown. The approximate current shape of the hill structure is outlined (red).*

3.11.2 Age Constraints:

The implications of the three loess units (see section 3.7) is that most of the underlying topography of Starvation Hill has to be older than the last glaciation (Otiran). Clearly not much older or the underlying surfaces would be deeply dissected before the loess units were deposited. Also, the weathered gravels are likely to be Woodlands, and this would be compatible with a penultimate glaciation aggradation onlapping the rising flanks of the growing anticline and grading to the high surfaces. The evidence of downcutting coeval with ongoing folding suggests that north-south fold growth was active at that time.

On the north side of Starvation Hill, the surfaces appear to dive into or be onlapped by the Ashley-Cust related surfaces, but there are no raised terraces or any sign of those surfaces being warped. Therefore, there is not much obvious young activity propagating on the north trending anticline.

The south side of Starvation Hill is different in the way the younger surfaces are affected and this is compatible with active uplift on the flank of the folded surface defined by the deformation of surface S1, on an eastward trending anticline. There is also an indication that the north trending anticline may still be affecting the younger surfaces to the southwest corner of the hill, suggesting the formation of the north and east trends may be sequential, but overlapping in development.

3.11.3 Comparison of Starvation Hill and View Hill:

View Hill, the focus of Part Two, and Starvation Hill are predominantly used for farming livestock, mainly sheep. Like Starvation Hill, the ridges of View Hill are partially scrub-ridden, and the remaining and surrounding area is grass covered with little outcrop.

View Hill is substantially smaller in expanse (~1.2 km^2) than Starvation Hill (~4 km^2), although rises to a similar relative height above the surrounding plains (~90m for the

highest point). Unlike Starvation Hill, there do not appear to be any significant fluvial surfaces on the slopes of View Hill with potential to measure tilting or warping of the View Hill complex, although a low saddle across the southwestern end of the basalt strike-ridge may mark a former drainage course.

Unfortunately the geology of View Hill cannot be compared with that of Starvation Hill due to the lack of outcrop exposed at Starvation Hill. The geology of View Hill is discussed in further detail in section 2.3.

A tectonic linkage was initially inferred between the View Hill and Starvation Hill structures (Jongens et al. 1999). The distinct fault scarp striking northeast, on the northwest side of View Hill (View Hill Fault), was projected to curve eastwards and link with an inferred fault to the south of Starvation Hill, and continue, northeast, to link with the Ashley-Loburn Fault System (see figure 1.7). Thus, View Hill and Starvation Hill were initially thought to be on opposite sides of a connected fault.

Starvation Hill is now inferred to lie on the hangingwall sides of two faults, one dipping south and the other east-southeast. These two faults are currently not necessarily thought to be initially connected, but segments of a linkage that has propagated between the Ashley-Loburn Fault System in the east and the Springfield Fault in the west.

3.12 Starvation Hill Conclusions:

There is no scarp evident and no clear evidence of surface faulting at Starvation Hill. This posed the question of the extent to which folding may reflect both fault geometry and fault activity.

The investigation of the geomorphology of the Starvation Hill structure has lead to many inferences including:

- River systems to the north and south of the hill appear to have trimmed the structure, especially along the south side and potentially into the southwest corner, as is evident looking at a profile view of the hill. A series of surfaces lap up the flanks of the hill, leaving remnants uplifted by growth of the hill structure.

- The tectonic setting is complex, creating a pattern of at least two directions of folding on the hill resulting in a dual-limbed anticline. A model of this faulting through the area of Starvation Hill has been suggested.

    - A fault thought to be the westward extension of the Ashley-Loburn Fault System is inferred to curve southward, located to the northwest side of Starvation Hill. The fault dips to the southeast and produces the north trending hinge. The emergence of the resulting fold structure is inferred to be pre-Otiran.

    - A second fault, occurring after the first, is thought to underlie the hill on an eastward trend. This fault is inferred to be the eastward projection of the View Hill fault and dips to the south, producing the east trending hinge.

    - Neither fault appears to propagate to the surface.

- The inferred model for the tectonic setting and growth of the Starvation Hill structure in detail contains many anomalies and ambiguities unable to be resolved with the model derived from surface topographic data only. The model itself is suggestive of the merits of geomorphic studies of active tectonic structures providing significant insight into the tectonic setting and history, particularly where exposure limits observation of bedrock structure.

Part Four – Summary & Conclusions:

4.1 Tectonic Setting:

The township of Oxford, ~45 km northwest of Christchurch and nestled under the foothills of the Southern Alps, is surrounded by a tectonic setting much more complicated than only a range front fault system. The North Canterbury Plains, extending from the base of the foothills, contains an apparent series of thrust faults and back thrusts, approximately paralleling the Alpine Fault to the west. Few of these thrusts and back thrusts have substantial or continuous surface expressions.

Overlain on the northern extent of this thrust system, in the Oxford area, is a second fault trend reflecting of the general tectonic setting of the Marlborough Fault System. This fault system is the result of the transition zone of the boundary between the Australian and Pacific plates, as it changes from subduction southeast of the North Island, to oblique compression and transpressional strike-slip in the southwest, along the Alpine Fault. This transition manifests as disseminated deformation across a broad zone parallel to the plate boundary.

The Marlborough Fault System comprises the majority of this transition zone and trends east-northeast, from the northern section of the Alpine Fault, to the southern

extent of the Hikurangi Subduction Zone. This fault system produces a zone of deformation which functions as a migrating duplex system. The theoretical expectation is that such a fault-bounded duplex will tend to be bypassed by the propagation of a new fault system to the south, preceded by compression and contraction strains.

The Hope Fault is currently thought to take up most of the motion between the subduction to the northwest and the transpressional strike-slip to the southwest, with the juvenile Porters Pass-Amberley Fault Zone recently recognised as a significant zone for future tectonic activity.

An east-west orientated tectonic linkage is inferred to pass near Oxford, intersecting the northern end of the northeast striking thrusts. This linkage is located south of the Porters Pass – Amberley Fault Zone and approximately parallels its alignment.

Overprinting of the northeast striking thrust system by the east-west tectonic linkage through the Oxford area, may reflect the preceding compression and contraction strains of significant plate motion being diverted through the Porters Pass-Amberley Fault Zone. The strain is thought to be manifesting through such tectonically affected features as View Hill and Starvation Hill to the west and east of Oxford respectively.

The tectonic setting of these features alone is complex, with multiple faults inferred in close proximity to each structure, and this is typical of many tectonic features of North Canterbury. Where multiple faults affecting features are of significantly differing alignment, complex fold structures can result such as the Cust Anticline where the western end appears to bend almost 90° relative to the alignment of the eastern. Both View Hill and Starvation Hill appear to lie within the same zone of the east-west orientated tectonic linkage inferred through the Oxford area.

4.2 View Hill:

Located ~12 km west of Oxford, this distinctive topographic feature comprises two ~northeast striking ridges separated by a saddle-like area. The northwest ridge exposes Torlesse Group basement and the southeast ridge exposes View Hill Volcanics of the Eyre Group, separated by poorly exposed undifferentiated sediment of the Eyre Group.

The View Hill structure is inferred to be the result of a thrust fault located to the northwest of the hill. The fault produces a distinct scarp of ~4 m height to the southwest, changing in scarp morphology as it is traced to the northeast, becoming a series of less distinct, interfingered scarp splays.

Some constraint as to subsurface structure can be made on the basis of available outcrop. The relative elevations of the basalt outcrops low on the bank of the Waimakariri River compared to View Hill infer a minimum total throw of ~120 m. This throw would translate into a net slip substantially larger than the elevation difference depending upon the unknown dip of the thrust plane. Downstream in the Waimakariri River, further repetition of outcrops of Torlesse Group capped by cover rocks at Burnt Hill are inferred as the result of a similar thrust fault. The repeated pattern of upthrusted basement and the dips of the cover beds implies the faults dip gently and may flatten at depth.

To the northeast of View Hill, an anomalous section in gravels showing evidence of faulting was exposed in the river bed of the Eyre River. The fault dips to the southeast, but displacement is uncertain. An inferred tendency for the fault to propagate along the base of the scarp implies the youngest ruptures are to be found on the downthrown side. This faulting is therefore likely to be related to the youngest event, but, the relative timing of this event in the context of the river terrace sequence presents some problems. This appears to be a late Holocene event, but is difficult to date by any material seen in the exposure.

Fault scarp profile surveys have shown significant change as the scarp is traced around the northwest side of View Hill. The prominent and distinct scarp on the west side becomes a dispersed and topographically smaller feature on the north side. Suggested implications of this varying scarp morphology include variation in the strike and consequential slip vector of the fault from northeast to east, variation in near surface dip of the fault, increasing thickness of gravels as depth to basement rock increases, variations in the surface lithologies, or a combination of these.

The decrease in total throw is possibly more related to the decrease in age of the displaced surfaces as they are modified by slip-off of the Eyre River. The relative step up in scarp height from ~1.4 to ~4 m, plus the problematic late Holocene displacement in the Eyre River implies multiple post-glacial rupture events. Poorly constrained slip rates are estimated to be in the order of 0.5 mm per year.

4.3 Starvation Hill:

Located ~3 km east of Oxford, Starvation Hill was previously interpreted to be the result of an oblique strike-slip fault to the southeast of the hill, running from the View Hill Fault, to south of the Oxford township and continuing to north of the Cust Anticline. The fault was thought to form a restraining bend, causing the uplift of the Starvation Hill structure to the north of the fault. Reconciliation of the relative uplift of these structures and fault dips for a single fault presents considerable geometric problems.

There is no scarp evident and no clear evidence of surface faulting at Starvation Hill. This posed the question of the extent to which fault generated folding may reflect both fault geometry and fault activity.

River systems to the north and south of the hill appear to have trimmed the structure, especially along the south and southwest sides, as is evident looking at

the profile view of the hill. A series of surfaces have lapped up the flanks of the hill, leaving remnants uplifted and warping by growth of the hill structure.

The manner in which these surfaces wrap around the structure allow for partial 3D reconstruction as compared to the more common 2D cross-sections derived in many studies of antecedent gorges across fold ridges

Examination and interpretation of the various remnants of the inferred fluvial surfaces on the hill and their 3D reconstructions has provided various insights into the growth of the Starvation Hill structure. The hill is not representative of a typical antiform, suggesting complexities in its growth.

Reconstructed surfaces on the north side of the hill appear to be upwarped in the middle of the structure, suggesting a fold axis trending north. The highest of the surfaces on the southwest side dips more gently to the west compared to high surfaces on the north side. This suggests the antiformal structure is broader across the south than the north sections of the hill.

The southwest corner of the hill is complex, with the former course of the Eyre River having wrapped around the southern side of the hill, leaving a series of triangular shaped slip-off terraces, culminating to a point on the south side of the hill structure.

Further up the southwest side of the hill, surfaces show compound warping both rising to the east, correlating with a north trending fold axis towards the middle of the hill structure, and also warped up over the southwest corner. This suggests a second axis of folding trending in an easterly direction.

Evidence of the continuation of this second fold axis on the eastern side is limited to the extended interfluve to the east of the hill, and the possible correlation of surface remnants on the eastern side suggesting an upwarping.
Examination of the cover sequence of the Starvation Hill area found a thick cover of three loessal units on the majority of the hill structure. Many questions remain as to

what underlies the third loess unit of the hill, as weathered gravels, possibly of the Woodlands Formation, were only found at two locations. At other locations on the hill, the base of the loess was not reached. The plains to the north and south consist of gravels from Burnham and Springston degradation events respectively. The eastern extent of the hill is inferred to represent a relict topography partially buried by overbank deposits of Windwhistle age, capped by two loess units, indicative of uplift and preservation of this interfluve area between the Cust and Eyre channels.

The complexities of the southwest corner of the hill and surrounding flight of terraces is suggestive of episodes of degradation eroding into Woodlands Formation Gravels. These terraces show a change in channel alignment from easterly, to more north-east, cutting into the southern flank of the hill truncating older surfaces. Aerial photograph interpretation indicates that the channels eventually migrated south from the hill to the present Eyre River course, probably as a result of the growth of the structure.

Seismic line interpretation provided some insight into the possible tectonic setting affecting the Starvation Hill structure. Coupled with the evidence of two axes of folding from examination and interpretation of the various remnants of fluvial surfaces on the hill, a model suggesting the complexities of the tectonics of Starvation Hill is inferred.

The model suggests Starvation Hill is the result of two faults. The first fault is inferred to be a northeast striking thrust fault, dipping to the southeast. It is likely to be one of a zone of such faults connecting to the western end of the Ashley-Loburn Fault System, and creating the restraining bend responsible for the Cust Anticline, and possibly extending southwest to include the Burnt Hill – Waimakariri Gorge Road bridge area structure.

The emergence of the north trending fold component of the Starvation Hill structure is therefore interpreted as developing in on the hanging wall of a splay relating to

this system. The majority o uplift on this structure is inferred to be pre Otiran, based on the presence of the thick loess cover, but was clearly actively warping during the preceding fluvial modification of the land surface.

The second fold was generated by emergence of a later fault, dipping south and propagating across the earlier fold. Possibly this relates to development of a transfer fault related to the View Hill Thrust Fault. Evidence for later Pleistocene and continued Holocene growth of this structure comes from the relatively similar dips to the south of both the older loess covered surfaces and the younger gravel terraces below and the way in which the later also climb around this structure to elevations above surfaces which retain the thick loess cover. Southward slip-off of Holocene terraces to the Eyre channel is consistent.

4.4 Tectonic Linkage:

Although there is no surface exposure of a scarp in the course of the Eyre River, a tectonic linkage is inferred between the View Hill and Starvation Hill structures. The distinct fault scarp of the View Hill Fault trends northeast, on the northwest side of View Hill. The fault appears to align with the Springfield Fault to the southwest although the distance between these two features is significant. To the northeast, the View Hill Fault is projected to curve eastwards and link with the inferred fault underlying Starvation Hill.

A second fault along the northwest side of Starvation Hill is inferred to curve northeast, to link with the Ashley-Loburn Fault System to the north of the Cust Anticline. Thus View Hill and Starvation Hill are thought to be part of an approximately east-west tectonic linkage between the Ashley-Loburn Fault System in the east, and the Springfield Fault to the west.

It is clear that deformation on both the View Hill and Starvation Hill structures is coeval, and of a similar magnitude in terms of uplift, and indirectly, shortening rates.

REFERENCES

Allmendinger, R. (1998). Inverse and forward modelling of trishear fault-propagation folds. *Tectonics*, 17:640-656.

Allmendinger, R. (1997 – 2000). Trishear for Windows ™ v 4.5 ©1997 – 2000.

Balster, C.A. and Parsons, R.B. (1968). Geomorphology and soils, Willamette Valley, Oregon. Oregon State University Agriculture Experiment Station Special Report 265p.

Barnes, P. (1994). Continental extension of the Pacific Plate at the southern termination of the Hikurangi subduction zone: The North Mernoo Fault Zone, offshore New Zealand. *Tectonics* 13:735-754

Barnes, P. (1996). Active folding of Pleistocene unconformities on the edge of the Australian-Pacific Plate boundary zone, offshore North Canterbury, New Zealand. *Tectonics* 15:623-640

Berger, W., Pillans, B., and Tonkin, P. (2001). Luminescence chronology of loess-paleosol sequences from Canterbury, South Island, New Zealand. *New Zealand Journal of Geology and Geophysics* 44:501-516.

Billen, M., Gurnis, M., and Simons, M. (2003). Multiscale dynamics of the Tonga-Kermadec subduction zone. *Geophysical Journal International* 153:359-388.

Bradshaw, J. (1989). Cretaceous geotectonic patterns in the New Zealand region. *Tectonics*, 8:803-820.

Brown, L., and Wilson, D. (1988). Stratigraphy of the Late Quaternary deposits of the northern Canterbury Plains, New Zealand. *New Zealand Journal of Geology and Geophysics* 31:305-335.

Browne, G., and Field, B. (1985). The lithostratigraphy of Late Cretraceous to Early Pleistocene rocks on Northern Canterbury, New Zealand. *New Zealand Geological Survey. Record 6*, 63p.

Campbell, J. (1991). Styles of deformation associated with the Marlborough fault system. Structural transition from Alpine Fault to Hikurangi margin in time and space conference, Lower Hutt, New Zealand. *Geological Society of New Zealand Miscellaneous Publication* 56:10-13.

Campbell, J. Bennet, D., and Brand, R. (2000). Actively emergent, fault-related fold structures beneath the Canterbury Plains. 2000 New Zealand Petroleum Conference. Pre-conference Field Trip Guide.

Cowan, H. (1992). Structure, seismicity and tectonics of the Porter's Pass-Amberley fault zone, North Canterbury, New Zealand. University of Canterbury Thesis: PhD, 181p.

Daniels, R.B., Gamble, E.E., and Cady, J.G. (1971). The relation between geomorphology and soil morphology and genesis. Advances in Agronomy, 23:51-88.

Daniels, R. B. and Hammer, R. D. (1992). Soil Geomorphology. Published by John Wiley & Sons. New York.

Darby, D., and Bevan, J. (2001). Evidence from GPS measurements for contemporary interpolate coupling on the southern Hikurangi subduction thrust and for partitioning of strain in the upper plate. *Journal of Geophysical Research* 106:30881-30891.

Estrada, B. (2003). Seismic hazard associated with the Springbank Fault, North Canterbury Plains. University of Canterbury Thesis: MSc, 193p.

Evans, S. (2000). Paleoseismic analysis of the Springfield Fault, Central Canterbury. University of Canterbury Thesis: BSc Hons.

Field, B., Browne, G. and others (1989). Cretaceous and Cenozoic sedimentary basins and geological evolution of the Canterbury region, South Island, New Zealand. New Zealand Geological Survey basin studies 2.

Gage, M. (1958). Late Pleistocene glaciations of the Waimakariri Valley, Canterbury, New Zealand. *New Zealand Journal of Geology and Geophysics* 1:123-155.

Gile, L. H., Hawley, J. W. and Grossman, R. B. (1981). Soils and geomorphology in the Basin and Range area of Southern New Mexico – Guide Book to the Desert Project. New Mexico Bureau of Mines and Mineral Resources Memoir 39p.

Gregg, D. (1964). Geological Map of New Zealand 1:250,000. Sheet 18 "Hurunui". N.Z. DSIR, Wellington.

Indo-Pacific Ltd (1998). Seismic line data printout (Survey Line 002).

Ives, D. (1973). Nature and distribution of loess in Canterbury. *New Zealand Journal of Geology and Geophysics* 16:587-610.

Jongens, R., Pettinga, J., and Campbell, J. (1999). Stratigraphic and structural overview of the onshore Canterbury Basin: North Canterbury to the Rangitata River. Unpublished Report for Indo-Pacific Energy (NZ) Ltd. University of Canterbury. 31p

Kear, B. S., Gibbs, H. S. and Miller, R. B. (1967). Soils of the Downs and Plains, Canterbury and North Otago, New Zealand. *Soil Bureau Bulletin* 14. Published by D.S.I.R. Wellington New Zealand. 92p.

Milne, J., Clayden, B., Singleton, A., and Wilson, A. (1995). Soil Description Handbook (Revised Ed). Published by Manaaki Whenua Press, Lincoln, Canterbury, New Zealand. 157 p.

McLennan, J. (1981). The Cretaceous – Tertiary rocks of Avoca, Oxford and Burnt Hill, Central Canterbury. University of Canterbury Thesis: MSc, 234p.

Munsell® Colour (firm) - Munsell® Soil Colour Charts, Year 2000 revised washable edition. Published by Gretag Macbeth, 617 Little Britain Road, New Windsor, NY 12553.

Lin, C., Lee, Y., Huang, M., Lai, W., Yuan, B., & Huang, B. (2003). Characteristics of surface ruptures associated with the Chi-Chi earthquake of September 21, 1999. *Engineering Geology* 71:13-31.

Melhuish, A., Sutherland, R,. Davey, F., and Lamarche, G. (1999). Crustal structure and neotectonics of the Puysegur oblique subduction zone, New Zealand. *Tectonophysics* 313:335-362.

New Zealand Digital Elevation Model. Produced by Landcare Research, based on New Zealand 1:50,000 scale Terralink Topographic Database.

Nicol, A. (1991) Structural styles and kinematics of deformation on the edge of the New Zealand plate boundary zone, Mid-Waipara region, North Canterbury. University of Canterbury Thesis: PhD. 171 p.

Norris, R., Koons, P., and Cooper, A. (1990). The obliquely-convergent plate boundary in the South Island of New Zealand; implications for ancient collision zones. *Journal of Structural Geology* 12:715-725.

North Canterbury Active Tectonics GIS. Unpublished data, Department of Geological Sciences, University of Canterbury.

Pettinga, J., Chamberlain, C., Yetton, M., Van Dissen, R., and Downes, G. (1998). Earthquake source identification and characterisation: Stage 1 (Part A) Earthquake hazard and risk assessment study. Canterbury Regional Council, publication No. U98/10. 121p.

Pettinga, J., Yetton, M., Van Dissen, R., and Downes, G. (2001). Earthquake source identification and characterisation for the Canterbury region, South Island, New Zealand. *Bulletin of New Zealand Society for Earthquake Engineering* 34:282-317.

Powell, S. (2000). Active deformation and structural relationships of the Mt. Lawry Fault and the hillside anticline, White Rock, North Canterbury. University of Canterbury Thesis: BSc Hons.

Ruhe, R. V. (1969). Quaternary Landscapes of Iowa. Iowa State University Press. Ames Iowa USA. 255p.

Savage, H., and Cooke, M. (2004). The effect of non-parallel thrust fault interaction on fold patterns. *Journal of Structural Geology* 26:905-917.

Sibson, R. and Rowland, J. (2001). Faulting, fluid redistribution, and seismic style; case studies from an active arc. 2001 Earth system processes conference, Edinburgh, United Kingdom, June 24-28. Programmes with Abstracts.

Sisson, R. (1999). Paleoseismic investigation of the Ashley Fault, North Canterbury, New Zealand. University of Canterbury Thesis: BSc Hons. 124p.

Sissons, R., Campbell, J., Pettinga, J., and Milner, D. (2001). Paleoseismicity of the Ashley and Loburn Faults, North Canterbury, New Zealand. Report prepared for Earthquake Commissions Research Foundation. Project No. 97/237. 31p plus figures.

Suggate, R. (1963). The Alpine Fault. Transactions of the Royal Society of New Zealand, *Geology* 2:105-129.

Suggate, R. (1990). Late Pliocene and Quaternary Glaciations of New Zealand. *Quaternary Sciences Reviews* 9, 2-3:175-197.

Tappenden, V. (2003). Magmatic response to the evolving New Zealand Margin of Gondwana during the Mid-late Cretaceous. University of Canterbury Thesis: PhD.

Terralink. Producer of Land Information New Zealand 1:50,000 scale Topographic Database.

Tonkin, P. and Almond, P. (1998). Using Loess Soil Stratigraphy to Reconstruct the Late Quaternary History of Piedmonts Adjacent to Large Strike-slip Faults, South Island, New Zealand. In Geological Society of New Zealand / New Zealand Geophysical Society 1998 Joint Annual Conference, 30 Nov to 3 Dec, University of Canterbury, Christucrch: Programme and Abstracts.

Trangmar, B. (1987). Overview of Canterbury loess deposits. In: Heine, J. ed., Tour guide for International Symposium on Loess. Lower Hutt, New Zealand Soil Bureau. P 5-22.

Waimakariri Irrigation Ltd (2000). The rivers of the Waimakariri plains. [online]. Available: http://www.wil.co.nz.

Wilson D. (1989). Quaternary geology of Northwestern Canterbury Plains. Miscellaneous series map 14, 1:100,000 scale, New Zealand Geological Survey, Department of Scientific and Industrial Research.

APPENDIX I -
AUGER CORE PROFILE DESCRIPTIONS:

Details of the profiles discussed in sections 2.6.3 and 3.7.3 are provided below. Variation in the detail collected resulted from varying purposes of the profiles. Many profiles were conducted for the sole purpose of measuring depth to gravels, and as such, loess units are not differentiated. Other profiles give detailed accounts of the loess stratigraphy recording variations of thickness and number of loess units.

Locations of the View Hill profiles are given in figure 2.10, and locations of the Starvation Hill profiles are given in figure 3.12. Summary profile diagrams for the Starvation Hill profiles are given in figures 3.13a, b & c.

Soil Horizon nomenclature is based on the Milne et al. (1995) soils descriptions.

Fragmental Component relates to the >2mm diameter fraction i.e. gravels

f.gr	– few gravels (>5%)	sli.gr	– slightly gravely (5-15%)
m.gr	– moderately gravely (15-35%)	gr	– gravely (35-70%)

Fine Earth Texture: corresponds to a field soil texture assessment:

sl – sand loam zl – silt loam cl – clay loam c – clay

to – …grades down to…

(Prefixed e.g. scl – sandy clay loam, lms – loamy medium sand)

Soil Colour as recorded using the Munsell colour chart notation (Munsell®, 2000).

Mottle colour patterns record the colours of either iron concentrations or depletions. The matrix colour is that dominated by either uniform oxidised or reduced colours (as recorded using the Munsell colour chart). These patterns are recorded in terms of their abundance, size and contrast as follows:

Abundance:

vf – very few (<2%) f – few (2-10%) c – common (10-25%)

m – many (25-50%) vm – very many (50-75%)

Size:

vf – very fine (2-6mm) f – fine (6-10mm) m – medium (10-20mm)

c – coarse (20-60mm) vc – very coarse (60-100mm)

Contrast:

f – faint d – distinct p – prominent

(e.g. c.m.d. – common, medium sized, distinctive mottles)

Sedimentary Unit relates to the classification of the sediment into either:

L – Undifferentiated Loess, or

L1 – Loess Unit 1

L2 – Loess Unit 2

L3 – Loess Unit 3

as defined in Part 3, section 3.7.5

Or

A1 – Alluvial Unit 1

A2 – Alluvial Unit 2

A3 – Alluvial Unit 3

Or

S1 –Sedimentary Unit 1

S2 – Sedimentary Unit 2

Miscellaneous terms:

EOA (End of Auger) – profiling ended due to the reaching the limits of the auger

View Hill Soil Profiles:

Soil Profile 1

Horizon	Depth (cm)	Fragmental Component	Fine Earth Texture	Fine Earth Colour	Mottles			Sed. Unit	Other
					Colour		Pattern		
					High Chrome	Low Chrome			
A	20		scl	2.5Y 4/2					sticky and plastic
Bw	50	sli. gr	sl	2.5Y 4/4					20%+ of clay
C(ox)	140+		sl	10YR 4/6					M. plastic, not sticky

Soil Profile 2

Horizon	Depth (cm)	Fragmental Component	Fine Earth Texture	Fine Earth Colour	Mottles			Sed. Unit	Other
					Colour		Pattern		
					High Chrome	Low Chrome			
A	20							L	
?	70	sli. gr						Sand	Mottled grey/brown oxidised sands grad up into loess

Soil Profile 3

Horizon	Depth (cm)	Fragmental Component	Fine Earth Texture	Fine Earth Colour	Mottles			Sed. Unit	Other
					Colour		Pattern		
					High Chrome	Low Chrome			
A	25		zl	10YR 5/2					
Bg	40	sli. gr	zl	10YR 5/2					f.m. concretions 10YR 2/2 & 10YR 6/8
Bwg	70		lms	2.5Y 5/3		10YR 4/3	f.m.d.		
Cr	140+		lms to sl	2.5Y 6/3	10YR 4/6		m.m.d.		Fine Earth colour & mottles grade to 10YR 4/3 & 10YR 4/3

Soil Profile 4

Horizon	Depth (cm)	Fragmental Component	Fine Earth Texture	Fine Earth Colour	Mottles			Sed. Unit	Other
					Colour		Pattern		
					High Chrome	Low Chrome			
A	28		zl						
Bg	55	sli. gr	s.f.g ls						
Bwf	100		ls					Sand	brown sand grades down to grey sand
C	140+		s					Sand	coarse and medium sand

Soil Profile 5

Horizon	Depth (cm)	Fragmental Component	Fine Earth Texture	Fine Earth Colour	Mottles			Sed. Unit	Other
					Colour		Pattern		
					High Chrome	Low Chrome			
A	30		zl	10YR 3/2					
Br	70		scl	7.5Y 5/6		2.5Y5/2	f.f.f.		sli. sticky and plastic
Bw(g)	100		sl	2.5Y 5/2	2.5Y 6/3	7.5Y 5/6	m.m.d.		
C	140+		lms to s	2.5Y 4/3					

Starvation Hill Profiles:

Profile 1 (on surface N1)

Horizon	Depth (cm)	Fragmental Component	Fine Earth Texture	Fine Earth Colour	Mottles			Sed. Unit	Other
					Colour		Pattern		
					High Chrome	Low Chrome			
A	35		zl	10YR 4/2				L	
Btg	120		cl	10YR 4/6	7.5YR 5/8	2.5Y 6/2		L	Grey veins running vertically
Bt	165		cl	10YR 5/6				L	
Rock?									

Profile 2 (on surface N3)

Horizon	Depth (cm)	Fragmental Component	Fine Earth Texture	Fine Earth Colour	Mottles			Sed. Unit	Other
					Colour		Pattern		
					High Chrome	Low Chrome			
A	15		zl	10YR 3/3				L	clear boundary
Btg	75		zcl	10YR 5/4	7.5YR 5/6	2.5Y 6/1		L	gradual boundary
Bt	130		zcl	2.5Y 5/4				L	gradual boundary
2bBtg	300		cl	10YR 4/3	10YR 4/6	10YR 6/3	c.m.d.	L	
3b2Bt	325		cl	10YR 5/4	7.5YR 5/6	2.5Y 6/1		L	diffuse boundary
3b2Btgc	375		cl	2.5Y 6/3		2.5Y 7/1		L	m.c.d. 10YR 2/1 Conc.
3b2Btg	432		cl	7.5YR 6/8		10YR 7/1		L	
Rock?									

Profile 3 (on surface N5)

Horizon	Depth (cm)	Fragmental Component	Fine Earth Texture	Fine Earth Colour	Mottles			Sed. Unit	Other
					Colour		Pattern		
					High Chrome	Low Chrome			
A	40							L	
?	605							L	
Rock?									

Profile 4 (on surface N5)

Horizon	Depth (cm)	Fragmental Component	Fine Earth Texture	Fine Earth Colour	Mottles			Sed. Unit	Other
					Colour		Pattern		
					High Chrome	Low Chrome			
A	30			10YR 4/1				L1	
Br	60			7.5YR 5/8	2.5Y 7/1		vm.c.d.	L1	
Bx(g)	130		scl	2.5Y 4/6	7.5YR 5/6	7.5YR 7/1	c.m.d.	L1	grey veins
Bw	270		zcl	7.5YR 5/6				L1	
2bBtg	400		c	7.5YR 5/6		2.5Y 5/3	vm.m.d.	L2	
2bBt(g)	480		c	10YR 5/4	10YR 5/6	2.5Y 7/1	m.l.d.	L2	grey veins
3b2Btg1	530		cl	10YR 5/4	10YR 6/2	2.5Y 6/4	m.l.d.	L3	grey veins and f.f.d. concretions
3b2Btg2	580		zc	10YR 7/3	10YR 6/6		m.m.d.	L3	grey veins
3b2Btg3	630		c	7.5YR 5/6		2.5Y 7/1	vm.l.d.	L3	grey veins
3bBt(g)	>645		c	10YR 5/4		2.5Y 7/1	f.m.d.	L3	grey veins
EOA									

Profile 5

Horizon	Depth (cm)	Fragmental Component	Fine Earth Texture	Fine Earth Colour	Mottles			Sed. Unit	Other
					Colour		Pattern		
					High Chrome	Low Chrome			
A	20		zl	10YR 3/2				L	
Bw	50		cl	10YR 5/4				L	Imature brown soil
Gravels									

Profile 6 (on surface E4)

Horizon	Depth (cm)	Fragmental Component	Fine Earth Texture	Fine Earth Colour	Mottles			Sed. Unit	Other
					Colour		Pattern		
					High Chrome	Low Chrome			
A	25							L	
?	540							L	water at 430cm
Too water logged to continue									

Profile 7 (on surface E4)

Horizon	Depth (cm)	Fragmental Component	Fine Earth Texture	Fine Earth Colour	Mottles			Sed. Unit	Other
					Colour		Pattern		
					High Chrome	Low Chrome			
A	20			10YR 4/2				L1	L1 - mottled argillic Pallic soil
AB(g)	40		cl	10YR 4/2		2.5Y 7/2		L1	
Bgt	170		zl	10YR 5/6		2.5Y 7/2	m.m.d	L1	
Bw	185		sl	10YR 5/4	7.5YR 5/6	2.5Y 7/2	f.m.d.	L1	
2bBw1	200		scl	10YR 5/4				L2	L2 - buried brown soil
2bBw2	230		sl					L2	
2bBw3	320		cl to sl	10YR 4/4				L2	290 = few greywacke pepples see fig 3.19a
3C	415+		sl					S1	Overbank deposits?
Burried landscape ?									

Profile 8 (on surface E3)

Horizon	Depth (cm)	Fragmental Component	Fine Earth Texture	Fine Earth Colour	Mottles			Sed. Unit	Other
					Colour		Pattern		
					High Chrome	Low Chrome			
A	30		cl					L1	
Bg	75		zcl	7.5YR 5/7		10YR 6/2		L1	large grey veins at 40cm
Bg(x)	90		zcl	10YR 5/4				L1	
B(x)	145		zcl	10YR 5/4				L1	
2bB(f)	165		zcl	2.5Y 6/4	7.5YR 5/7			L1	may be old burried A horizon
2bBg	245		zcl	10YR 6/4	10YR 5/6	10YR 7/1		L2	
2bBw(f)	300		cl	10YR 6/4	10YR 5/6	10YR 7/1		L2	
2bBw(f)	420		cl	10YR 5/4				L2	
3b2Btg1	480		cl	2.5Y 6/2	10YR 5/6			L2	
3b2Btg2	560		cl	10YR 6/6	2.5Y 6/4	2.5Y 6/2		L2	
3b2Btg3	580		c	7.5YR 5/6		10YR 7/2		L3	vertical grey veins
3b2Bw	620		cl	10YR 4/6		10YR 7/2		L3	some grey veins
Gravels									

Profile 9 to 11

Horizon	Depth (cm)	Fragmental Component	Fine Earth Texture	Fine Earth Colour	Mottles			Sed. Unit	Other
					Colour		Pattern		
					High Chrome	Low Chrome			
A	25	sli. gr	zl	10YR 3/1				A1	
Bw	30	gr	zl	2.5Y 5/4				A1	
Gravels									

Profile 12 (on surface S1)

Horizon	Depth (cm)	Fragmental Component	Fine Earth Texture	Fine Earth Colour	Mottles			Sed. Unit	Other
					Colour		Pattern		
					High Chrome	Low Chrome			
A	35							L	
?	>645							L	some concretion layers scattered thoughout unit
EOA									

Profile 13 (on surface S1)

Horizon	Depth (cm)	Fragmental Component	Fine Earth Texture	Fine Earth Colour	Mottles			Sed. Unit	Other
					Colour		Pattern		
					High Chrome	Low Chrome			
A	25							L1	
Btg	121							L1	
Bw	350+							L2	dark concretion layers scattered thoughout unit

Profile 14 (on surface S1)

Horizon	Depth (cm)	Fragmental Component	Fine Earth Texture	Fine Earth Colour	Mottles			Sed. Unit	Other
					Colour		Pattern		
					High Chrome	Low Chrome			
A	25								
Btg	121							L1	
Bw	350+							L2	

Profile 15 (on surface S1)

Horizon	Depth (cm)	Fragmental Component	Fine Earth Texture	Fine Earth Colour	Mottles			Sed. Unit	Other
					Colour		Pattern		
					High Chrome	Low Chrome			
A	27							L1	
Btg ?	110							L1	
Bw ?	>645							L2	dark concretion layers scattered throughout unit
EOA									

Profile 16 (on surface S2)

Horizon	Depth (cm)	Fragmental Component	Fine Earth Texture	Fine Earth Colour	Mottles			Sed. Unit	Other
					Colour		Pattern		
					High Chrome	Low Chrome			
A	35		zl		2.5Y 2/1			A2	
Br	50				7.5YR 4/6	7.5YR 4/6	c.f.d.	A2	
Gravels									

Profile 17 (on surface S2)

Horizon	Depth (cm)	Fragmental Component	Fine Earth Texture	Fine Earth Colour	Mottles			Sed. Unit	Other
					Colour		Pattern		
					High Chrome	Low Chrome			
A	15							A2	
Gravels									

Profile 18 (on surface S3)

Horizon	Depth (cm)	Fragmental Component	Fine Earth Texture	Fine Earth Colour	Mottles			Sed. Unit	Other
					Colour		Pattern		
					High Chrome	Low Chrome			
A	35		zl	2.5Y 3/3				L1	
Bg	85		zl	10YR 5/6		2.5Y 7/2		L1	gleyed argillic? Pallic soil
Bw	205		zl	2.5Y 6/4				L1	
2bBtg	430		cl	2.5Y 5/4		2.5Y 6/3	m.f./m.d.	L2	
3b2Btg	520		cl	10YR 6/8	7.5YR 5/8	2.5Y 7/3	f.m.d.	L3	additional mottle colour of 10YR 7/1
3b2Bw(x)	565			10YR 6/4				L3	Brittle
Gravels									

Profile 19 (on surface S4)

Horizon	Depth (cm)	Fragmental Component	Fine Earth Texture	Fine Earth Colour	Mottles			Sed. Unit	Other
					Colour		Pattern		
					High Chrome	Low Chrome			
A	10							L	
?	70	sli. gr						L	
Gravels									

Profile 20 (on surface S4)

Horizon	Depth (cm)	Fragmental Component	Fine Earth Texture	Fine Earth Colour	Mottles			Sed. Unit	Other
					Colour		Pattern		
					High Chrome	Low Chrome			
A	15		zl	2.5Y 3/2					clear boundary
Btg	50	sli. gr	cl	2.5Y 6/3	10YR 5/6	2.5Y 6/2	m.m.d		
Gravels									

Profile 21 (on surface S4)

Horizon	Depth (cm)	Fragmental Component	Fine Earth Texture	Fine Earth Colour	Mottles			Sed. Unit	Other
					Colour		Pattern		
					High Chrome	Low Chrome			
A	30								
?	60								
Gravels									

Profile 22 (on surface S4)

Horizon	Depth (cm)	Fragmental Component	Fine Earth Texture	Fine Earth Colour	Mottles			Sed. Unit	Other
					Colour		Pattern		
					High Chrome	Low Chrome			
A	20							L	
Loess (test site)									

Profile 23 (on surface S4)

Horizon	Depth (cm)	Fragmental Component	Fine Earth Texture	Fine Earth Colour	Mottles			Sed. Unit	Other
					Colour		Pattern		
					High Chrome	Low Chrome			
A	10		zl	2.5Y 6/3				L1	
Bw	80		zl	2.5Y 5/4				L1	imature pallic soil
2bBgt	115		scl to cl	7.5YR 5/8	2.5Y 7/4	5Y 7/2		S2	Looks similar to L3
2bBw	175		sl	10YR 4/4				S2	
3C	210	sli. gr	sl	10YR 5/4		2.5Y 7/1		S2	grey veins top 10cm
Gravels									

Profile 24 (on surface S4)

Horizon	Depth (cm)	Fragmental Component	Fine Earth Texture	Fine Earth Colour	Mottles			Sed. Unit	Other
					Colour		Pattern		
					High Chrome	Low Chrome			
A	25		cl	2.5Y 4/2				L	Scattered stones & Gr
Bw(f)	30	sli. gr	cl	10YR 6/3	10YR 6/8		f.m.d.	L	additional mottle colour 7.5Y 6/8
Gravels									

Profile 25 (on surface S4)

Horizon	Depth (cm)	Fragmental Component	Fine Earth Texture	Fine Earth Colour	Mottles			Sed. Unit	Other
					Colour		Pattern		
					High Chrome	Low Chrome			
A	15							L	
?	40							L	
Gravels									

Profile 26 (on surface S4)

Horizon	Depth (cm)	Fragmental Component	Fine Earth Texture	Fine Earth Colour	Mottles			Sed. Unit	Other
					Colour		Pattern		
					High Chrome	Low Chrome			
A	25	sli.gr						L	
?	40	sli.gr						L	
Gravels									

Profile 27 (on surface S5)

Horizon	Depth (cm)	Fragmental Component	Fine Earth Texture	Fine Earth Colour	Mottles			Sed. Unit	Other
					Colour		Pattern		
					High Chrome	Low Chrome			
A	30	zcl	zcl	2.5Y 3/2				A3	
?	40	gr	zl	2.5Y 5/3				A3	
Gravels									

Profile 28 (on surface S5)

Horizon	Depth (cm)	Fragmental Component	Fine Earth Texture	Fine Earth Colour	Mottles			Sed. Unit	Other
					Colour		Pattern		
					High Chrome	Low Chrome			
A	20	m. gr	zl	10YR 3/2				A3	m. gr thoughout (almost 50%)
?	50	m. gr	zcl	10YR 5/4				A3	Lismore or Hororata Profile ?
Gravels									

Profile 29

Horizon	Depth (cm)	Fragmental Component	Fine Earth Texture	Fine Earth Colour	Mottles			Sed. Unit	Other
					Colour		Pattern		
					High Chrome	Low Chrome			
A	35	f. gr	zl	10YR 3/2				A4	few gr within top 40cm
Bw	70		cl	10YR 5/4				A4	Fine Earth colour grades down to 10YR 5/6
Gravels									

Note: Horizon Bw has the morphology of a brown soil, but could be a deeper version of profiles 30 & 31

Profile 30

Horizon	Depth (cm)	Fragmental Component	Fine Earth Texture	Fine Earth Colour	Mottles			Sed. Unit	Other
					Colour		Pattern		
					High Chrome	Low Chrome			
A	30		zcl	2.5Y 4/2				A4	clear boundary
Bw(f)	57		cl	10YR 4/6		10YR 5/4		A4	mottled sub-soil - redeposited loess or overbank silts?
Gravels									

Profile 31

Horizon	Depth (cm)	Fragmental Component	Fine Earth Texture	Fine Earth Colour	Mottles			Sed. Unit	Other
					Colour		Pattern		
					High Chrome	Low Chrome			
A	30		zcl	2.5Y 4/2				A4	
Bw(f)	35		cl	2.5Y 5/4	10YR 5/6		f.f.f.	A4	
Gravels									

APPENDIX II -
GLOBAL POSITIONING SYSTEM

This appendix presents an introduction and brief description of the GPS technology and surveying techniques. The information was mainly extracted from the online tutorial of Trimble®, the equipment used during this investigation. For additional reading, many references in the specialized literature and Internet exist.

A II.1 Introduction:

The Global Positioning System (GPS) is a worldwide radio-navigation system formed by 24 NAVSTAR satellites and their ground stations. The NAVSTAR satellites orbit the earth every 12 hours and are used as reference points to calculate accurate positions on the Earth.

Ground Stations monitor both the performance and the exact position in space of the GPS satellites. These stations transmit corrections for the satellite's orbits (ephemeris) constants and clock offsets back to the satellites themselves. This information is incorporated and sent to GPS receivers on the Earth.

A II.2 How GPS Works:

Satellites in space are used as reference positions to locate points on the Earth. The exact orbit and position of each satellite is known, and is continually monitored by the ground stations. In order to determine the exact location of a point of interest on the Earth, the distance between a satellite and the point is calculated using the travel time of a radio signal sent from the satellite to a receiver located at the point of interest. The radio signal is a very complicated digital code, named pseudo-random code, and is different for each satellite.

The receiver calculates the travel time of the signal by comparing its own pseudo-random code with an identical code in the signal sent from the satellite. The receiver's code is delayed with respect to the signal from the satellite, and it is "moved" until it matches perfectly. This amount of "movement" is equal to the travel time of the signal. Knowing the travel time and the velocity of the signal (i.e. the speed of light), the distance between the receiver and the satellite can be calculated. With the distances between three different satellites and the receiver located at a specific point, a "trilateration" process (a process similar to triangulation but without angles involved) is used to calculate the position of the point. A fourth satellite is employed to determine the exact position and to remove time errors.

A II.3 Differential GPS Technique:

Different GPS techniques exist in order to achieve better accuracy in the measurements. During this study, the differential GPS technique was used to minimize positional errors. Differential GPS involves two receivers working at the same time. One of them remains stationary while the other one is moving making positional measurements. The stationary receiver (base station) is located at a point of very well known position, usually a survey mark such as a trig station. This attaches the satellite measurements to a local reference and allows us to make position corrections if necessary.

The time signal that travels from the satellites to a receiver and that is used to calculate the position of a particular point, may contain errors related to technological or environmental factors. These errors may be caused by clock and/or satellite orbit inaccuracies, changes in signal travel path due to atmospheric layers, and environmental noises. The well known position of the base station permits us to determine and correct timing errors and provides the positional corrections to the moving receiver, improving the overall accuracy of the measurements.

Instead of using timing signals to calculate its position, the base station uses its known position to calculate timing. It compares the calculated travel time (what the travel time of the GPS signals should be according to its position), with the actual

measured travel time. The difference is an “error correction” factor that is used to correct the measurements of the moving receiver.

A II.3.1 Code Phase and Carrier Phase GPS:

There are two different modes of determining positional locations in differential GPS technique: code and carrier phase. Both were used as part of this study. As explained above, the GPS receivers determine the signal travel time from the satellites by comparing pseudo-random codes. In code phase, pseudo-random codes that have a cycle width of almost a microsecond are compared. Due to the wide cycle of the signals, the compared pseudo-random codes can be out of phase and this will introduce an error on the location. This error may be of about 1 m or more.

Carrier-phase uses a shorter wavelength signal which significantly reduces the positional errors. A carrier signal is a particularly high frequency signal also transmitted by the satellites. The pulses of this signal are much closer together and consequently provide greater accuracy. The positional error in carrier-phase may be of around 10 cm.